Maritime Emission Regulations and Operations Research in Shipping

Yewen Gu

Department of Business and Management Science, Norwegian School of Economics, Bergen, Norway

Contents

Acknowledgements

8310 kilometers, from Shanghai to Bergen, the distance I travelled for knowledge. 1461 day-and-nights, from 2014 to 2018, the time I spent for truth. These two numbers vividly illustrates the nature of the PhD program, exciting and challenging. However, when I finally stand at the end of this journey and look back, I find that it is not a lonely fight but a collective victory. Many people offered their kindly help and support during my journey and without them I may not make it to the end. Therefore, I using this opportunity here to express my most sincere gratitude to these people.

First of all, I would like to thank my primary supervisor Professor Stein W. Wallace at the Department of Business and Management Science, Norwegian School of Economics. His patient and experienced guidance significantly helped me to overcome different difficulties and challenges during my research work. Second, I would like to express my deep appreciation to Dr. Xin Wang at the Department of Industrial Economics and Technology Management, Norwegian University of Science and Technology. As one of my co-supervisor, we worked closely on most of my research projects during my PhD program. As a young scholar, I learnt a lot from him through our cooperation. Third, I am also grateful to the other two of my co-supervisors, Roar Os Ådland at the Department of Business and Management Science, Norwegian School of Economics, and Kjetil Fagerholt at the Department of Industrial Economics and Technology Management, Norwegian University of Science and Technology. Both of them have offered valuable inputs and comments about my work, which helps me to improve my research. Fourth, I need to say thank you to Norwegian School of Economics and the Department of Business and Management Science for the opportunity they offered me to pursuer my PhD degree. Lastly, I also need to say thank you to my family and friends. It is their encouragement that supports and guides me when I am depressed and feel lost.

General Introduction

Since the first cargoes were moved by sea about 5000 years ago, shipping has played a critical role in the world economy (Stopford, 2009). Today, this old business continues to contribute and is serving more than 90 percent of the global trade (ICS, 2017). With such importance, the shipping industry attracts substantial attention from various disciplines which certainly include the field of operations research.

In operations research, people try to build different kinds of optimization models which can help a shipping company to minimize its cost or maximize its profit in their business operations. One of the main purposes of solving these optimization models is to find out how optimal decisions are made so that they can also be applied in the real world by the shipping companies. Moreover, exploring the underlying interrelationship among different variables and parameters through computational studies using optimization also offers valuable managerial insights to this industry. The decisions considered by a shipping company can be roughly divided into three levels, namely strategic decisions, tactical decisions and operational decisions.

First, the strategic decisions in the shipping industry normally concern a shipping company's long-term interests. Such strategic decisions may include, for example, ordering newbuildings, purchasing second-hand vessel, retrofitting an exiting fleet with new technologies and demolition of old ships. These strategic decisions bring long-lasting or permanent effects on the size and capability of a shipping company's fleet and therefore influences the company's transport capacity. Due to the intensive capital involvement and long-term impact, strategic decisions are only made occasionally based on specific cases. Second, the shipping company needs to make some decisions regularly as well. For instance, every week or month the shipping company may temporarily adjust its fleet size through the chartering market in order to adapt to the volatile demand. Every few months a forward contract may be negotiated and signed by the shipping company and its fuel supplier for risk control purposes, which guarantees the volume and price of the marine fuels supplied to the shipping company for the next planning period. Such decisions made on a regular basis with medium-term impact are considered as tactical decisions in the shipping industry. Unlike the strategic decisions, which are usually irreversible, tactical decisions can be fixed or adjusted afterwards with certain costs. Last, operational decisions which determine a ship's sailing behavior (e.g., route and speed choice) during the voyage are made on a daily basis. These operational decisions directly affects a ship's travelling time and fuel consumption.

Although decisions on different levels are normally made separately by different people in the shipping company, they may actually interact with each other. For example, the delivery of a new vessel (strategic level) will significantly decrease the shipping company's incentive to charter-in additional vessel from the spot market (tactical level). Furthermore, chartering-out the shipping company's own ship for profit during a booming market (tactical level) may force the rest of the fleet to speed up (operational level) so as to maintain the total transport capacity for certain contractual demand. Because of the interaction, the decisions on different levels, even though made separately, should be considered with integration. The importance of such integrated decision making is also commonly recognized in operations research.

However, the world is continuously changing and maritime transportation is no exception.

Several environmental regulations have been implemented or proposed in this industry. Among these regulations, the Emission Control Areas (ECA or SECA) and the Maritime Emission Trading Scheme (METS) catch most attentions from both industry and academia due to their international coverage and enormous impact. The ECA was introduced in 2005, but its policy has been gradually upgraded and stricter requirements have been enforced during the past decade. The latest ECA regulation covers the North Sea, the Baltic Sea, and the North American and US Caribbean coasts. The vessels entering these regulated zones need to either install scrubber on board or switch to marine gasoline oil (MGO) so that their sulphur emission can be restricted within the allowed limit. On the other hand, METS is a market-based measure (MBM) proposed to the International Maritime Organization (IMO) for discussion and evaluation. Different from ECA, METS aims to control the greenhouse gases (GHGs), mainly CO_2, emitted from ships. The concept of emission allowance, which can be freely traded on the market, is used in the METS to offer incentives for the shipping company to reduce its CO_2 emissions through more efficient operations and more advanced technology. More detailed information of these two environmental regulations will be introduced in the following chapters.

The implementation of these new regulations not only affects the sustainability of maritime transportation, but also impacts the shipping company's decisions on all levels. For instance, the introduction of ECA may affect a shipping company's decisions on the strategic level. New ships with emission abatement technology may be ordered, while old vessels may be retrofitted to comply with the regulation or sent for scrapping. Moreover, the ships may start slow steaming during daily operations if the METS comes into force in the future, since speed reduction can help to decrease the consumption of fuel and thus CO_2 emissions, which finally leads to a lower cost for emission allowance..

Although ECA and METS have been implemented or proposed for a while, the regulations continue to upgrade and evolve, which brings new challenges to the industry and new research interests to the academia. The purpose of this thesis is to study the impacts of the latest environmental regulations on the shipping company's decision making on all levels.

Some knowledge gaps brought by the new regulations to the literature of operations research in maritime transportation are filled by the works in this thesis. Moreover, this thesis also offers valuable insights for the shipping industry and maritime policy makers, so that more efficient business operations and regulations can be achieved in the future. The following four chapters focus on several classical optimization models in maritime transportation and extend them by taking new environmental regulations into account.

In Chapter 1 we study how the ECA regulation affects the traditional maritime fuel management (MFM) problem. Before ECA was introduced, the tactical and operational decisions in the MFM problem were normally made separately in shipping companies. Similarly, the literature about MFM also choose to focuses on either the tactical level or the operational level in the problem. Although it is commonly recognized in operations research that the tactical and operational decisions should be considered with integration, the special situation in MFM has its reason. However, the implementation of ECA changed the case. We develop a stochastic programming model involving both tactical and operational decisions in MFM with the consideration of the new regulation. The model minimizes the total expected cost while controlling the risk in the worst scenarios. The results of the computational study show that isolated decision making on either tactical or operational level in MFM will lead to various problems after ECA came into force. The most severe consequences occurs when tactical decisions are made in isolation.

In Chapter 2 we focus on how a shipping company's bunker risk management influences the CO_2 emissions of its fleet. The study in this chapter is conducted based on the model developed in Chapter 1. However, instead of discussing the importance of integrated decision making in MFM, we examine the emission performances of ships when the shipping company

holds different risk attitudes on its bunker cost. The findings of this study show that a shipping company's bunker risk management does have substantial impact on its emission during the fleet operation. We also demonstrate that with a properly designed risk control policy and hedging strategies, a shipping company can sometimes achieve noticeable emission reductions with little financial sacrifice.

In Chapter 3 we study a new challenge faced by a shipping company due to the latest ECA regulation. A choice of emission abatement equipment installed on board the ship needs to be made by the company so that the regulation can be complied with while the relevant cost can be minimized. In this chapter, we integrate the optimization of a ship's sailing pattern into the traditional lifespan cost assessment of the emission control technology for vessels. This study shows that a substantial overestimation of the value of scrubbers, and hence a considerable loss, can occur if a ship's sailing pattern is not considered in the decision making process. Moreover, we also find that such a concern is more relevant and important when the port call density inside ECA is low.

In Chapter 4 the impact of a Maritime Emission Trading Scheme (METS) on the short-term CO_2 emission reductions in shipping is examined. A new model integrating the classical fleet composition and deployment problem and the METS is developed. In the computational study, we use this model as a tool to test the emissions of a fleet under different scenarios when minimizing total cost. We find that the implementation of METS may not guarantee further emission reduction in certain scenarios. Otherwise, a more substantial short-term emission reduction is experienced in the scenarios with low bunker price, high allowance cost or global METS coverage.

Chapter 1

Integrated maritime fuel management with stochastic fuel prices and new emission regulations

Published at: Journal of the Operational Research Society, 2018

Yewen Gu[1], Stein W. Wallace[1], Xin Wang[2]

[1]Department of Business and Management Science, Norwegian School of Economics, Bergen, Norway
[2]Department of Industrial Economics and Technology Management, Norwegian University of Science and Technology, Trondheim, Norway

Abstract

Maritime fuel management (MFM) controls the procurement and consumption of the fuels used on board and therefore manages one of the most important cost drivers in the shipping industry. At the operational level, a shipping company needs to manage its fuel consumption by making optimal routing and speed decisions for each voyage. But since fuel prices are highly volatile, a shipping company sometimes also tactically procures fuel in the forward market to control risk and cost volatility. From an operations research perspective, it is customary to think of tactical and operational decisions as tightly linked. However, the existing literature on MFM normally focuses on only one of these two levels, rather than taking an integrated point of view. This is in line with how shipping companies operate; tactical and operational fuel management decisions are made in isolation. We develop a stochastic programming model involving both tactical and operational decisions in MFM in order to minimize the total expected fuel costs, controlled for financial risk, within a planning period. This paper points out that after the latest regulation of the Sulphur Emission Control Areas (SECA) came into force in 2015, an integration of the tactical and operational levels in MFM has become important for shipping companies whose business deals with SECA. The results of the computational study show that isolated decision making on either tactical or operational level in MFM will lead to various problems. Nevertheless, the most severe consequence occurs when tactical decisions are made in isolation.

Keywords: Maritime fuel management, Emission Control Areas, Speed optimization, Risk management, Forward contract, Stochastic programming

1.1 Introduction

Maritime transportation is one of the major freight transportation modes in the world. As of 2015, more than 90 percent of the global trade is carried by sea (ICS, 2017). The shipping industry is indispensable for global trade and the world economy, as it is, by far, the most cost effective choice for intercontinental transport of large-volume goods.

Marine fuel costs represent a major portion of a ship's operating costs. It is estimated that bunker costs constitute more than half of the operating costs of a vessel (Stopford, 2009; Ronen, 2011). Based on this, as well as environmental concerns, fuel management has become vital for both financial and environmental reasons.

Maritime fuel management (MFM) normally addresses decisions and management policies at both operational and tactical levels. At the operational level, a shipping company needs to manage its fuel consumption by making optimal routing and speed decisions on each voyage, while obeying some time constraints. On the other hand, since fuel prices are highly volatile, shipping companies sometimes also need to control the risk of their fuel costs, at a tactical level, by entering into fuel contracts in the forward market. Such forward contracts of marine bunker are normally specified by a predetermined fuel price, supply amount and bunkering port (Ghosh et al., 2015). The two levels in MFM are connected through fuel allocation decisions which allocate the actual fuel consumption to different fuel sources, in our case the spot- and forward-fuel markets. The total bunker costs, including fuels from both spot- and forward markets, can then be obtained, and minimizing these costs, taking financial risks into account, is the main goal of MFM.

It is standard in most industrial settings, as well as in the operations research literature, to take operational decisions into consideration when tactical decisions are made, and certainly to consider tactical decisions already made when making operational decisions. After all, tactical decisions are mostly made to prepare the ground for operations, and operations must live with the tactical decisions made, whether they are good or not. Good examples would be location-routing problems (Prodhon and Prins, 2014) and fleet composition and routing problems (Hoff et al., 2010). The former combines tactical depot allocations and operational vehicle routing, while the latter considers both tactical fleet composition and operational routing decisions. Other examples in maritime transportation, such as ship routing and scheduling problems, can be found in Meng et al. (2013) and Christiansen et al. (2004). However, this common practice is not generally witnessed in MFM. For most shipping companies, the two levels of MFM are separated, i.e., the tactical forward-fuel procurement decisions and the operational routing-speed decisions do not interact with each other. Under normal circumstances, no matter how much forward-fuel the procurement department has purchased, the operations team would always sail a vessel along its usual (often also the shortest) path between two ports with the lowest possible speed as long as the agreed arrival time between shippers and the shipping company is fulfilled. On the other hand, the procurement department normally does not pay too much attention to future fleet operations, since the sailing patterns are relatively fixed. They would make their decisions for procuring forward-fuels mainly based on such as the shipping company's risk aversion, historical fuel consumption data and their judgement about future fuel market developments. So there have been good reasons for this rather unusual separation.

This disconnection is also found in the literature. At the tactical level, although widely applied in the industry (Pedrielli et al., 2015), forward contracts (offered by several main fuel suppliers, such as Shell and Chevron) have not been much discussed in the literature (Ghosh et al., 2015). Wang and Teo (2013) provided an overview of the available forward contracts and financial instruments for marine bunker and developed a model that considered fuel hedging in liner network planning. Pedrielli et al. (2015) developed a game theory based model to optimize the bunker contract design problem for both bunker suppliers and shipping companies. Plum

et al. (2014) formulated a mixed integer programming model to solve the *bunker purchasing with contract problem* which provided an efficient tool for the shipping company to plan bunker purchasing and assess new contracts on a global level. At the operational level, more papers on fuel management can be found in the literature. Wang et al. (2013) offered a comprehensive literature review on this topic. Norstad et al. (2011), Fagerholt et al. (2010), Xia et al. (2015) and Wang and Meng (2012) focused on sailing speed optimization and fuel cost minimization; Psaraftis and Kontovas (2010) and Ronen (2011) investigated the relationship between slow steaming and fleet size in container shipping; Yao et al. (2012) and Wang and Meng (2015) proposed optimization models regarding choice of bunkering port. However, most of these papers focus on only one of the two levels. Very few works have studied the MFM problem with an integrated point of view involving both tactical and operational considerations. To the best of our knowledge, only one paper (Ghosh et al., 2015) has included considerations from both levels of MFM. In their problem, the authors aim to find the optimal bunkering strategy at the operational level, but using forward contracts of given amounts only as input to their model. In contrast to their settings, the amounts of forward-fuels to be purchased are also important decisions in our paper.

Significant changes have taken place in maritime transportation after the Sulphur Emission Control Areas (SECA) were introduced by Annex VI of the 1997 MARPOL Protocol, which was finally implemented in May 2005. The geographical locations of the SECA are marked by the dark areas in Fig. 1.1. These regions include the North Sea, the Baltic Sea, and the North American and US Caribbean coasts. The SECA were established to apply stricter controls over the emission of sulphur oxides, such as sulphur dioxide (SO_2), from ships. The latest regulation applied in SECA came into effect on 1st January 2015. For vessels sailing inside the regulated areas, the new regulation restricts the level of sulphur content in the bunker fuel to a maximum of 0.1%. Therefore, the conventional marine fuel – heavy fuel oil (HFO) – which has about 3.5% sulphur content, is no longer permitted inside the SECA. This forces some shipping companies to switch to the marine gasoline oil (MGO) in these areas by carrying both types of fuel on board and performing a fuel change-over when crossing the SECA border. MGO has a sulphur content level that meets the SECA requirements, but a much higher price. After 2020, the global sulphur cap which increases the sulphur standard outside SECA from 3.5% to 0.5% will be implemented. By then the traditional HFO must be replaced by certain Ultra Low Sulphur Fuel Oil (ULSFO) with 0.5% sulphur content. However, a price difference between MGO and ULSFO is still expected. Other methods for SECA compliance, such as liquefied natural gas (LNG) powered propulsion or scrubber systems are also used in the shipping industry. In this paper we only consider the fuel switching approach.

Due to the considerable price difference between the two fuels (MGO and HFO), shipping companies no longer necessarily sail their ships in the old-fashioned way. They now have an incentive to change their sailing behavior in order to minimize costs while simultaneously complying with SECA regulations. The changes in sailing behavior can be classified into two categories: speed differentiation and SECA-evasion (Doudnikoff and Lacoste, 2014; Fagerholt et al., 2015). For instance, when a voyage involves both SECA and normal sea areas, the ship may prefer to sail at different speeds inside and outside SECA. It may slow down when sailing inside SECA so as to consume less MGO which is far more expensive. The speed may then be increased during the rest of the voyage outside SECA so that the total travel time is maintained. The consumption of HFO will increase, but it is much cheaper. Such a strategy is referred to as speed differentiation, see Fig. 1.2(a). Furthermore, if a vessel needs to sail from Port A to Port B and both ports are located inside the same SECA, as illustrated in Fig. 1.2(b), it may choose to first leave the SECA zone after departing from Port A, then sail along the edge of the SECA zone and re-enter the zone when approaching Port B, rather than taking the shortest route between the two ports. This strategy is called SECA-evasion. SECA-evasion normally

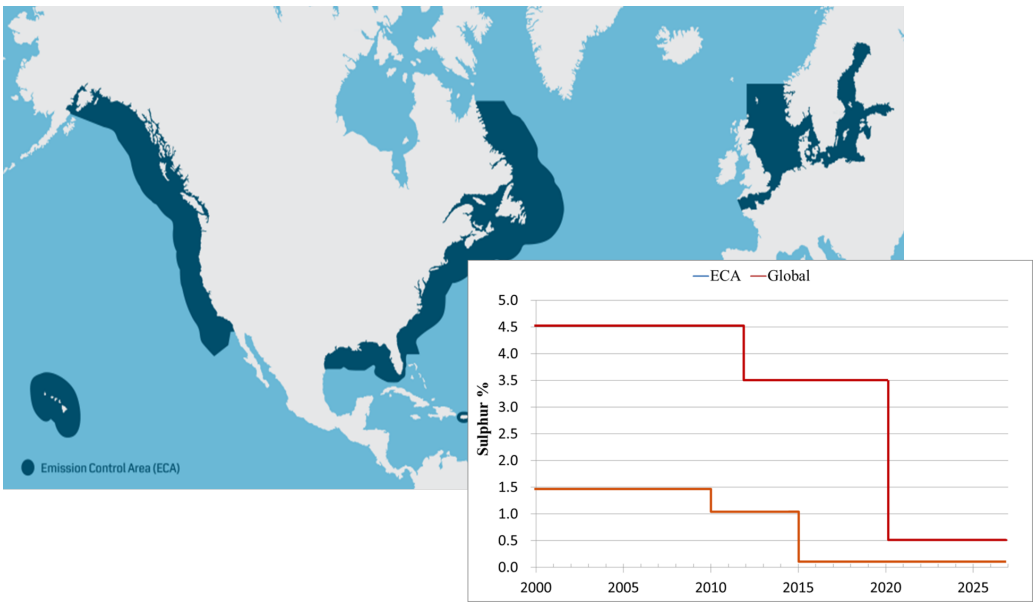

Figure 1.1: Map of the current Sulphur Emission Control Areas

leads to a longer total sailing distance and requires a higher average speed to stay inside the schedules, it however avoids a substantial involvement of SECA sailings and thus reduces the need for expensive MGO. To what extent these two strategies will be applied depends on the price gap between the two fuels. As a whole, the application of these two types of changes in sailing behavior may result in lower total fuel costs. Similarly, such operational changes are still expected after 2020 as long as the price of ULSFO used outside SECA is lower than the price of MGO.

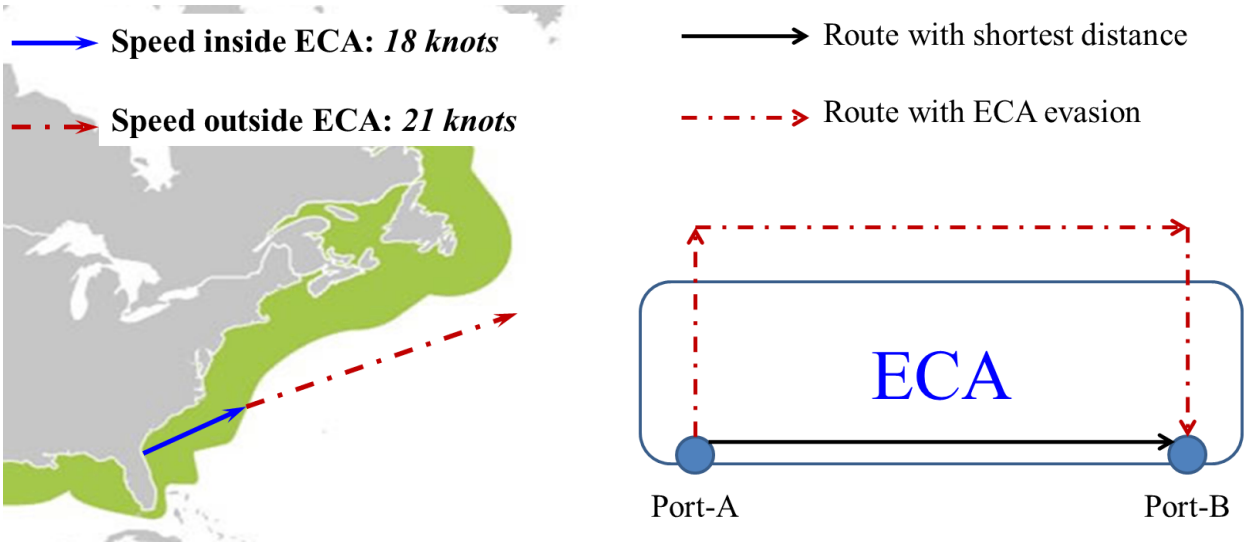

(a) Speed Differentiation

(b) SECA Evasion

Figure 1.2: Two classifications of ship's sailing behavior changes

It is important to notice that adopting speed differentiation and SECA-evasion strategies at the operational level may affect the tactical fuel management decisions (forward contracts) for the two fuels (MGO and HFO), because the demand for the two fuels is no longer fixed but depends on the routing and speed decisions made while operating the ships. Similarly, different strategies of forward-fuel procurement at the tactical level have impacts on future operations, as forward contracts lock in the purchasing prices for some amounts of the fuels which affect the price gap between MGO and HFO (relative to the gaps in the spot markets). Hence, with the

complexity of MFM increasing dramatically with SECA taken into account, the MFM problem needs to be treated from a new integrated angle. It is no longer appropriate to make tactical and operational decisions in isolation when managing bunker in maritime transportation, and one should include simultaneous consideration of both levels in MFM.

Therefore, the main purpose of this paper is to answer the following research question: After SECA came into force, how important is it to integrate the tactical and operational decisions? To this end, we develop a stochastic programming model that integrates the tactical (forward-fuel purchasing) and operational (routing and speed optimization) decisions, taking into account uncertain fuel prices and the latest SECA regulations. In the computational study, this model is applied to a transatlantic liner service of Wallenius Wilhelmsen Logistics (WWL), one of the world's largest liner service providers for rolling equipment.

The paper is organized as follows. Section 1.2 describes the problem and the relevant assumptions. We then present the mathematical formulation of the model in Section 1.3. Section 1.4 introduces the test case and the scenario generation process. In Section 1.5 we show and analyze the results of the computational study. We then conclude in Section 1.6.

1.2 Problem description and assumptions

In this section a detailed description of the MFM problem is given. Section 1.2.1 defines some important terms used in the paper. Section 1.2.2 describes the problem setting, and the relevant assumptions are stated in Section 1.2.3.

1.2.1 Terminology

We refer to a *loop*, see Fig. 1.3(a), as a round trip involving several port calls in a predetermined sequence. A *leg* is then defined as the voyage between two consecutive ports within a loop. Fig. 1.3(b) further shows three *leg options* for one of the legs, each representing a possible path for navigating the leg. The leg options for the same leg normally differ in terms of both total traveling distance and sailing distance inside SECA.

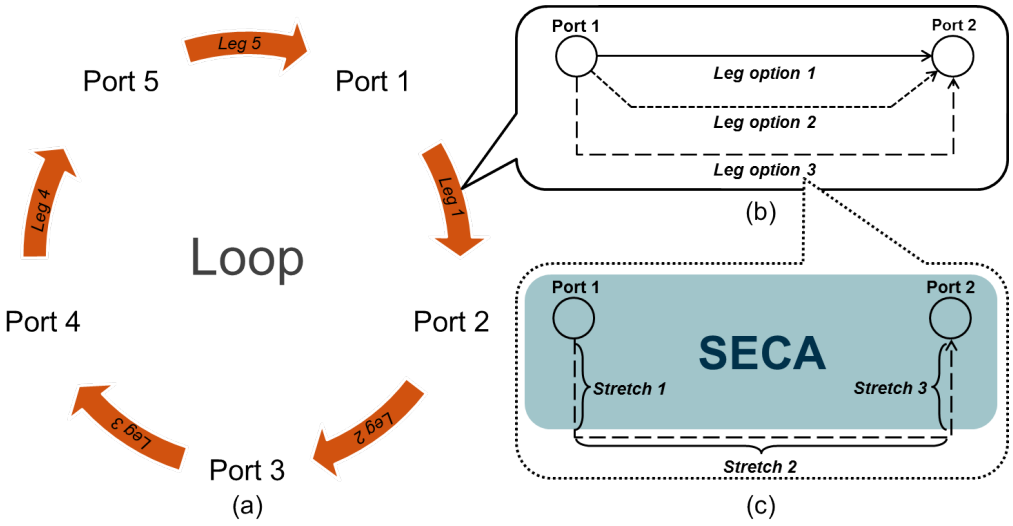

Figure 1.3: Illustration of: (a) loop and legs, (b) leg options, and (c) stretches.

A leg option may contain one or more *stretches*, as shown in Fig. 1.3(c). The first stretch starts when the vessel departs from the origin port and the last stretch ends when the vessel arrives at the destination port. According to the chosen leg option, a new stretch starts whenever the vessel enters or leaves SECA, at which point fuel switching is performed. Although

one leg option may have numerous stretches, we assume that the same sailing speed is adopted on stretches of the same type. For example in Fig. 1.3(c), we assume the ship sails the same speed on stretches inside SECA, i.e., on Stretches 1 and 3. Therefore, we combine the stretches of the same type for every leg option, and hence characterize each leg option with two parts: the SECA stretch and the non-SECA stretch.

1.2.2 Problem setting

A typical liner company offers services with fixed routes, schedules and frequencies, like bus services. The number of ships involved in a particular service route depends on the desired service frequency. Our problem is based on a trading loop operated by a liner company which involves SECA sailings, and considers the company's bunker procurement strategy (both forward- and spot-fuels) as well as its routing, speed and fuel allocation decisions for the next planning period on the trading loop. The aim is to minimize the expected total bunker costs with uncertain fuel prices taken into account, while restricting the risk in total bunker costs within a desired level.

In order to reduce the exposure to fuel cost volatility, using forward contract is one of the most common approaches used by large fuel consumers, such as airlines and shipping companies. The specific type of forward contract considered in this paper is the *Fixed Price Agreement* (FPA in the following) (Dan-Bunkering, 2016). Upon signing the FPA the shipping company purchases (or commits to purchase), at a fixed price, a certain amount of a specified type of bunker which may be delivered later at a certain bunkering port within a given time period, while the bunker supplier has the obligation to deliver regardless of future spot price developments. The contract also states that, during the execution of the FPA or on its expiration, the shipping company also has the right to terminate the contract before its full amount has been delivered and get a "refund" for the unused amount (leftovers). However, to protect the bunker supplier (seller of the FPA) the unused forward-fuel will be refunded at either the forward price or the spot price on the market at the time when terminating the FPA depending on which has a lower value. For example, if the spot price is higher than the forward price agreed in the FPA, the shipping company will only be refunded at the forward price; if, on the contrary, the spot price is lower, the bunker supplier will refund based on the spot price. Also note that instead of terminating the FPA and getting a refund, the shipping company can always require delivery of the remaining unused fuel in the FPA and sell it on the spot market.

1.2.3 Assumptions

The following assumptions are made when developing the model.

- The shipping company is risk averse. The main purpose of the tactical decisions (forward-fuel procurement) in MFM is risk control. Hence, it is reasonable to assume that a shipping company that actually enters the forward-fuel market is risk averse. Forward-fuel contracts may also be used for speculation, but that is not what we study.

- For simplicity, we only consider one ship in our problem. The length of a complete planning period for the MFM problem is set to be the time needed for the ship to finish a round trip on a specific trading loop.

- The port visiting sequence and the corresponding leg information (such as the leg options for each leg, and the characteristics of the associated stretches for every leg option) of the trading loop are assumed to be given and used as input to our model.

- During the operational phase, the shipping company has access to an exogenous and transparent spot-fuel market where the spot-fuel prices are uncertain.
- The fuels purchased from forward contracts are always used first before buying from the spot market. At the end of the planning period, the residual value of any unused fuel in the forward contract is treated as if the FPA is terminated or has just expired. This is to properly evaluate the end-of-horizon values of the uncompleted FPAs which may still be in effect after the end of our planning period. In this case, the shipping company either gets a refund or requires delivery of the remaining amount which is subsequently sold in the spot market.
- When selling the unused fuel in the spot market, the shipping company always gets a price lower than the spot price. This is to reflect the fact that the quantity of the unused fuel may be small and that the bunkering port may be fixed which can lead to inconvenience for the potential buyers.
- The shipping company cannot enter a new FPA during the operational stage.

1.3 The Model

In this section we present the mathematical model for the MFM problem. Section 1.3.1 introduces several important components of the model. The mathematical formulation is presented in Section 1.3.2.

1.3.1 Model development

We propose a two-stage stochastic programming model. The uncertain phenomena we seek to capture are the spot prices for MGO and HFO fuels during the planning period, which are represented by using scenarios. The first-stage decisions, made before the planning period, are the amounts of both fuels to buy in an FPA (forward contract), which belong to the tactical level of MFM. In the second stage, where the two spot-fuel prices (which are assumed to be constant during the planning period in each scenario) are realized, operational decisions will be made based on the realized scenario and the already made first-stage decisions. These operational decisions include: (a) the speed and routing choices on each leg; and (b) the fuel allocation decisions regarding how much forward- and spot-fuels should be used, respectively, in order to satisfy the ship's actual fuel consumption based on the chosen speeds and routes. The aim of the model is to minimize the total bunker costs, which comprise the costs of forward-fuels consumed, and the *expected* costs of spot-fuels purchased, with residual values for unused forward amounts (if any), and financial risk taken into account.

To model the risk attitude of the shipping company, we include *conditional value-at-risk* (CVaR) constraints which are imposed on the total bunker costs. Two key parameters, a confidence level and a maximum CVaR value, are predetermined for our model. The confidence level and the maximum CVaR value, together, reflect the degree of risk aversion held by the shipping company. In our problem, for example, given a confidence level of 95% and a maximum CVaR value of \$300,000, the CVaR constraints would restrict the average bunker costs in the worst 5% scenarios to under \$300,000.

Another challenge is the modeling of the fuel consumption rate relative to speed. It has been shown in the literature that fuel consumption per time unit for a cargo ship is approximately proportional to the third power of its sailing speed (Ronen, 1982; Psaraftis and Kontovas, 2013), and the cubic function can be transferred to a quadratic function that provides a good estimation of the relationship between fuel consumption per distance unit and speed (Norstad

et al., 2011). Nevertheless, shipping companies normally have fuel consumption data only for a group of discrete speed points rather than a function, which is also the case in our study. We therefore use the piece-wise linearization approach, proposed by Andersson et al. (2015), to approximate the fuel consumption rate under different sailing speeds. This approach uses linear combinations of the fuel consumption rates at given speed points to provide an estimation between these speed points, as shown in Fig. 1.4. For instance, if some particular speed v^* can be written, using two weight values a, b, $a + b = 1$, and two speed points v_{Low}, v_{Medium}, as $v^* = a * v_{Low} + b * v_{Medium}$; then the estimated fuel consumption rate F^* at speed v^* can be calculated as $F^* = a * F_{Low} + b * F_{Medium}$. Although this approach normally leads to an overestimation (see Andersson et al. for explanations), the gap is usually acceptable as long as enough discrete speed points are used. This method also gives a proper approximation for the relation between sailing time and speed on each leg and stretch.

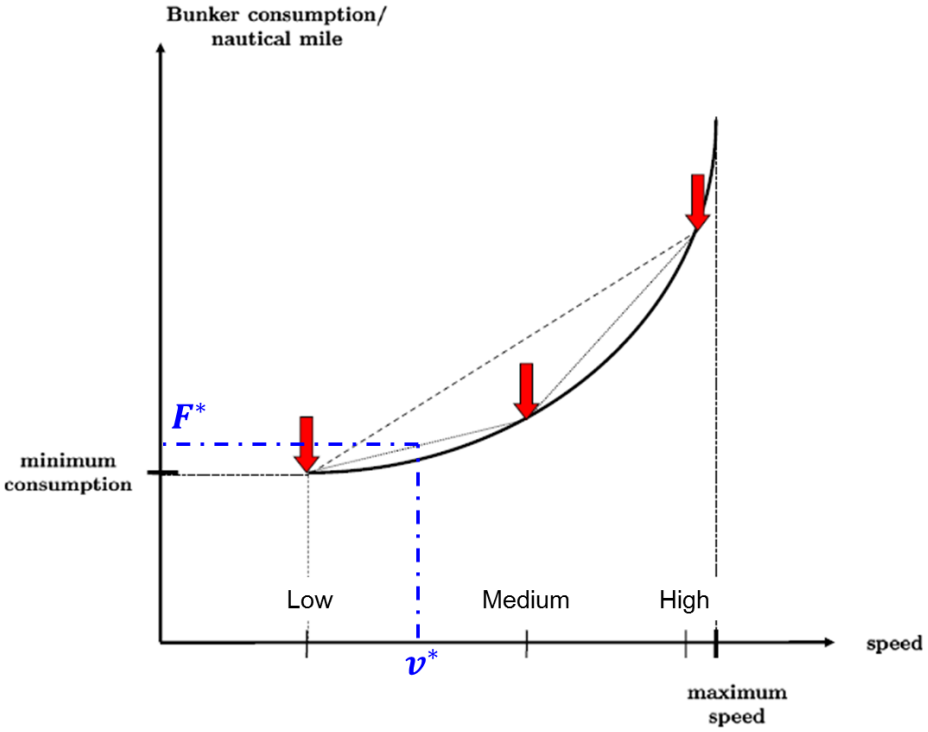

Figure 1.4: Piecewise linearisation of fuel consumption (Andersson et al., 2015)

As mentioned in Section 1.2.3, the unused fuels in a FPA are assumed to be either refunded, or delivered and sold to other fuel consumers (at a discounted price based on the spot price). Therefore, the shipping company will only choose one of the two options so that the residual value of the leftover fuels can be maximized. For example, if the selling price (discounted spot price) of the unused fuels is higher than the fixed price agreed in the FPA, the shipping company will then require delivery and sell these fuels to other buyers. In this case, the residual value of the unused fuels equals "*spot price* $*$ *discount rate* $*$ *unused amount*". Otherwise, the forward contract will be terminated and the contract value of the leftovers (*fixed price* $*$ *unused amount*) will be the residual value. In the model, the residual value in each scenario is pre-calculated based on the logic described above and the actual spot price realized in that scenario.

1.3.2 Mathematical formulation

The notation used in the formulation is as follows:

Sets

J	Set of sailing legs along the loop
R_j	Set of leg options for Leg j
V	Set of feasible discrete speed points for the ship
S	Set of price scenarios

Parameters

P^{MGO-F}	Price per ton of MGO agreed in the forward-fuel contract
P^{HFO-F}	Price per ton of HFO agreed in the forward-fuel contract
P_s^{MGO-S}	Price per ton of MGO on spot market under scenario s
P_s^{HFO-S}	Price per ton of HFO on spot market under scenario s
R_s^{MGO}	Residual value per ton for the unused MGO left in the FPA under scenario s
R_s^{HFO}	Residual value per ton for the unused HFO left in the FPA under scenario s
$\overline{W}_j$	Latest starting time for Leg j
W_j^S	Service time for Leg j in the departing port
W_{jrv}^{SECA}	Sailing time on SECA stretches on Leg j under Leg option r with speed v
W_{jrv}^{N}	Sailing time on non-SECA stretches on Leg j under Leg option r with speed v
D_{jr}^{SECA}	Sailing distance on SECA stretches on Leg j under Leg option r
D_{jr}^{N}	Sailing distance on non-SECA stretches on Leg j under Leg option r
F_v	Fuel consumption per unit distance sailed with speed alternative v (same for both HFO and MGO)
p_s	Probability of scenario s taking place
M_1	Largest possible amount of MGO consumption on this loop
M_2	Largest possible amount of HFO consumption on this loop
γ	Confidence level applied in CVaR
A_γ	The maximum tolerable CVaR value under confidence level γ

Decision variables

x_{jrvs}^{SECA}	Weight of speed choice v used on SECA stretches on Leg j with Leg option r under scenario s
x_{jrvs}^{N}	Weight of speed choice v used on non-SECA stretches on Leg j with Leg option r under scenario s
y_{jrs}	Binary variables representing the decisions on route selection, equal to 1 if Leg option r is sailed on Leg j under scenario s, and 0 otherwise
z_{js}^{MGO-S}	Amount of MGO from spot market used on Leg j under scenario s
z_{js}^{MGO-F}	Amount of MGO from forward contract used on Leg j under scenario s
z_{js}^{HFO-S}	Amount of HFO from spot market used on Leg j under scenario s
z_{js}^{HFO-F}	Amount of HFO from forward contract used on Leg j under scenario s
u_{s}^{MGO-F}	Amount of unused forward MGO left at the end of the planning period under scenario s
u_{s}^{HFO-F}	Amount of unused forward HFO left at the end of the planning period under scenario s
m^{MGO-F}	Agreed amount of MGO in the forward contract
m^{HFO-F}	Agreed amount of HFO in the forward contract
i_{s}^{MGO-F}	Auxiliary binary variable for MGO under scenario s
i_{s}^{HFO-F}	Auxiliary binary variable for HFO under scenario s
α	Auxiliary variable for CVaR constraints
h_s	Auxiliary variables for CVaR constraints under scenario s

The mathematical formulation is as follows:

$$\begin{aligned}\min \quad & P^{MGO-F}m^{MGO-F} + P^{HFO-F}m^{HFO-F} \\ & + \sum_{s\in S} p_s \Bigg\{ \sum_{j\in J} \left(P_s^{MGO-S} z_{js}^{MGO-S} + P_s^{HFO-S} z_{js}^{HFO-S}\right) \\ & - R_s^{MGO} u_s^{MGO-F} - R_s^{HFO} u_s^{HFO-F} \Bigg\}\end{aligned} \tag{1.1}$$

subject to

$$\overline{W}_{j+1} \geq \overline{W}_j + W_j^S + \sum_{r\in R_j}\sum_{v\in V} \left(W_{jrv}^{SECA} x_{jrvs}^{SECA} + W_{jrv}^{N} x_{jrvs}^{N}\right) \qquad s\in S, j\in J \tag{1.2}$$

$$\sum_{v\in V} x_{jrvs}^{SECA} = y_{jrs} \qquad s\in S, j\in J, r\in R_j \tag{1.3}$$

$$\sum_{v\in V} x_{jrvs}^{N} = y_{jrs} \qquad s\in S, j\in J, r\in R_j \tag{1.4}$$

$$\sum_{r\in R_j} y_{jrs} = 1 \qquad s\in S, j\in J \tag{1.5}$$

$$z_{js}^{MGO-F} + z_{js}^{MGO-S} = \sum_{r \in R_j} \sum_{v \in V} F_v D_{jr}^{SECA} x_{jrvs}^{SECA} \qquad s \in S, j \in J \tag{1.6}$$

$$z_{js}^{HFO-F} + z_{js}^{HFO-S} = \sum_{r \in R_j} \sum_{v \in V} F_v D_{jr}^{N} x_{jrvs}^{N} \qquad s \in S, j \in J \tag{1.7}$$

$$\sum_{j \in J} z_{js}^{MGO-F} + u_s^{MGO-F} = m^{MGO-F} \qquad s \in S \tag{1.8}$$

$$\sum_{j \in J} z_{js}^{HFO-F} + u_s^{HFO-F} = m^{HFO-F} \qquad s \in S \tag{1.9}$$

$$u_s^{MGO-F} \leq M_1 i_s^{MGO-F} \qquad s \in S \tag{1.10}$$

$$\sum_{j \in J} z_{js}^{MGO-F} \leq M_1 (1 - i_s^{MGO-F}) \qquad s \in S \tag{1.11}$$

$$u_s^{HFO-F} \leq M_2 i_s^{HFO-F} \qquad s \in S \tag{1.12}$$

$$\sum_{j \in J} z_{js}^{HFO-F} \leq M_2 (1 - i_s^{HFO-F}) \qquad s \in S \tag{1.13}$$

$$y_{jrs} \in \{0, 1\} \qquad s \in S, j \in J, r \in R_j \tag{1.14}$$

$$x_{jrvs}^{SECA}, x_{jrvs}^{N} \geq 0 \qquad s \in S, j \in J, r \in R_j, v \in V \tag{1.15}$$

$$z_{js}^{MGO-F}, z_{js}^{MGO-S}, z_{js}^{HFO-F}, z_{js}^{HFO-S} \geq 0 \qquad s \in S, j \in J \tag{1.16}$$

$$u_s^{MGO-F}, u_s^{HFO-F} \geq 0 \qquad s \in S \tag{1.17}$$

$$i_s^{MGO-F}, i_s^{HFO-F} \in \{0, 1\} \qquad s \in S \tag{1.18}$$

CVaR constraints:

$$\alpha + \frac{1}{1 - \gamma} \sum_{s \in S} p_s h_s \leq A_\gamma \tag{1.19}$$

$$h_s \geq 0 \qquad s \in S \tag{1.20}$$

$$\begin{aligned} h_s \geq\ & P^{MGO-F} m^{MGO-F} + P^{HFO-F} m^{HFO-F} \\ & - R_s^{MGO} u_s^{MGO-F} - R_s^{HFO} u_s^{HFO-F} \\ & + \sum_{j \in J} \left(P_s^{MGO-S} z_{js}^{MGO-S} + P_s^{HFO-S} z_{js}^{HFO-S} \right) - \alpha \qquad s \in S \end{aligned} \tag{1.21}$$

The objective function (1.1) minimizes the sum of the expected expenditure on forward-fuels (initial costs on forward contracts subtracted by their end-of-horizon values) and the expected spot-fuel costs. The first line in the objective function refers to the initial costs for the agreed amounts of MGO and HFO in the forward contracts, while the expected costs for spot-fuels

consumed in the second stage are expressed as the second line of the objective function. The last line represents the residual value of the unused fuels left in the forward contracts at the end of the planning period.

Constraints (1.2) ensure that the time constraints for all sailing legs are respected. Constraints (1.3) and (1.4) connect x- and y-variables with respect to the speed-routing choices in SECA and non-SECA stretches, respectively. They ensure that the sums of the speed weights, x^{SECA}_{jrvs} and x^{N}_{jrvs} respectively for SECA and non-SECA stretches, are equal to 1 if Leg option r is chosen for Leg j in Scenario s, and 0 otherwise. Constraints (1.5) ensure that only one leg option is used on any specific leg. Constraints (1.6) - (1.9) are bookkeeping constraints. Constraints (1.6) and (1.7) make sure that for each scenario the sum of the spot- and forward-fuels used on each leg equals the actual fuel consumption on that leg based on the speeds and leg options chosen. Constraints (1.8) and (1.9) ensure that the forward-fuels used plus the leftovers equal the agreed amounts in the forward contract. Constraints (1.10) - (1.13) enforce that for each type of fuel the unused forward amount and the spot amount will not be simultaneously positive, i.e., at least one of them is zero. This is to ensure that the fuels purchased from forward contracts are always used first, before buying from the spot market. Constraints (1.14) - (1.18) define the domains of the decision variables. Constraints (1.19) - (1.21) are the CVaR constraints representing the risk (aversion) attitude of the shipping company, restricting the risk on the total bunker costs to be within an acceptable level.

1.4 Test case and scenario generation

In this section, we describe our test case in Section 1.4.1, followed by the scenario generation process in Section 1.4.2.

1.4.1 Basic information of the case

We consider a liner service based on Wallenius Wilhelmsen Logistics (WWL), a major roll-on roll-off (RoRo) liner shipping company for transporting cars, trucks and other heavy rolling equipment. The service loop and the corresponding schedules are adopted from one of WWL's Europe-Americas trade lanes, see Fig. 1.5. The port visit sequence of the loop is shown in Table 1.1. In reality, this service loop has several more port calls in Europe besides the Port of Bremerhaven. However, these ports are close to each other, and are all located inside the North Sea SECA. There are, therefore, no feasible alternative leg options and different types of stretches for the shipping company to carry out SECA-evasion or speed differentiation strategies among these ports, apart from the direct (shortest) routes with the same slowest possible speed. We therefore only use one port inside the North Sea SECA, and the schedule information in that area is aggregated and adjusted accordingly. The time needed to finish a round trip in this case is 35 days. Hence, the planning period here is also set to be 35 days according to the assumption made in Section 1.2.3.

Table 1.1: Port visit sequence of the considered service loop

	From	To
Leg 1	Brunswick	Galveston
Leg 2	Galveston	Charleston
Leg 3	Charleston	New York
Leg 4	New York	Bremerhaven
Leg 5	Bremerhaven	Brunswick

(a) Trade lanes from Europe to Americas

(b) Trade lanes from Americas to Europe

Figure 1.5: All trade lanes operated by WWL between Europe and Americas (WWL, 2016)

The fuel consumption data for a number of discrete speed points used in this paper is collected from historical data of a real RoRo ship under normal conditions. From the raw data, we have selected 7 discrete speed points ranging from 15 knots to 24 knots. Fig. 1.6 shows the fuel consumption values (in tons/nautical mile) for the selected speed points. Note that, since the fuel consumption function is monotonically increasing and convex, the discrete speed points are placed more densely towards higher speeds.

For the considered service loop in our case study, we have constructed five leg options for each leg of the loop. When constructing these leg options, the main principle can be described as follows: for each leg, Leg option 1 is to sail the shortest possible distance without any consideration of reducing SECA involvement, which is also the sailing route used before SECA regulation was established; Leg option 5 has the lowest possible SECA involvement in spite of a significant increase in total sailing distance; and the other three leg options are in between the two extreme cases. An illustration of all five leg options of Leg 3 (Charleston-New York) is shown in Fig. 1.7. The solid black line is the SECA border (IMO, 2016), while the dotted lines marked with numbers refer to Leg options 1, 2, 3, 4 and 5, respectively. Leg option 1 has the shortest sailing distance and Leg option 5 has the lowest SECA involvement. The detailed sailing distances within SECA and non-SECA for each leg option of every leg are presented in Table 1.2.

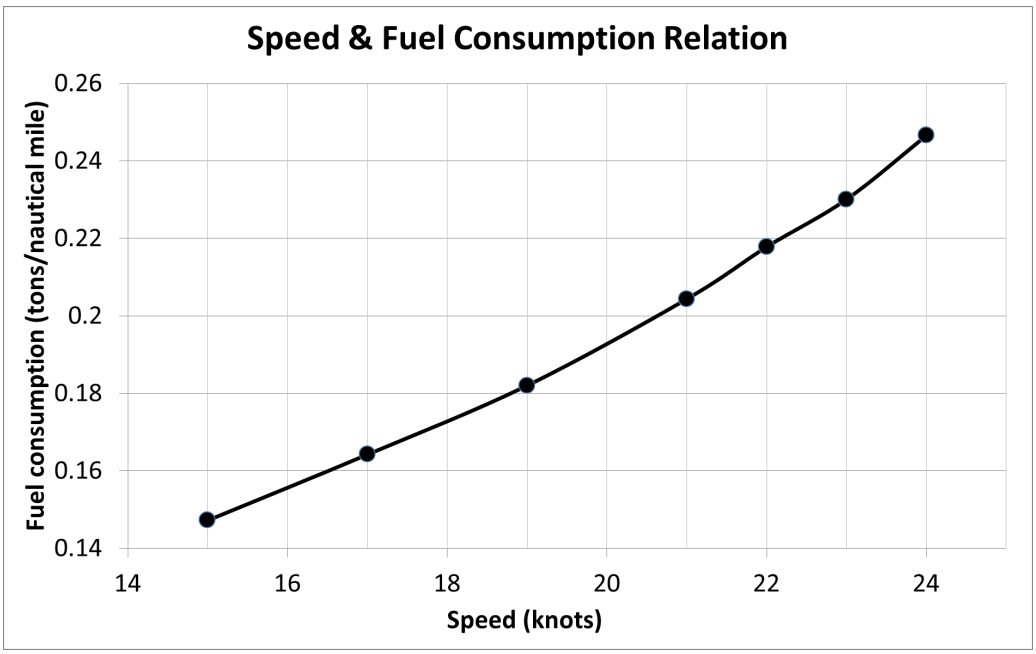

Figure 1.6: Fuel consumption (tons/nautical mile) for the selected discrete speed points

Table 1.2: Sailing distances within SECA/non-SECA for each leg option of every leg

SECA/non-SECA (nautical mile)	Option 1	Option 2	Option 3	Option 4	Option 5
Leg 1	1191/35	569/774	495/870	469/905	408/1062
Leg 2	1271/34	686/704	524/906	458/1083	397/1241
Leg 3	632/0	560/330	499/429	443/515	423/602
Leg 4	1767/1629	1379/2125	1042/2503	899/2652	752/2903
Leg 5	2393/1626	1110/2984	1013/3109	817/3337	751/3428

1.4.2 Scenario generation

The stochastic phenomena in our problem are, as mentioned earlier, the spot prices for MGO and HFO. Given their respective marginal distributions and correlation, we use a version of the scenario-generating heuristic proposed by Høyland et al. (2003). This approach can generate scenarios that match the input distribution properties. When constructing the scenarios for the spot-fuel prices for the next planning period, we use the latest observed prices on the spot market as base prices, and generate (positive or negative) price increments to be added to the base prices. The reason is that fuel prices are highly dependent over time. It would be problematic to directly use historical fuel prices from the past booming period (e.g., 2008) to generate future fuel price scenarios since the market is in depression. However, the development of fuel price can be considered as a Lévy process (Krichene, 2008; Gencer and Unal, 2012) which has independent increments.

To obtain appropriate distributions and correlation for the price increments of the two types of fuels, we use the historical data provided by Clarkson Research Services Limited (Clarkson, 2018a), which is one of the largest data and consulting service providers in the shipping industry. The raw data contains the average weekly fuel prices recorded in three major ports, Rotterdam, Houston and Singapore, from January 2000 to December 2015. Based on these weekly fuel prices, the difference between the fuel prices of week n and week $n+5$ is calculated to represent the monthly increment. In this way, we have in total obtained 834 data points as monthly increment samples for each type of fuel. The distributions of the samples are shown in Fig. 1.8.

In Fig. 1.8, we see that the distributions for the two fuels' monthly price increments are

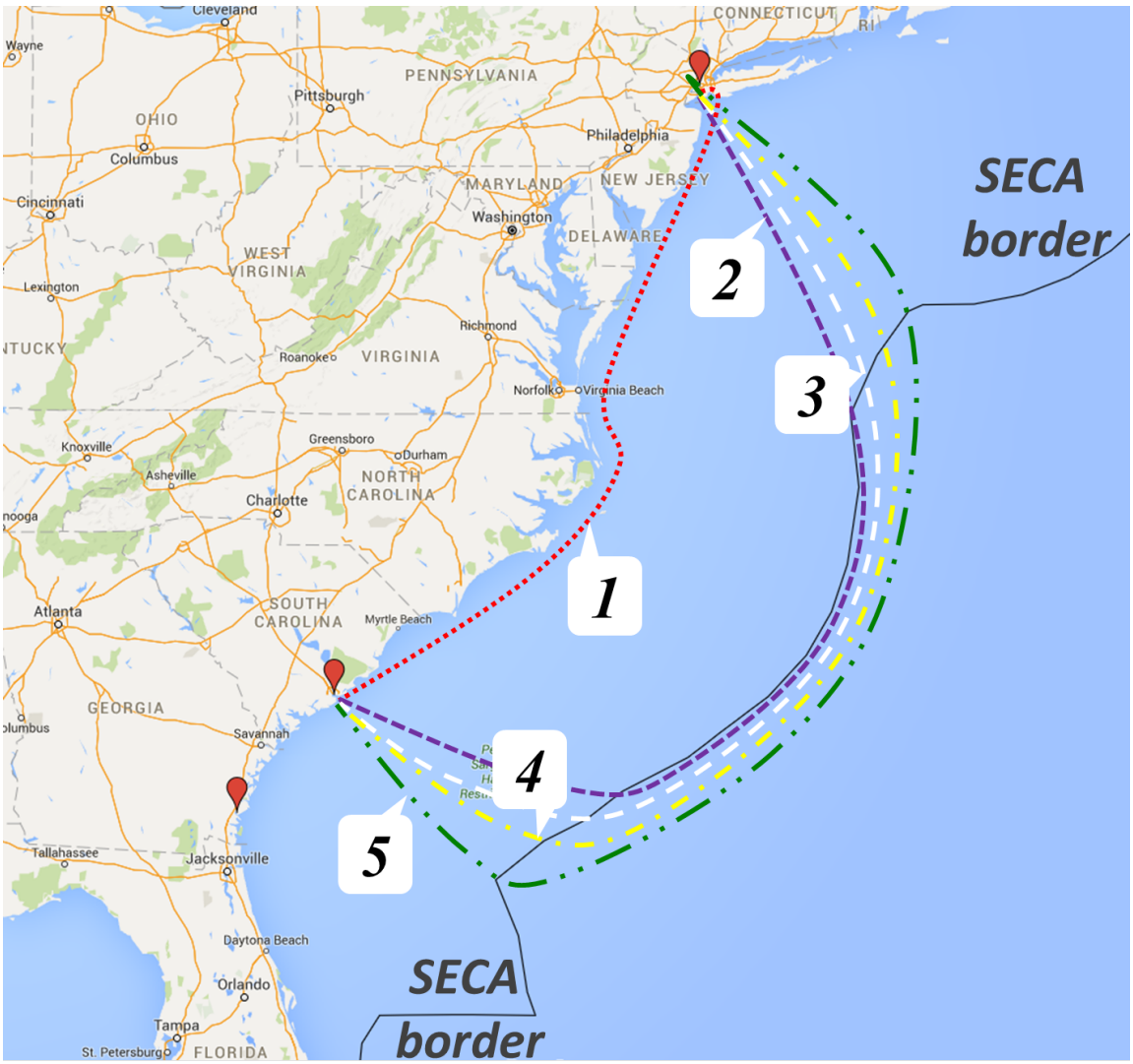

Figure 1.7: Illustration of the five leg options for Leg 3 (Charleston - New York). (Google Maps, 2016)

relatively symmetrical. For each fuel type, we assume a triangular distribution that fits the distribution of the samples reasonably well, also shown in the figures. The small and thin tails would of course be of importance if we were developing a model meant for actual decision-making. However, for our principal discussion of the integration of tactical and operational decisions, we felt that the triangle was enough. Nothing principal would change if we added them (and it would be easy enough to do). The means of the triangular distributions are set to 0, otherwise speculation may occur which is not the focus of this research. The symmetrical triangular distributions are then used as input for the scenario generation procedure. In particular, the lower limit, mode and upper limit of the triangular distribution is set to $(-40, 0, 40)$ for HFO, and $(-120, 0, 120)$ for MGO. The correlation between the HFO and MGO price increments is estimated at 0.75, which is also derived from the historical fuel price data. For the last observation in December 2015, we ended up with 150 USD/ton for HFO, while for MGO it was about 375 USD/ton. These latest prices are used as the basis for the fuel price scenarios in the planning period. Since the expected values of the price increments equal 0, the expected values of the spot-fuel prices in the second stage are assumed to be equal to the latest observed fuel prices. This is a reasonable assumption for our model, since if there is a known increase or decrease in expected prices, which means a guaranteed expected gain or loss, speculation may occur and that is not what we analyze.

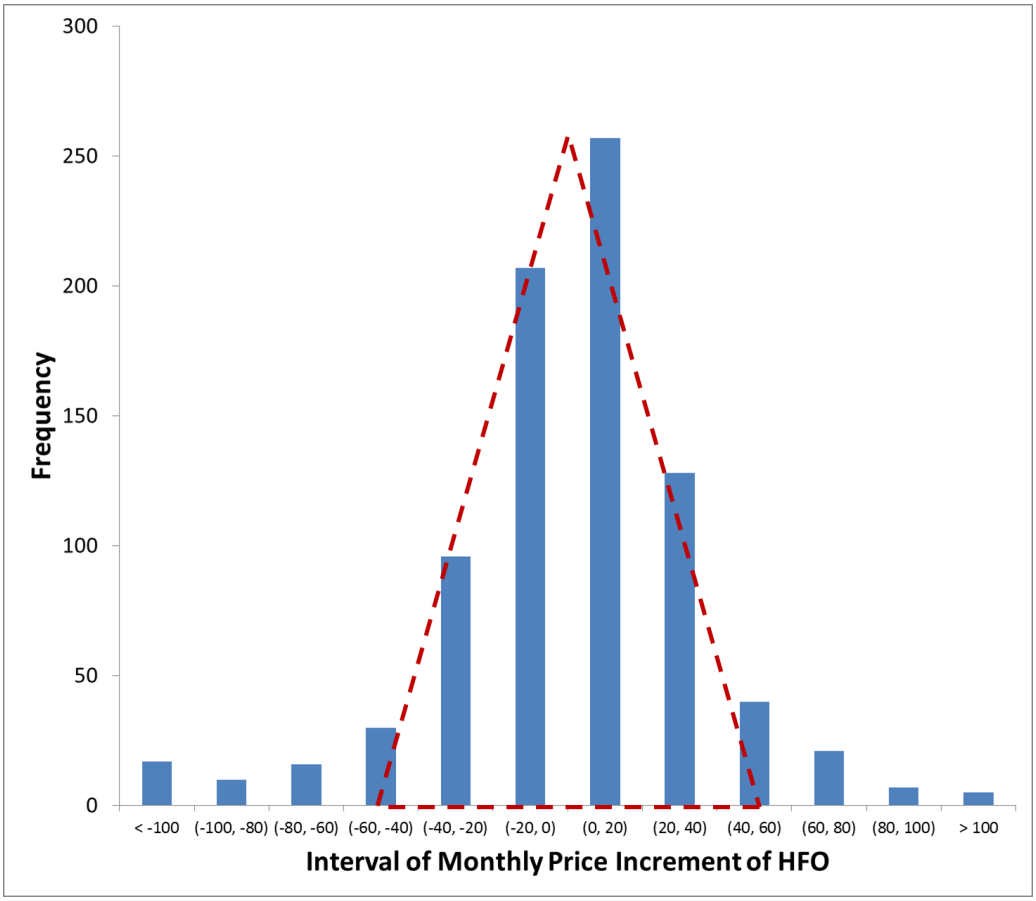

(a) HFO

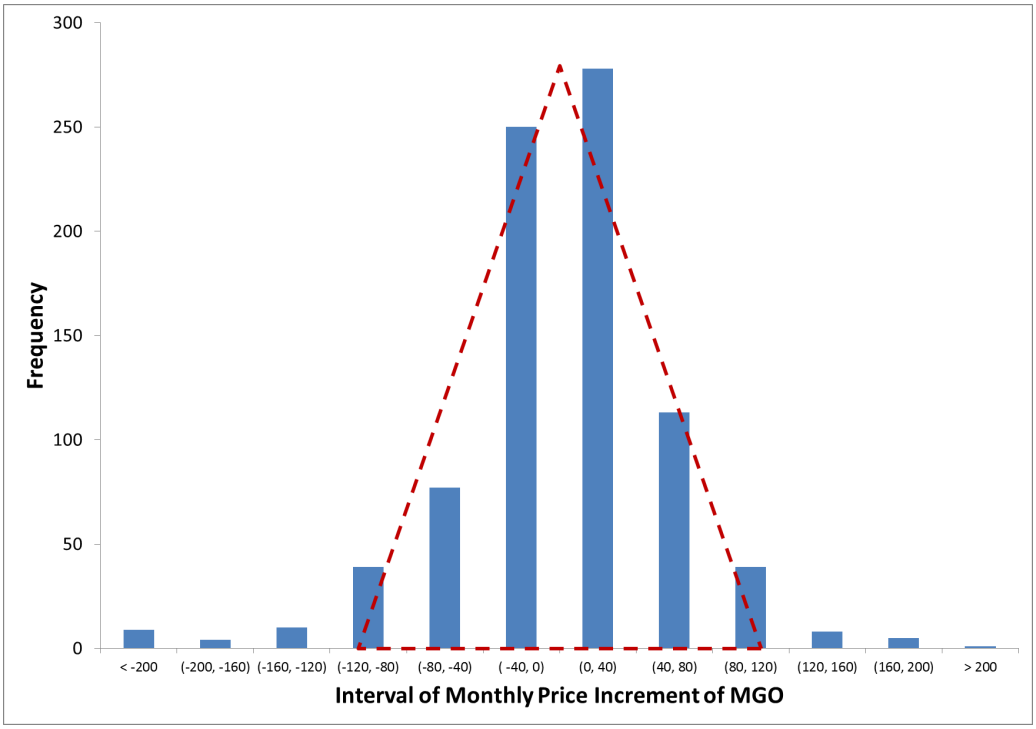

(b) MGO

Figure 1.8: Distribution of the monthly increments for the two fuels

Furthermore, we also check the reliability of the scenario generation approach we use. The in-sample stability test (Kaut and Wallace, 2007) is performed in order to ensure that the solution of the stochastic model does not depend too much on the particular scenario tree used. We generate 10 scenario trees, each consisting of 100 scenarios, using the same generating approach and parameters. We then solve the problem with each scenario tree and are able to observe approximately the same objective function values. The gap among the objective values in the in-sample stability test is less than 0.02%, which is small enough to ensure stability when using 100 scenarios in our problem.

1.5 Computational study

This section presents our computational study. Section 1.5.1 introduces the comparison and analysis tests. Section 1.5.2 offers other important details in the computational study. Numerical results and managerial insights are given in Section 1.5.3.

1.5.1 Tested situations

In order to understand the interaction between the tactical and operational levels of MFM, and the importance of integrated decision-making, we introduce several situations in the following, representing different types of integration between the two levels.

Situation 1. *Decisions on both tactical and operational levels are made with complete integration.*

In **Situation 1**, the tactical and operational levels of MFM are well connected. This means that the purchasing department will take the potential sailing behavior changes during future fleet operation into account when contracting forward-fuels, while the operation team makes routing decisions, such as leg option and speed choices, based on not only the realized spot-fuel prices but also the forward contracts which have already been signed. Note that this situation is represented by solving the problem with the proposed formulation in Section 3 without any changes.

We then introduce **Situation 2** where the tactical and operational levels of MFM are somewhat disconnected. We consider three sub-situations.

Situation 2.a. *Decisions on both tactical and operational levels are made in isolation.*

In *Situation 2.a*, the tactical and operational levels of MFM are completely separated. Neither of them includes the other party in its decision-making. On the tactical level, the purchasing department assumes that the operation team will still sail their fleet in the traditional way, i.e., according to patterns used before SECA regulations were implemented. The operational SECA-related strategies including SECA evasion and speed differentiation are therefore not taken into account at the tactical level. On the other hand, the operation team also ignores the prices and amounts of forward-fuels bought and makes its routing plans solely based on the spot-fuel prices.

To implement this sub-situation, we first obtain the tactical decisions (amounts of forward-fuels) the way they would be made in isolation. We keep only Leg option 1 for each leg (removing all the others), representing the traditional route sailed before SECA was introduced. Moreover, an additional group of constraints (1.22) are added to the model in order to ensure the speeds used on SECA and non-SECA stretches are the same, which means no speed differentiation.

We then solve the problem and observe the first-stage tactical decisions, i.e., the amounts of MGO and HFO purchased in the "traditional" way in a forward contract, denoted $m^{MGO-F}_{traditional}$ and $m^{HFO-F}_{traditional}$, respectively.

$$x^{SECA}_{jrvs} = x^{N}_{jrvs} \qquad s \in S, j \in J, r \in R_j, v \in V \tag{1.22}$$

We then obtain the operational decisions as they would be if made in isolation, disregarding any forward-fuels bought. We start with the original formulation, i.e., without constraints (1.22), but take out the CVaR constraints (1.19) - (1.21) since they are intended for risk control when making the tactical forward contract. We solve the problem with both m^{MGO-F} and m^{HFO-F} set to zero and with full leg options for every leg, and observe the purchased amounts of spot-fuels in each scenario $s \in S$, denoted z^{*MGO}_{js} and z^{*HFO}_{js}. In fact, these values are also the actual consumption in operation as the amounts of forward-fuels are set to zero, and therefore represent the operational decisions made in isolation.

To evaluate this sub-situation in terms of total costs, we combine the tactical and operational decisions obtained ($m^{MGO-F}_{traditional}$, $m^{HFO-F}_{traditional}$ and z^{*MGO}_{js}, z^{*HFO}_{js}), and recalculate the objective function value using the scenarios for spot-fuel prices and the following Equation (1.23).

$$\begin{aligned}
\textbf{Recalculated Total Cost} = {} & m^{MGO-F}_{traditional} P^{MGO-F} + m^{HFO-F}_{traditional} P^{HFO-F} \\
& + \sum_{s \in S} p_s \Bigg\{ \left[\sum_{j \in J} z^{*MGO}_{js} - m^{MGO-F}_{traditional} \right]^+ P^{MGO-S}_s \\
& \quad + \left[\sum_{j \in J} z^{*HFO}_{js} - m^{HFO-F}_{traditional} \right]^+ P^{HFO-S}_s \\
& \quad - \left[m^{MGO-F}_{traditional} - \sum_{j \in J} z^{*MGO-S}_{js} \right]^+ R^{MGO}_s \\
& \quad - \left[m^{HFO-F}_{traditional} - \sum_{j \in J} z^{*HFO-S}_{js} \right]^+ R^{HFO}_s \Bigg\}
\end{aligned} \tag{1.23}$$

The $[\ \ ]^+$ operator in Equation (1.23) outputs the original value of the expression inside the operator if it is positive, and 0 otherwise. The first line of (1.23) represents the expenses of purchasing two forward-fuels. The second and third lines represent the expected costs of spot-fuels when the actual fuel consumption (e.g., $\sum_{j \in J} z^{*MGO}_{js}$) is larger than the forward amount (e.g., $m^{MGO-F}_{traditional}$) in certain scenarios. The last two lines compute the residual value of the unused forward-fuels, if any.

Situation 2.b. *Decisions on the tactical level are made with integration while decisions on the operational level are made in isolation.*

In *Situation 2.b*, we assume that tactical decisions (forward contract) are made with operational considerations taken into account, while the operation team still makes its decisions in isolation. To implement this sub-situation, we obtain the operational decisions the same way as in *Situation 2.a*. However, instead of the "traditional" amounts of forward-fuels contracted without SECA considerations, we recalculate the total costs with Equation (1.23) using the "smart" amounts of forward-fuels as in **Situation 1**.

Situation 2.c. *Decisions on the tactical level are made in isolation while decisions on the operational levels are made with integration.*

In *Situation 2.c*, the tactical decisions (forward contract) are made assuming "traditional" sailing patterns, but the operation team optimizes its sailings in the light of both SECA consideration and the forward contract already signed. To implement, we set the variables m^{MGO-F} and m^{HFO-F} to $m^{MGO-F}_{traditional}$ and $m^{HFO-F}_{traditional}$, respectively, which are the "traditional" amounts of two forward-fuels as obtained in *Situation 2.a*. We then solve the problem (without the CVaR constraints), and observe the objective function value.

1.5.2 Other important details

Before we show the numerical results, some other important details applied in the computational study must be stated.

In all tested situations the forward price is set to be 5% higher than the expected value of the stochastic spot price over the planning period, representing the cost for removing the risks. It also prevents potential speculation on fuels since that is not the focus of the paper. Furthermore, the discounting rate for selling the unused forward-fuels in a spot market (compared to the spot price) is set to 10%, so as to provide the other fuel consumers the incentive to choose the unused fuels (small quantity and fixed bunkering port) over the fuels available on the spot market. Therefore, if the spot price of the fuel is 400 USD/ton, the shipping company will sell its leftovers for 360 USD/ton. Note that the shipping company may also choose to just terminate the contract and get a refund.

In order to ensure the comparability of different situations, we apply the same level of risk aversion in all of our tests, whenever the CVaR constraints (1.19) - (1.21) are active. The maximum CVaR value (A_γ) is set to be 5% higher than the optimal expected costs obtained under a risk neutral assumption (the lowest possible expected cost) and the confidence level (γ) is set to 95%. These parameters can of course be adjusted according to the shipping company's actual risk attitude. However, since removing risk comes at a cost and shipping is an industry with very low profit margin, we argue that restricting the total costs in the extreme cases to a maximum of 5% increase is a reasonable risk control setting for the purpose of this paper.

1.5.3 Numerical results

The aggregated numerical results for all tested situations are displayed in Table 1.3. For each situation, the first-stage decisions (forward-fuel procurement) as well as the second-stage decisions (fuel allocation) are presented in detail.

The average consumption of one type of fuel equals the sum of the actual fuel consumption of that type in each scenario multiplied by the probability of the scenario. Similar logic applies to the average unused fuels. Moreover, the expected total costs is the objective value of the optimization while the standard deviation refers to the cost volatility among all the scenarios. Given a 95% confidence level, the last row in the table shows the risk level in extreme cases (CVaR value) which equals the average of the realized total costs in the worst 5% scenarios in that situation.

Comparison between Situation 1 and Situation 2.a

To compare *Situation 2.a* with **Situation 1**, we use a box plot to show the scope and variability of the total costs produced across all 100 scenarios for each of the two situations, see Fig. 1.9. The whisker on either side of a box represents the 5% scenarios with the highest (right

Table 1.3: Major numerical results of optimization in different situations

	Situation 1	Situation 2.a	Situation 2.b	Situation 2.c
First-stage				
Amount of MGO contracted (tonne)	473.14	1139.42	473.14	1139.42
Amount of HFO contracted (tonne)	1371.72	521.99	1371.72	521.99
Second-stage				
forward managing				
Average consumption of forward MGO (tonne)	466.57	466.83	466.83	474.08
Average consumption of forward HFO (tonne)	1371.00	521.99	1371.72	521.99
Average unused forward MGO (tonne)	6.57	672.59	6.31	665.34
Average unused forward HFO (tonne)	0.72	0	0	0
spot managing				
Average consumption of spot MGO (tonne)	6.02	0	0	0
Average consumption of spot HFO (tonne)	34.05	898.65	48.92	879.35
Overview				
Expected total costs (USD)	405692	420961	406850	419700
Difference (%)	-	3.8%	0.3%	3.5%
Cost standard deviation	615	17808	798	17956
Difference (%)	-	2749%	30%	2819%
CVaR value (95%) (USD)	406818	462339	408826	461225
Difference (%)	-	13.6%	0.5%	13.4%

whisker) or the lowest (left whisker) total costs, while the box represents the remaining 90%. From the results in Table 1.3 and Fig. 1.9, we can clearly see severe consequences when the decisions on both levels are made in isolation (*Situation 2.a*). The total cost on average (of all 100 scenarios) in *Situation 2.a* is 3.8% higher than that in **Situation 1**. Also, the total costs in *Situation 2.a* are much more volatile. The standard deviation of the total costs across all scenarios in *Situation 2.a* is 27.5 times higher than that in **Situation 1**. Moreover, the CVaR value under a 95% confidence level in *Situation 2.a* is 13.6% higher than that in **Situation 1**.

Hence, we see that the shipping company will face considerably higher expected total costs as well as higher cost volatility and risk in extreme cases under uncertain fuel prices if both tactical and operational decisions of MFM are made in isolation. In *Situation 2.a*, the shipping company tends to buy too much MGO and too little HFO in the forward contract, compared to **Situation 1**, as the purchasing department assumes the fleet will sail the shortest routes as before, i.e., assumes a lot of sailings in SECA. However, this turns out to be incorrect since the

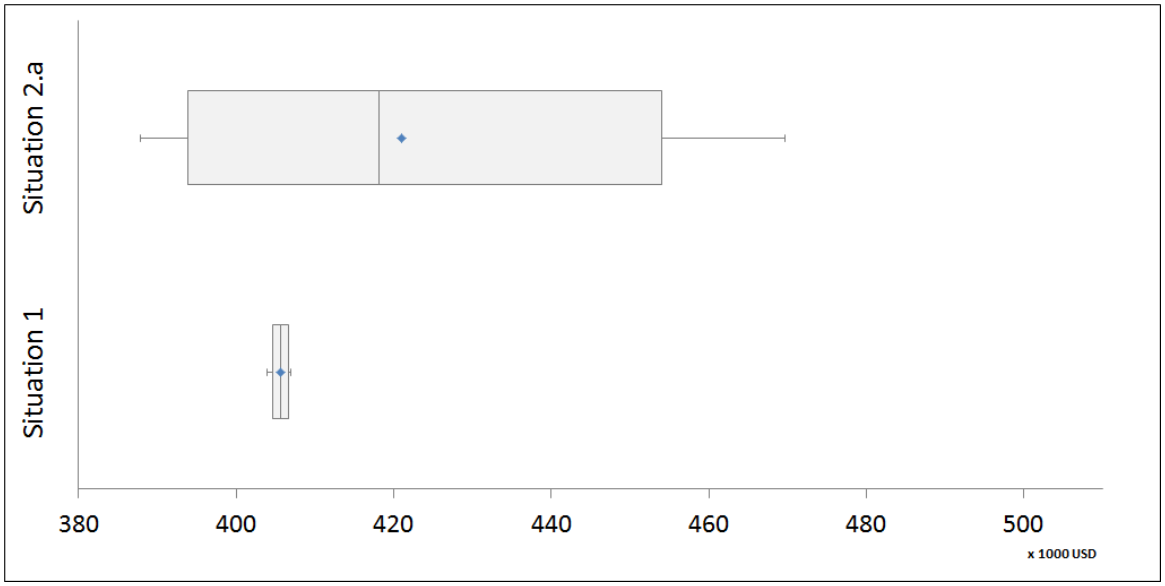

Figure 1.9: Box plot for cost comparisons between Situation 1 and Situation 2.a

operation team will try to reduce their SECA involvement by applying speed differentiation and SECA-evasion. As a result, the amounts of MGO and HFO bought in the forward contract in *Situation 2.a* are too high and too low, respectively, compared to the "optimal" amounts in **Situation 1**, which leads to large amounts of both unused forward MGO (loss in residual value) and spot HFO purchased (high volatility and risk). We can see this from the *Average unused MGO* and *Average spot HFO consumption* values in Table 1.3.

Comparison between Situation 1 and Situation 2.b

We now investigate the consequences of the case where only the decisions at the operational level are made in isolation, i.e., *Situation 2.b*. We show in Fig. 1.10(a) a scenario-by-scenario comparison of total costs between *Situation 2.b* and **Situation 1**, and in Fig. 1.10(b) a box plot comparing the two situations similar to Fig. 1.9.

From Fig. 1.10 and Table 1.3, we see that although the expected total costs in *Situation 2.b* is still higher than that in **Situation 1**, the difference (0.3%) is small. Even so, the cost volatility in *Situation 2.b* is still 30% higher than that in **Situation 1**. And Fig. 1.10(a) shows that the shipping company ends up with a higher total bunker cost in all scenarios if the operational decisions are made in isolation. The largest cost increase in such a case can reach 0.6% which can be significant in an industry with low profit margin.

From a risk perspective, Table 1.3 and Fig. 1.10(b) also show that the CVaR value (95%) in *Situation 2.b* is 0.5% higher than in **Situation 1**. Therefore, although the consequences caused by the ignorance in the operational decision-making are not as severe as the ones witnessed in *Situation 2.a*, it is still problematic for the shipping company since they will face a higher risk in the extreme cases.

By looking into the experimental results in detail, we have learned that although the amounts of forward-fuels bought in *Situation 2.b* are the same as the "optimal" amounts in **Situation 1**, the sailing choices (leg option or speed) in the scenarios with a higher total cost are "incorrect" because they are made without taking the forward contract into consideration.

To further illustrate, we present the detailed sailing operations under **Situation 1** and *Situation 2.b* for two particular scenarios, scenario No.34 and scenario No.41, in Figure. 1.11. Only the differences in sailing behaviors of the two situations are shown here, more details can be found in the Appendix 1.1. For scenario No.34 in Fig. 1.11(a), *Situation 2.b* makes incorrect leg option choices on both Leg 3 and Leg 4 which are unnecessarily "aggressive" compared

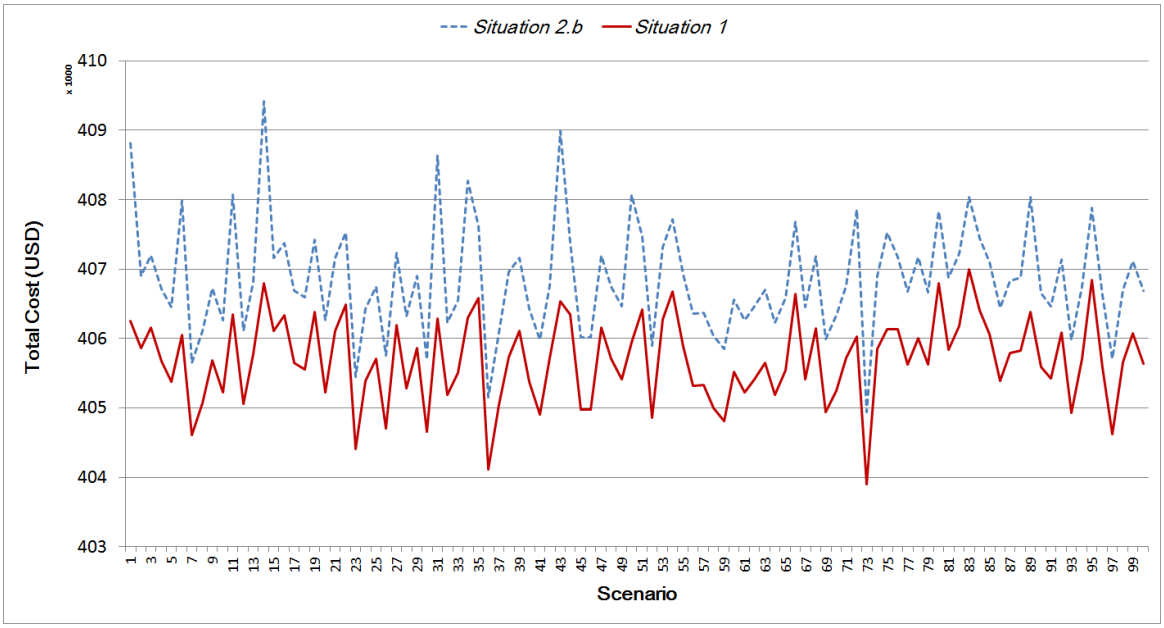

(a) Total cost comparisons across all scenarios for Situation 1 and Situation 2.b

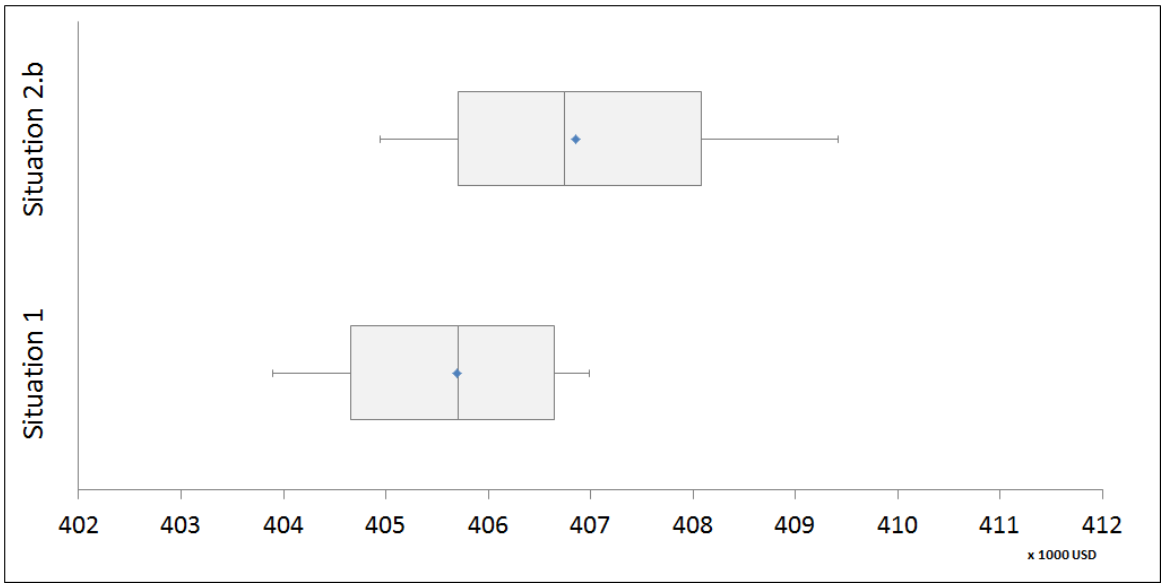

(b) Box plot for cost comparisons between Situation 1 and Situation 2.b

Figure 1.10: Comparison between Situation 1 and Situation 2.b

to the optimal ones, i.e., with less SECA involvement but longer total sailing distance. In addition, a larger speed difference when sailing in and out of SECA is also seen on Leg 4 under *Situation 2.b*. For scenario No.41 in Fig. 1.11(b), although the same leg option is chosen for Leg 4 in both situations, an unnecessarily "conservative" speed combination, i.e., small speed difference in and out of SECA, is used in *Situation 2.b* which also results in a higher total cost.

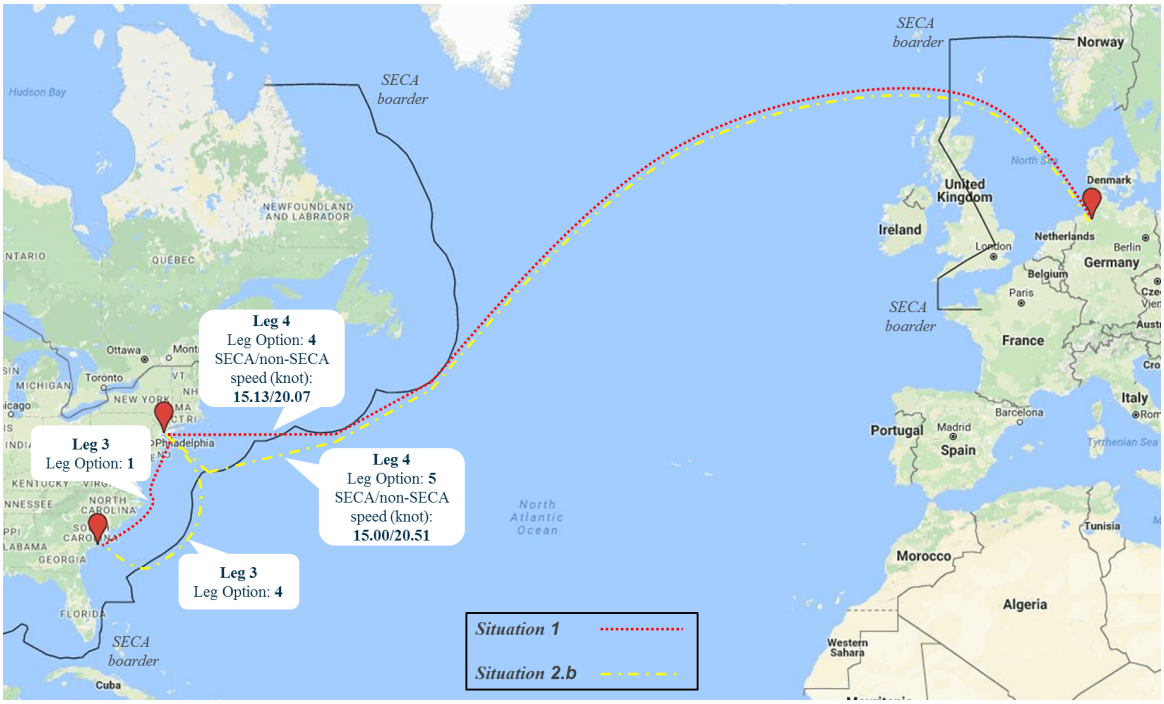

(a) Different sailing behaviors between Situation 1 and Situation 2.b in Scenario No.34

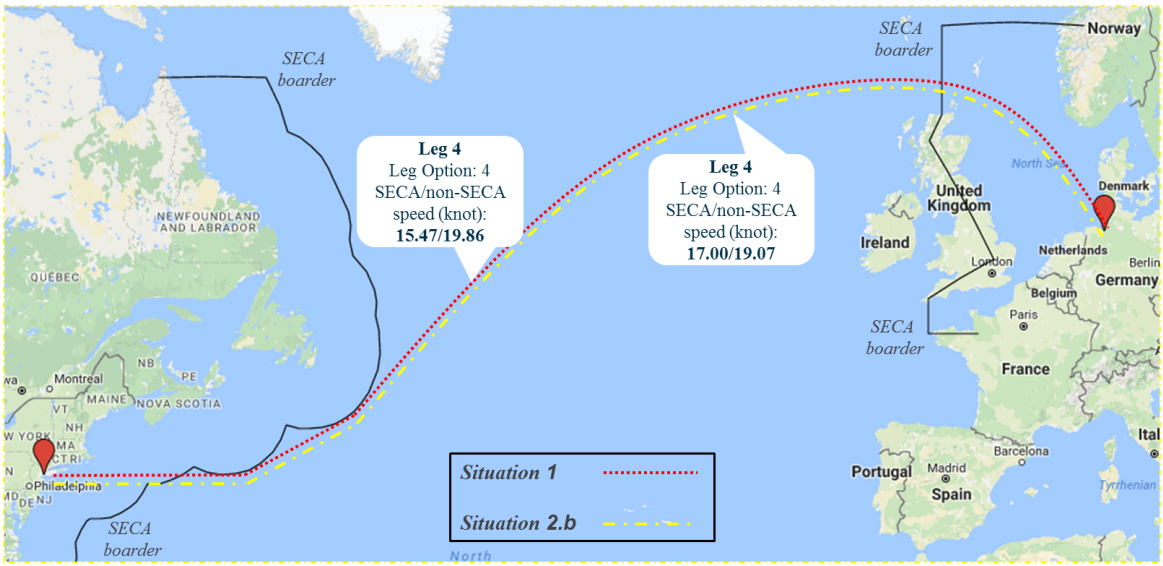

(b) Different sailing behaviors between Situation 1 and Situation 2.b in Scenario No.41

Figure 1.11: Comparison between Situation 1 and Situation 2.b

Comparison between Situation 1 and Situation 2.c

The results from comparing **Situation 1** and *Situation 2.c* are also shown with a box plot in Fig. 1.12. Recall that in *Situation 2.c*, the tactical forward-fuels purchasing decisions are made in isolation and thus assume "traditional" sailing patterns. The amounts of forward-fuels

bought are therefore the same as in *Situation 2.a*, while the operation team actually optimizes its sailings based on both SECA consideration and the "traditional" (and incorrect) forward-fuel amounts purchased.

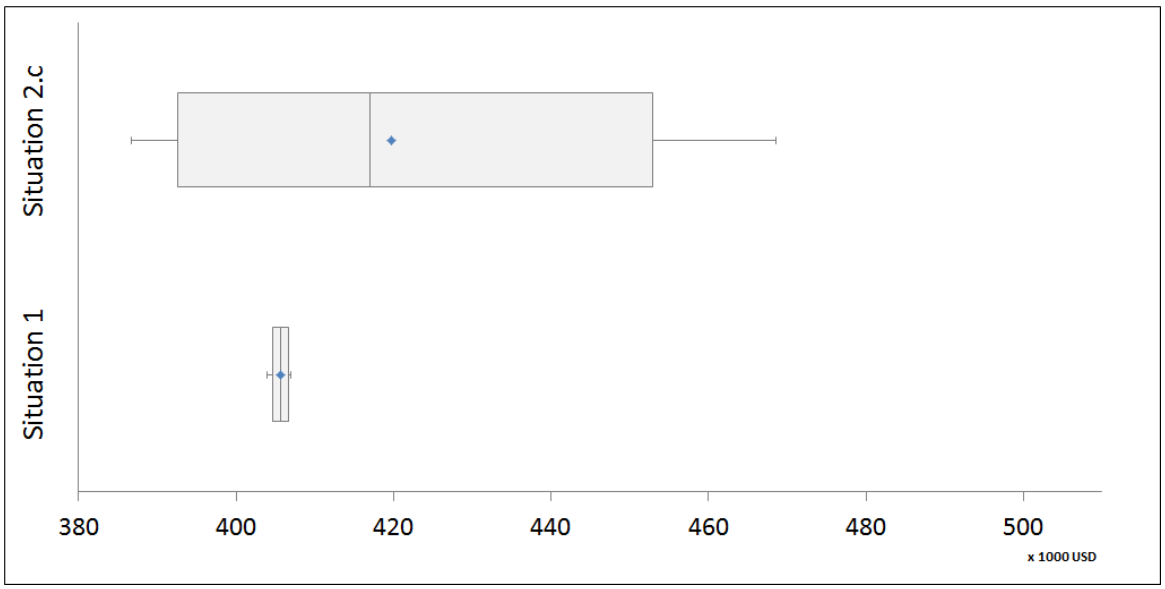

Figure 1.12: Box plot of comparison between Situation 1 and Situation 2.c

From Fig. 1.12 and Table 1.3, we can see that the expected total costs in *Situation 2.c* are 3.5% higher than that in **Situation 1**, while the standard deviation is 28.2 times higher. The CVaR value under 95% confidence level in *Situation 2.c* is also 13.4% higher than that in **Situation 1**.

Other remarks on the comparison of situations

From Table 1.3, we see that although the operation team optimizes its sailings, taking the tactical decisions (forward contract) already made into consideration in *Situation 2.c*, its performance, in terms of both expected total costs and volatility, is still as bad as *Situation 2.a*. This is mainly due to the fact that the shipping company made their first-stage tactical decisions in isolation. This led to significant mistakes regarding the contracted amounts of both forward-fuels (too much MGO and too little HFO bought), which dramatically decreased the operational flexibility in the second stage. After that, not much can be done by the operation team to remedy this mistake. In fact, the operation team in *Situation 2.c* usually has to take a more "conservative" sailing pattern due to the excess MGO and insufficient HFO purchased in the forward contracts, which resembles the traditional behavior before the introduction of SECA regulations – sailing the shortest distance. Whereas in **Situation 1**, the operation team can carry out a more "aggressive" sailing pattern (less SECA involvement but longer total distance), which is proved to be more cost-efficient if supported with better forward-fuel purchasing decisions.

Furthermore, when comparing *Situation 2.b* and *Situation 2.a*, one may notice that as long as the tactical decisions in MFM are made with integration, the consequences brought by the isolation of operational decision-making are much less critical. However, if operating under *Situation 2.b*, the shipping company still has to face increased cost volatility and risk compared to the optimal case, which means isolated decision-making in operation is still problematic and should be avoided.

1.6 Conclusion

Maritime fuel management is one of the most important issues in the shipping industry. It involves decision-making on both tactical level (forward-fuel procurement) and operational level (routing and speed). These two levels are usually treated separately in the literature as well as in the industry. After the latest SECA regulation came into force, the complexity of MFM increased dramatically. The new challenges include not only the involvement of the expensive MGO required for the voyages inside SECA, but also the possible changes in sailing behavior induced by the price gap between MGO and the traditional bunker HFO which can still be used outside SECA. Therefore we study the MFM problem with a new integrated point of view.

In this paper, we have proposed a stochastic programming model integrating the tactical and operational levels of MFM, taking uncertain fuel prices and SECA into account. We utilize the model to explore how the tactical and operational decisions in the problem interact. Through a computational study we have pointed out that the tactical and operational levels in MFM do affect and interact with each other. Isolated decision-making on either tactical or operational level in MFM will lead to various problems such as higher expected total costs, higher cost volatility and higher risk. However, the most critical situation is when tactical decisions are made in isolation. Therefore, it is important for the shipping company to have an integrated approach to MFM in light of SECA. Such an integrated view is standard in most businesses, but was not necessary in MFM before the introduction of SECA.

This work has two major contributions. Firstly, it fills a gap in the present literature, where only very few studies include and integrate both tactical and operational considerations in MFM. Secondly, it demonstrates that tactical and operational decisions must be integrated in MFM after SECA regulations were introduced, and shows the consequences for a company if the integration does not happen.

Appendix 1.1

In this appendix, all the detailed information about the sailing patterns under **Situation 1** and *Situation 2.b* in scenario No.34 and No.41 are offered in Table 1.4 and Table 1.5 respectively.

Table 1.4: Fuel consumption and sailing pattern in the scenario No.34

Scenario No.34	*Situation 1*	*Situation 2.b*
Leg 1		
Leg Option	5	5
SECA/non-SECA/*Total* distance (nautical mile)	408/1062/*1470*	408/1062/*1470*
SECA/non-SECA speed (knot)	15.00/15.00	15.00/15.00
Leg 2		
Leg Option	5	5
SECA/non-SECA/*Total* distance (nautical mile)	397/1241/*1638*	397/1241/*1638*
SECA/non-SECA speed (knot)	15.00/15.00	15.00/15.00
Leg 3		
Leg Option	**1**	**4**
SECA/non-SECA/*Total* distance (nautical mile)	**632/0/*632***	**443/515/*958***
SECA/non-SECA speed (knot)	15.00/15.00	15.00/15.00
Leg 4		
Leg Option	**4**	**5**
SECA/non-SECA/*Total* distance (nautical mile)	**899/2652/*3551***	**752/2903/*3655***
SECA/non-SECA speed (knot)	**15.13/20.07**	**15.00/20.51**
Leg 5		
Leg Option	5	5
SECA/non-SECA/*Total* distance (nautical mile)	751/3428/*4179*	751/3428/*4179*
SECA/non-SECA speed (knot)	15.00/18.09	15.00/18.09
Total SECA distance (nautical mile)	3087	2751
Total non-SECA distance (nautical mile)	8383	9149
MGO consumption (tonne)	455	405
HFO consumption (tonne)	1450	1589
Total costs (USD)	389151	398456

Table 1.5: Fuel consumption and sailing pattern in the scenario No.41

Scenario No.41	*Situation 1*	*Situation 2.b*
Leg 1		
Leg Option	4	4
SECA/non-SECA/*Total* distance (nautical mile)	469/905/*1374*	469/905/*1374*
SECA/non-SECA speed (knot)	15.00/15.00	15.00/15.00
Leg 2		
Leg Option	3	3
SECA/non-SECA/*Total* distance (nautical mile)	524/906/*1430*	524/906/*1430*
SECA/non-SECA speed (knot)	15.00/15.00	15.00/15.00
Leg 3		
Leg Option	1	1
SECA/non-SECA/*Total* distance (nautical mile)	632/0/*632*	632/0/*632*
SECA/non-SECA speed (knot)	15.00/15.00	15.00/15.00
Leg 4		
Leg Option	4	4
SECA/non-SECA/*Total* distance (nautical mile)	899/2652/*3551*	899/2652/*3551*
SECA/non-SECA speed (knot)	**15.47/19.86**	**17.00/19.07**
Leg 5		
Leg Option	5	5
SECA/non-SECA/*Total* distance (nautical mile)	751/3428/*4179*	751/3428/*4179*
SECA/non-SECA speed (knot)	15.00/18.09	15.00/18.09
Total SECA distance (nautical mile)	3275	3275
Total non-SECA distance (nautical mile)	7891	7891
MGO consumption (tonne)	497	482
HFO consumption (tonne)	1348	1379
Total costs (USD)	385773	387047

Chapter 2

The Impact of Bunker Risk Management on CO_2 Emissions in Maritime Transportation Under ECA Regulation

Published at: Sustainable Logistics and Transportation, Springer, 2018

Yewen Gu[1], Stein W. Wallace[1], Xin Wang[2]

[1]Department of Business and Management Science, Norwegian School of Economics, Bergen, Norway
[2]Department of Industrial Economics and Technology Management, Norwegian University of Science and Technology, Trondheim, Norway

Abstract

The shipping industry carries over 90 percent of the world's trade, and is hence a major contributor to CO_2 and other airborne emissions. As a global effort to reduce air pollution from ships, the implementation of the ECA (Emission Control Areas) regulations has given rise to the wide usage of cleaner fuels. This has led to an increased emphasis on the management and risk control of maritime fuel costs for many shipping companies. In this paper, we provide a novel view on the relationship between bunker risk management and CO_2 emissions. In particular, we investigate how different actions taken in bunker risk management, based on different risk aversions and fuel hedging strategies, impact a shipping company's CO_2 emissions. We use a stochastic programming model and perform various comparison tests in a case study based on a major liner company. Our results show that a shipping company's risk attitude on bunker costs have impacts on its CO_2 emissions. We also demonstrate that, by properly designing its hedging strategies, a shipping company can sometimes achieve noticeable CO_2 reduction with little financial sacrifice.

Keywords: Bunker risk management, Maritime fuel management, CO_2 emissions, Stochastic programming, ECA, Fuel hedging, Sailing behavior

2.1 Introduction

Maritime transport is one of the most important freight transportation modes in the world, since it is by far the most cost effective alternative for transporting large-volume goods between continents. In 2015, more than 90 percent of global trade is carried by sea (ICS, 2017), therefore the shipping industry plays a vital role in the world economy.

Due to the enormous amount of marine fuel consumed by the world fleet, the maritime sector is one of the biggest sources of CO_2 emissions among all transportation industries. International shipping emits approximately 2.2% of the world's anthropogenic CO_2 emissions. This number may further increase to 17% by 2050 if no effective control measure is applied (Cames et al., 2015). On the other hand, fuel cost is the major cost driver in the shipping industry. It is therefore critical for a shipping company to manage its bunker purchasing and consumption properly. In practice, fuel prices are highly volatile which could bring considerable risks. Bunker risk management is then commonly applied by shipping companies in order to control the risk brought by the high volatility of the fuel cost. For example, risk measures such as CVaR (Conditional Value at Risk) from the field of financial portfolio management may be used to represent a shipping company's risk aversion. Fuel hedging is also one of the popular risk control approaches in the shipping industry. As a contractual tool, it allows the shipping company to reduce its exposure to fuel risk by establishing a fixed or capped cost for its future fuel consumption.

On the other hand, fuel cost is the major cost driver in the shipping industry. It is therefore critical for a shipping company to manage its bunker purchasing and consumption properly. In practice, fuel prices are highly volatile which could bring considerable risks. Bunker risk management is then commonly applied by shipping companies in order to control the risk brought by the high volatility of the fuel cost. For example, risk measures such as CVaR (Conditional Value at Risk) from the field of financial portfolio management may be used to represent a shipping company's risk aversion. Fuel hedging is also one of the popular risk control approaches in the shipping industry. As a contractual tool, it allows the shipping company to reduce its exposure to fuel risk by establishing a fixed or capped cost for its future fuel consumption.

In Gu et al. (2018b), a Maritime Fuel Management (MFM) problem that combines tactical fuel hedging and operational ship routing and speed optimization is introduced, which aims to minimize a shipping company's expected total fuel costs based on its risk attitude. Using a case study, the authors show that the integration of the tactical and operational levels of MFM is vital for a shipping company after the implementation of Emission Control Areas (ECA) which regulate sulfur emissions. In this study, the same mathematical model and a similar case are used, but we focus on the impact of a shipping company's bunker risk management on its fleet's CO_2 emissions.

As individual research topics, both CO_2 emissions and bunker risk management have been intensively studied in the maritime transportation literature. Regarding CO_2 emissions, many studies focus on the relationship between speed reduction, also known as slow steaming, and emission reduction. Corbett et al. (2009) evaluate whether speed reduction is a cost-effective option to mitigate CO_2 emissions for ships calling on US ports. Cariou (2011) examines the break-even price of the maritime bunker at which the slow steaming strategy and the corresponding CO_2 emissions reduction are sustainable in the long run. Lindstad et al. (2011) investigate the impacts of slow steaming on CO_2 emissions and costs in maritime transport. They show that the emissions of CO_2 can be decreased by 19% with a negative abatement cost and by 28% at a zero abatement cost if a proper slow steaming strategy is applied. Maloni et al. (2013) show that under current conditions, extra slow steaming can achieve substantial reductions in both total cost and CO_2 emissions. Tai and Lin (2013) compare the unit

CO_2 emissions in the cases when daily frequency or slow steaming strategies is applied in international container shipping on Far East-Europe routes. Wong et al. (2015) generalize the traditional discrete cost-based decision support model in slow steaming maritime operations into novel continuous utility-based models which balance fuel consumption, carbon emission and service quality. Another research direction on CO_2 reduction in maritime transportation is green ship routing and scheduling. It extends the traditional ship routing and scheduling problems and integrates environmental concerns. Related studies can be found in, for instance, Qi and Song (2012), Kontovas (2014) and De et al. (2016).

As regards bunker risk management, fuel hedging is the most commonly used instrument in maritime transportation. Menachof and Dicer (2001) argue that the bunker surcharges widely applied in liner shipping can be eliminated and replaced by the utilization of oil commodity futures contracts. The hedging effectiveness of futures contracts among different fuel commodities is examined and compared in Alizadeh et al. (2004). Wang and Teo (2013) offer a comprehensive review of all the fuel hedging instruments available on the market and integrate fuel hedging into the modeling of liner network planning. Pedrielli et al. (2015) propose a game theory based approach to optimize the fuel hedging contract so that the expected profit for the bunker supplier and the expected refueling cost for the shipping company are maximized and minimized, respectively.

To the best of our knowledge, none of the studies in the literature has explored the relationship between bunker risk management and CO_2 emissions in maritime transportation. Such a gap in knowledge is, to a certain degree, expected as the former had no impact on the latter in the past. This is because in most circumstances, the sailing pattern of the fleet (and hence its CO_2 emissions) is relatively fixed and irrelevant to the shipping company's bunker risk management, i.e., the shortest path and the slowest possible speed is usually chosen during the whole voyage, no matter what actions are taken in terms of the company's bunker risk management, such as the amounts of marine fuel hedged.

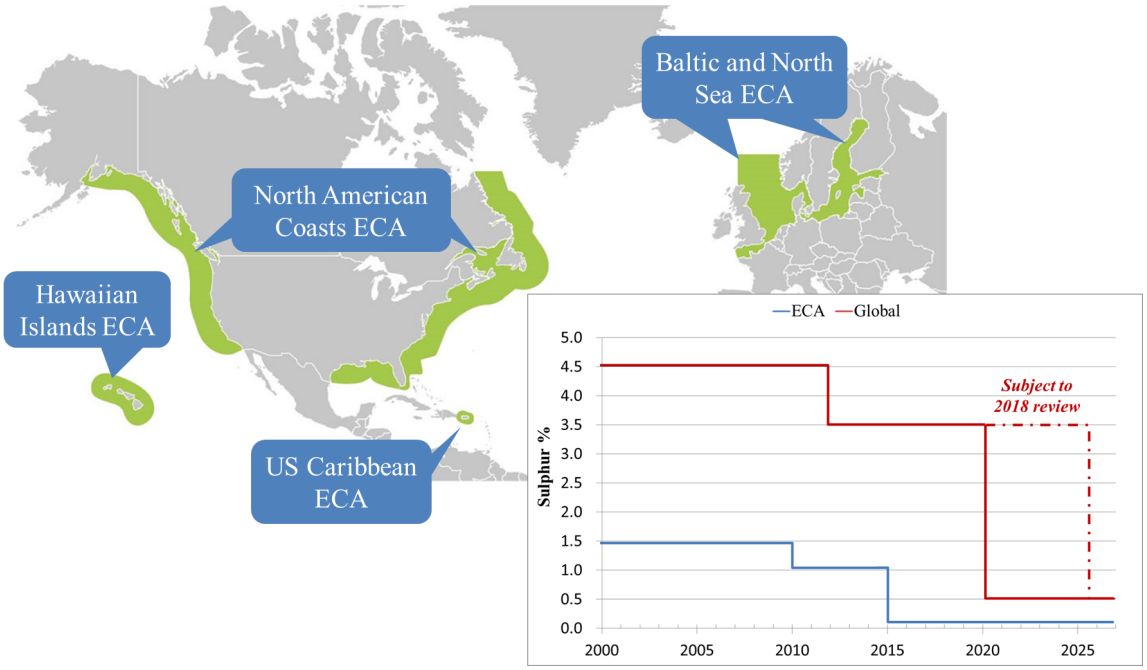

Figure 2.1: Map and requirements of the Emission Control Areas.

However, things have changed significantly in the shipping industry during the last decade due to the implementation of the ECA regulation. It is a regional sulfur emission control regulation that restricts the maximum sulfur content in the marine bunker burnt inside the regulated areas, see Fig. 2.1. The ECA regulation has forced the shipping companies, who

has not invested in sulfur emission reduction technologies (scrubber system or liquefied natural gas powered propulsion), to switch their fuels from the traditional heavy fuel oil (HFO) to the expensive marine gasoline oil (MGO) when their vessels navigate inside ECA.

One of the consequences of the ECA regulation and the substantial price difference between MGO and HFO is that the shipping companies no longer necessarily operate their fleet in the old-fashioned "shortest and slowest possible" way. They now have the motivation to change the sailing behavior of the vessels, so as to minimize the total bunker cost and simultaneously comply with the ECA regulation. Two types of potential change in sailing behavior, namely speed differentiation and ECA-evasion, are shown in Doudnikoff and Lacoste (2014) and Fagerholt et al. (2015). We illustrate these two types of sailing behavior change in Fig. 2.2. First, in order to reduce the consumption of MGO, a ship may choose to use different speeds inside and outside ECA, as shown in Fig. 2.2a, if the voyage involves both regulated and unregulated sea areas. Second, a vessel may make a detour so that the sailing distance inside ECA, and hence its MGO consumption, can be considerably decreased, see for example Fig. 2.2b. However, to what extent the speed differentiation and ECA-evasion strategies will be applied depends on the price difference between MGO and HFO. For example, if the price difference increases, so will the incentive to reduce MGO consumption, in which case sailing a route with lower ECA involvement may be more beneficial.

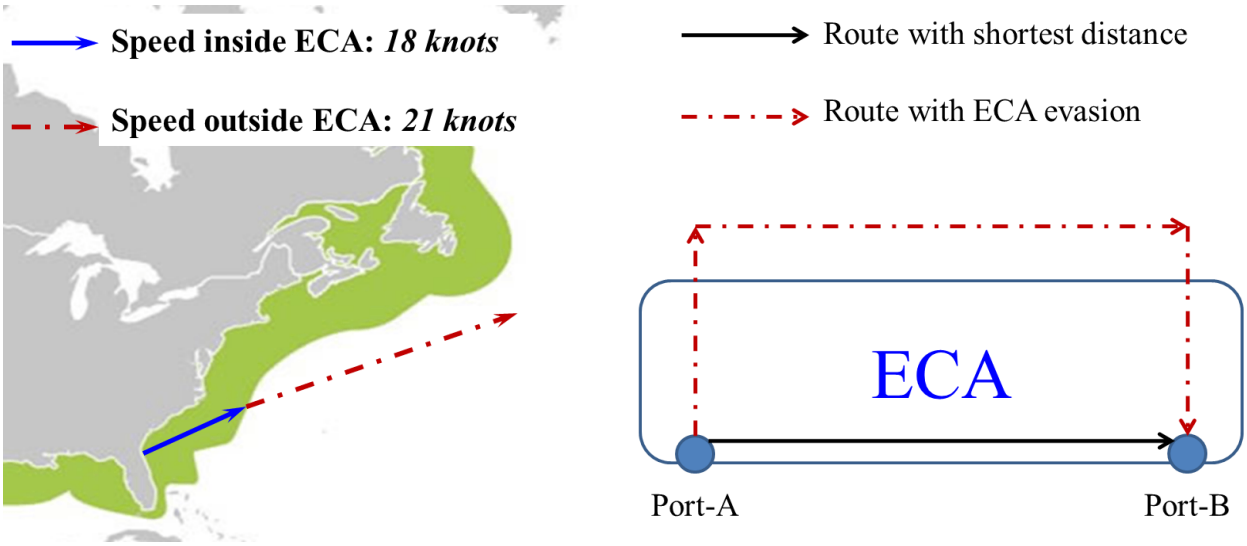

(a) Speed differentiation

(b) ECA-evasion

Figure 2.2: Two types of sailing behavior change after the implementation of ECA regulation.

A vessel's CO_2 emissions mainly depend on its fuel consumption. The CO_2 emission factors we use in this paper for MGO and HFO are 3.082 (tonnes/tonne fuel) and 3.021 (tonnes/tonne fuel), respectively (Psaraftis and Kontovas, 2009). Therefore, it is the total amount of the two fuels consumed that affects the CO_2 emissions the most, rather than the different combination of the two. Fuel consumption is further determined by the vessel's sailing speed and traveling distance. After the introduction of ECA, the shipping company's optimal speed and routing choices, which may include speed differentiation and ECA evasion, also depend on the prices of the two fuels and the associated hedging decisions made (Gu et al., 2018b). In this paper, we seek to investigate how different actions taken in bunker risk management, including different settings of risk aversion and fuel hedging strategies, impact the shipping company's optimal speed and routing choices and the corresponding CO_2 emissions.

We use the stochastic programming model introduced in Gu et al. (2018b), and propose various comparison tests based on different levels of risk aversion, fuel hedging strategies and fuel prices. The tests are performed on a case based on a real liner service offered by Walle-

nius Wilhelmsen Logistics (WWL), one of the world's largest liner service providers for rolling equipment. We aim to provide a novel view on the relationship between bunker risk management and CO_2 emissions, which would hopefully contribute to the worldwide effort in reducing greenhouse gas emissions.

The rest of the paper is structured as follows. Section 2.2 gives the description of the Maritime Fuel Management (MFM) problem and the mathematical model. In Sect. 2.3 we introduce the test case and the scenario generation process. Section 2.4 presents the results of our computational study. Our conclusion is given in Sect. 2.5.

2.2 The problem and mathematical model

The problem description and the mathematical formulation are given in this section. In Sect. 2.2.1, we summarize the settings and assumptions of the problem. The mathematical formulation is then presented in Sect. 2.2.2.

2.2.1 Problem statement

First, we introduce four important terms, *loop*, *leg*, *leg option* and *stretch*, which are frequently used in this paper, see Fig. 2.3 for illustration. A *loop* refers to a round trip calling several ports in a predetermined order, while a *leg* refers to the voyage between two consecutive ports in the loop. A *leg option* represents a possible sailing path for a leg. For different leg options of a same leg, the total sailing distance and the sailing distance inside ECA are also different. A leg option may have one or more *stretches*. When the vessel crosses the ECA border, the current stretch ends and a new one begins. We also combine the stretches of the same type (on which we assume the same speed) for every single leg option, and thus represent each leg option with only two segments: the ECA stretch and the non-ECA stretch. For example, in Fig. 3c, we combine Stretch 1 and Stretch 3 as the ECA stretch.

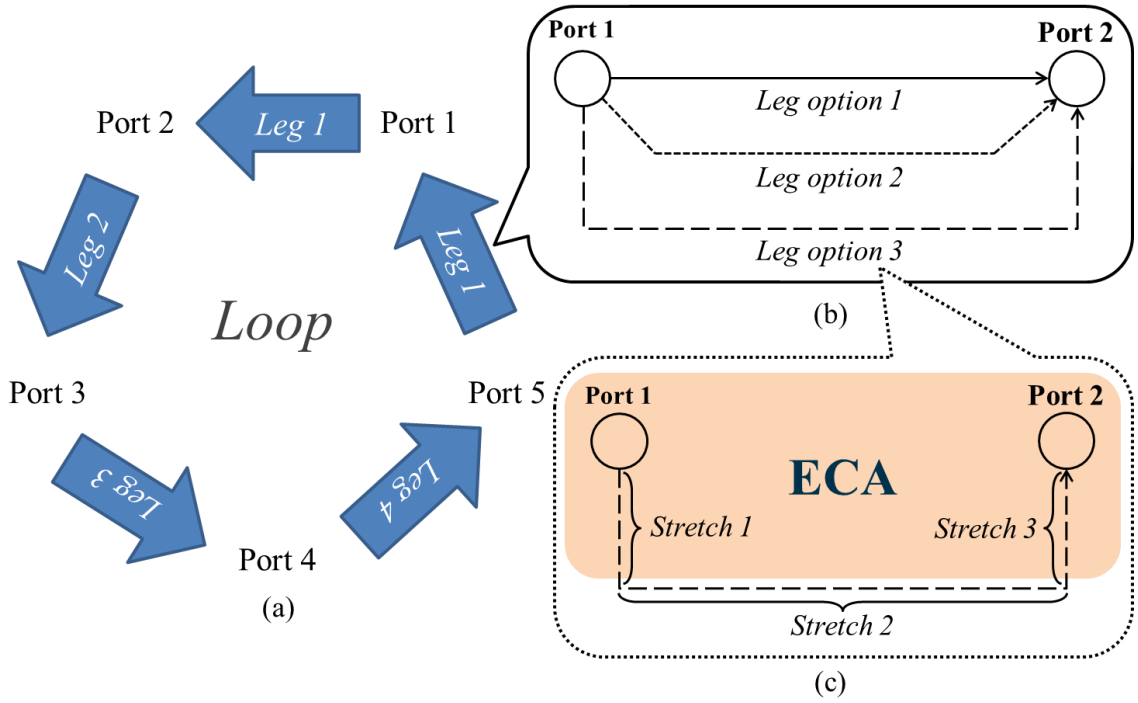

Figure 2.3: Illustration of a loop, and its associated legs, leg options and stretches.

For simplification, the MFM problem in this paper only considers one single vessel operating

on one single loop. The length of the planning period is assumed to be equal to the scheduled time for the vessel to finish a round trip on the loop. The sequence of the port calls on the loop and the related leg information, including all possible leg options for every leg and the associated stretches, are also assumed to be given as input to our model.

As an essential instrument in bunker risk management, fuel hedging reduces the fuel consumers' exposure to financial risk caused by volatile fuel prices. We consider the so called *forward-fuel contract with exit terms and physical supply* (FFC in the following) in this study. An FFC endows the shipping company with the right to buy a specified amount of a certain type of fuel with a predetermined price during an agreed time period. The forward price of a certain fuel in the FFC is normally higher than this fuel's expected price during the contract period. We assume this to be the case in our tests as well, and as a result, a risk-averse shipping company can, and normally will, use FFC for risk control purposes, while a risk-neutral one never enters the forward market due to the expected loss. However, if the shipping realizes that the remaining fuel in the ongoing FFC is no longer needed and decides to terminate the contract, the leftovers are sold back to the fuel supplier with a penalty.

The spot prices for MGO and HFO fuels during the planning period are assumed to be stochastic, and the MFM problem can be described using a two-stage model with scenarios representing the stochastics. In the first stage, decisions with respect to the amounts of MGO and HFO to be hedged in an FFC must be made at the beginning of the planning period. The spot prices of the two fuels in different scenarios are then realized in the second stage and are assumed to remain constant during the whole planning period. Several operational decisions will be made afterwards based on the realized fuel prices and the first-stage hedging decisions. These second-stage decisions are made of two major parts. The first consists of speed and routing choices on each leg. The second part consists of fuel allocation decisions, i.e. how much spot- and forward-fuels should be used during operations. The objective of the MFM problem is to minimize the total bunker cost which is the sum of the first-stage purchasing costs of the forward fuels and the expected second-stage costs on spot fuels and penalties for unused forward fuels, meanwhile control the bunker cost risk within a desirable level.

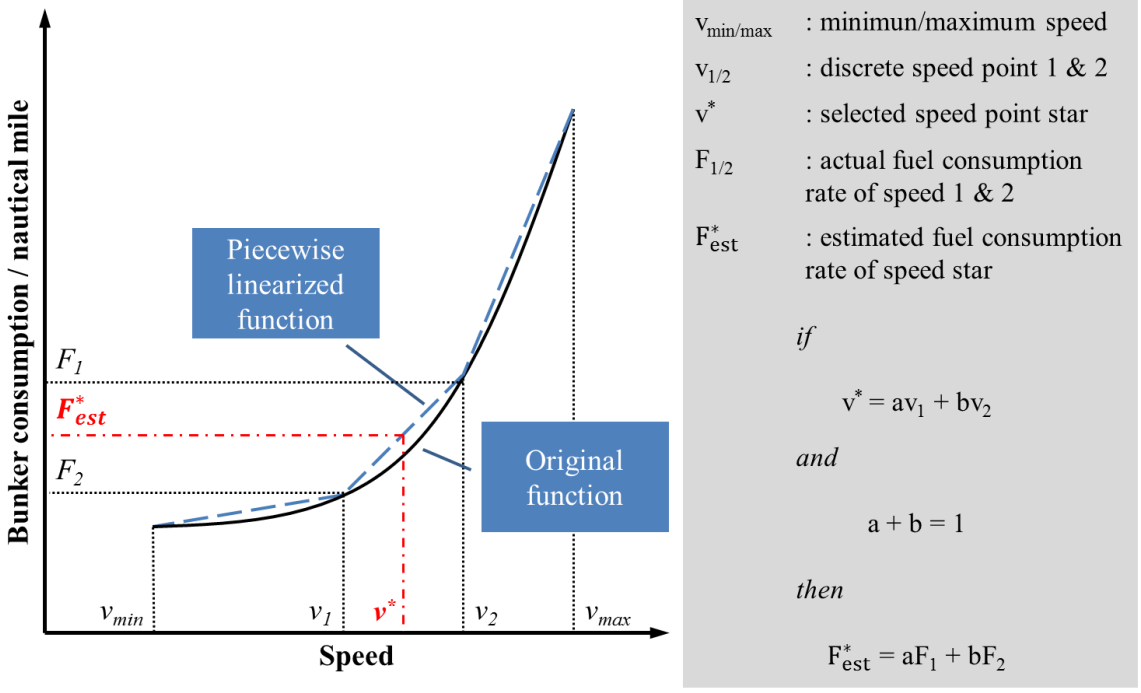

Figure 2.4: Piecewise linearisation of the fuel consumption function.

The relationship between a vessel's sailing speed and its fuel consumption per unit distance

is normally considered as a quadratic function (Norstad et al., 2011). We use a piecewise linearisation approach (Andersson et al., 2015) to approximate the fuel consumption rate for different sailing speeds, as shown in Fig. 2.4. Note that an overestimation is expected in the application of this approach (see Andersson et al. for detailed discussion), but it is normally insignificant as long as sufficient discrete speed points are used. A good estimation of the relation between speed and traveling time can also be made using this approach.

As part of the risk control measures for bunker risk management, we model the risk attitude of the shipping company using a Conditional Value-at-Risk (CVaR) approach, which is extensively used in the field of financial risk management to evaluate various risks. The standard expression of CVaR with a discrete probability distribution can be expressed as follows:

$$\mathrm{CVaR}_\gamma(\phi) = \frac{1}{1-\gamma} \sum_{s:f(\phi,\delta_s)\geq \mathrm{VaR}_\gamma(\phi)} p_s f(\phi, \delta_s) \tag{2.1}$$

In (2.1) ϕ are the decision variables, γ refers to the confidence level, $f(\phi, \delta_s)$ refers to the cost or loss function whose risk (expected value in the worst cases) needs to be controlled, δ are the random variables while δ_s represent the realization of the random variables in scenario s and p_s refers to the probability of scenario s. According to the definition of CVaR, only the scenarios in which the cost is larger than the VaR (value-at-risk) value ($s : f(\phi, \delta_s) \geq \mathrm{VaR}_\gamma(\phi)$) need to be accumulated for the calculation of CVaR. Since the expression of CVaR explicitly involves the VaR function, it becomes difficult to work with due to the non-linearity. Therefore, it is common to use its equivalent auxiliary alternative (Rockafellar and Uryasev, 2002):

$$\mathrm{CVaR}_\gamma(\phi, \alpha) = \alpha + \frac{1}{1-\gamma} \sum_{s:f(\phi,\delta_s)\geq \alpha} p_s[f(\phi, \delta_s) - \alpha] \tag{2.2}$$

$$\mathrm{CVaR}_\gamma(\phi, \alpha) = \alpha + \frac{1}{1-\gamma} \sum_{s\in S} p_s[f(\phi, \delta_s) - \alpha]^+ \tag{2.3}$$

Note that the VaR function in (2.1) is replaced by the artificial variable α in (2.2). Moreover, the expression of CVaR is further simplified to (2.3) through the $[\quad]^+$ operator which produces non-negative results.

In our model, we impose CVaR constraints on the total bunker costs to achieve the desired risk control effect. Two key parameters, a confidence level and a maximum tolerable CVaR value, are defined and used as inputs for our model. For instance, if the confidence level and the maximum CVaR value are set to 95% and 1.2 million USD, respectively, the CVaR constraints will then ensure that the expected total bunker costs in the worst 5% cases will not exceed 1.2 million USD during the planning period.

2.2.2 Mathematical formulation

The mathematical formulation is presented as follows:

Sets

J	Set of sailing legs along the loop
R_j	Set of leg options for Leg j
V	Set of feasible discrete speed points for the ship

S Set of scenarios

Parameters

P^{MGO-F} Price per ton of MGO agreed in the forward-fuel contract

P^{HFO-F} Price per ton of HFO agreed in the forward-fuel contract

P_s^{MGO-S} Price per ton of MGO on spot market under Scenario s

P_s^{HFO-S} Price per ton of HFO on spot market under Scenario s

P^{MGO-P} Penalty per ton for the unused MGO left in the forward-fuel contract

P^{HFO-P} Penalty per ton for the unused HFO left in the forward-fuel contract

$\overline{W}_j$ Latest starting time for Leg j

W_j^S Service time for Leg j in the departing port

W_{jrv}^{ECA} Sailing time on ECA stretches on Leg j under Leg option r with Speed v

W_{jrv}^{N} Sailing time on non-ECA stretches on Leg j under Leg option r with Speed v

D_{jr}^{ECA} Sailing distance on ECA stretches on Leg j under Leg option r

D_{jr}^{N} Sailing distance on non-ECA stretches on Leg j under Leg option r

F_v Fuel consumption per unit distance sailed with speed alternative v (same for both HFO and MGO)

p_s Probability of scenario s taking place

γ Confidence level applied in CVaR

A_γ The maximum tolerable CVaR value under confidence level γ

Decision variables

x_{jrvs}^{ECA} Weight of speed choice v used on ECA stretches on Leg j with Leg option r under scenario s

x_{jrvs}^{N} Weight of speed choice v used on non-ECA stretches on Leg j with Leg option r under scenario s

y_{jrs} Binary variables representing the decisions on route selection, equal to 1 if Leg option r is sailed on Leg j under scenario s, and 0 otherwise

z_{js}^{MGO-S} Amount of MGO from spot market used on Leg j under scenario s

z_{js}^{MGO-F} Amount of MGO from forward contract used on Leg j under scenario s

z_{js}^{HFO-S} Amount of HFO from spot market used on Leg j under scenario s

z_{js}^{HFO-F} Amount of HFO from forward contract used on Leg j under scenario s

u_s^{MGO-F} Amount of unused forward MGO left at the end of the planning period under scenario s

u_s^{HFO-F} Amount of unused forward HFO left at the end of the planning period under scenario s

m^{MGO-F} Agreed amount of MGO in the forward contract

m^{HFO-F} Agreed amount of HFO in the forward contract

α Artificial variable for CVaR constraints

h_s Artificial variables for CVaR constraints under scenario s

The mathematical formulation of the model starts here:

$$\begin{aligned}\min \quad & P^{MGO-F}m^{MGO-F} + P^{HFO-F}m^{HFO-F} \\ & + \sum_{s\in S} p_s \Bigg\{ \sum_{j\in J} \left(P_s^{MGO-S} z_{js}^{MGO-S} + P_s^{HFO-S} z_{js}^{HFO-S}\right) \\ & -(P^{MGO-F} - P^{MGO-P})u_s^{MGO-F} - (P^{HFO-F} - P^{HFO-P})u_s^{HFO-F} \Bigg\}\end{aligned} \tag{2.4}$$

Subject to

$$\overline{W}_{j+1} \geq \overline{W}_j + W_j^S + \sum_{r\in R_j}\sum_{v\in V} \left(W_{jrv}^{ECA} x_{jrvs}^{ECA} + W_{jrv}^{N} x_{jrvs}^{N}\right) \qquad s \in S, j \in J \tag{2.5}$$

$$\sum_{v\in V} x_{jrvs}^{ECA} = y_{jrs} \qquad s \in S, j \in J, r \in R_j \tag{2.6}$$

$$\sum_{v\in V} x_{jrvs}^{N} = y_{jrs} \qquad s \in S, j \in J, r \in R_j \tag{2.7}$$

$$\sum_{r\in R_j} y_{jrs} = 1 \qquad s \in S, j \in J \tag{2.8}$$

$$z_{js}^{MGO-F} + z_{js}^{MGO-S} = \sum_{r\in R_j}\sum_{v\in V} F_v D_{jr}^{ECA} x_{jrvs}^{ECA} \qquad s \in S, j \in J \tag{2.9}$$

$$z_{js}^{HFO-F} + z_{js}^{HFO-S} = \sum_{r\in R_j}\sum_{v\in V} F_v D_{jr}^{N} x_{jrvs}^{N} \qquad s \in S, j \in J \tag{2.10}$$

$$\sum_{j\in J} z_{js}^{MGO-F} + u_s^{MGO-F} = m^{MGO-F} \qquad s \in S \tag{2.11}$$

$$\sum_{j\in J} z_{js}^{HFO-F} + u_s^{HFO-F} = m^{HFO-F} \qquad s \in S \tag{2.12}$$

$$y_{jrs} \in \{0,1\} \qquad s \in S, j \in J, r \in R_j \tag{2.13}$$

$$x^{ECA}_{jrvs}, x^{N}_{jrvs} \geq 0 \qquad s \in S, j \in J, r \in R_j, v \in V \tag{2.14}$$

$$z^{MGO-F}_{js}, z^{MGO-S}_{js}, z^{HFO-F}_{js}, z^{HFO-S}_{js} \geq 0 \qquad s \in S, j \in J \tag{2.15}$$

$$u^{MGO-F}_{s}, u^{HFO-F}_{s} \geq 0 \qquad s \in S \tag{2.16}$$

CVaR constraints:

$$\alpha + \frac{1}{1-\gamma} \sum_{s \in S} p_s h_s \leq A_\gamma \tag{2.17}$$

$$h_s \geq 0 \qquad s \in S \tag{2.18}$$

$$\begin{aligned} h_s \geq\ & P^{MGO-F} m^{MGO-F} + P^{HFO-F} m^{HFO-F} \\ & - (P^{MGO-F} - P^{MGO-P}) u^{MGO-F}_s - (P^{HFO-F} - P^{HFO-P}) u^{HFO-F}_s \\ & + \sum_{j \in J} \left(P^{MGO-S}_s z^{MGO-S}_{js} + P^{HFO-S}_s z^{HFO-S}_{js} \right) - \alpha \qquad s \in S \end{aligned} \tag{2.19}$$

The objective function (2.4) minimizes the expected total bunker cost for the planning period. The purchasing costs for the stated amounts of both fuels in the FFC are given in the first line of (2.4). The second line of the objective function refers to the expected costs for the consumption of spot-fuels. The last line represents the treatment of the unused forward-fuels. At the end of the planning period, the leftovers in the FFC (if any) are sold back to the bunker supplier at "buyback" prices, computed as their contractual forward prices subtracted by a penalty.

Constraints (2.5) enforce the time constraints for all sailing legs according to the schedule. Constraints (2.6) and (2.7) connect x- and y-variables with respect to the speed-routing choices in ECA and non-ECA stretches, respectively. They ensure that the sums of the speed weights, x^{ECA}_{jrvs} and x^{N}_{jrvs} respectively for ECA and non-ECA stretches, are equal to 1 if Leg option r is chosen for Leg j in Scenario s, and 0 otherwise. Constraints (2.8) ensure that only one leg option is used on any specific leg. Constraints (2.9) and (2.10) make sure that for each scenario the sum of the spot- and forward-fuels used on each leg equals the actual fuel consumption on that leg based on the speeds and leg options chosen. Constraints (2.11) and (2.12) ensure that the forward-fuels used plus the leftovers equal the agreed amounts in the forward contract. Constraints (2.13) - (2.16) define the domains of the decision variables. Constraints (2.17) - (2.19) are the CVaR constraints representing the risk attitude of the shipping company, restricting the risk on the total bunker costs to be within an acceptable level. Constraint (2.17) ensures that the actual CVaR value during the optimization will not exceed the desired risk level (A_γ). On the other hand, the $[\quad]^+$ operator in (2.3) is replaced by the artificial variables h_s and Constraints (2.18) - (2.19) for optimization purpose.

It is important to notice that the CO_2 emissions are not directly considered in the formulation. Instead, they can be calculated based on the optimal solutions obtained using the CO_2 emission factors for the two fuels (see Sect. 2.1), 3.082 (tonnes/tonne fuel) and

3.021 (tonnes/tonne fuel) for MGO and HFO, respectively. More details will be discussed in Sect. 2.4.1.

2.3 The test case and scenario generation

In this section, we briefly describe the test case in Sect. 2.3.1, while the scenario generation process is discussed in Sect. 2.3.2.

2.3.1 The test case

The case considered in this paper is based on a liner service offered by Wallenius Wilhelmsen Logistics (WWL). The company offers roll-on roll-off (RoRo) services for transporting cars, trucks and other types of rolling equipment. In our case, the service loop and its corresponding schedule are adapted from one of WWL's Europe-Americas trade lanes. The sequence of the port calls in the loop is shown in Table 2.1. The scheduled total traveling time for a round trip on this loop is 35 days. We therefore also set the planning period to 35 days.

Table 2.1: Port visit sequence of the considered service loop

	From	To
Leg 1	Brunswick	Galveston
Leg 2	Galveston	Charleston
Leg 3	Charleston	New York
Leg 4	New York	Bremerhaven
Leg 5	Bremerhaven	Brunswick

We further assign five leg options to each leg in the case loop. Although different leg options of a specific leg share the same origin and destination ports, they differ in terms of ECA, non-ECA and total sailing distances. As an example, Fig. 2.5 illustrates all five leg options of Leg 3 (Charleston-New York), where Leg option 1 takes the shortest possible path which is completely inside ECA, and Leg option 5, on the contrary, has the least ECA sailing. The detailed information about sailing distances for each leg option of every leg is displayed in Table 2.2.

Table 2.2: Sailing distances within SECA/non-SECA for each leg option of every leg

SECA/non-SECA (nautical mile)	Option 1	Option 2	Option 3	Option 4	Option 5
Leg 1	1191/35	569/774	495/870	469/905	408/1062
Leg 2	1271/34	686/704	524/906	458/1083	397/1241
Leg 3	632/0	560/330	499/429	443/515	423/602
Leg 4	1767/1629	1379/2125	1042/2503	899/2652	752/2903
Leg 5	2393/1626	1110/2984	1013/3109	817/3337	751/3428

Additionally, the fuel consumption data we use is collected from the historical record of a real RoRo ship under normal conditions. Fig. 2.6 shows the fuel consumption per nautical mile for seven selected discrete speed points ranging from 15 to 24 knots.

2.3.2 Scenario generation

As mentioned earlier, the uncertainties considered in our problem refer to the spot prices for MGO and HFO. We assume we know their marginal distributions and the correlation between

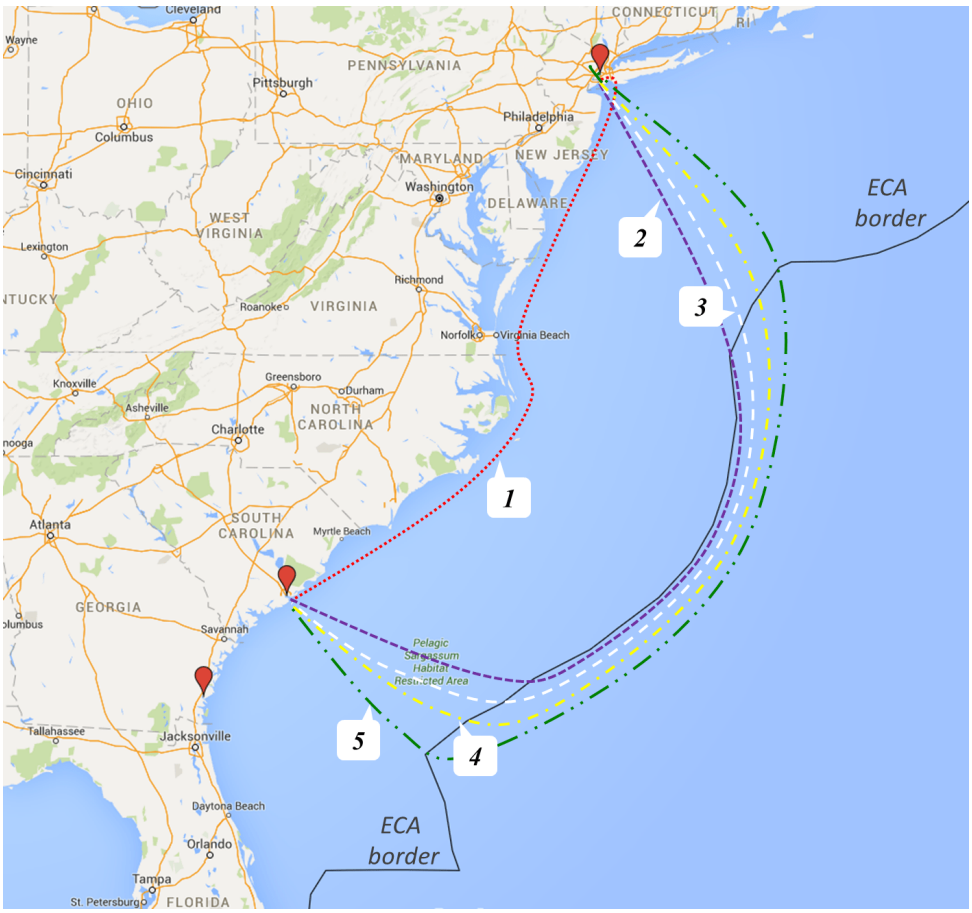

Figure 2.5: Five leg options for Leg 3 (Charleston - New York). (Google Maps, 2016)

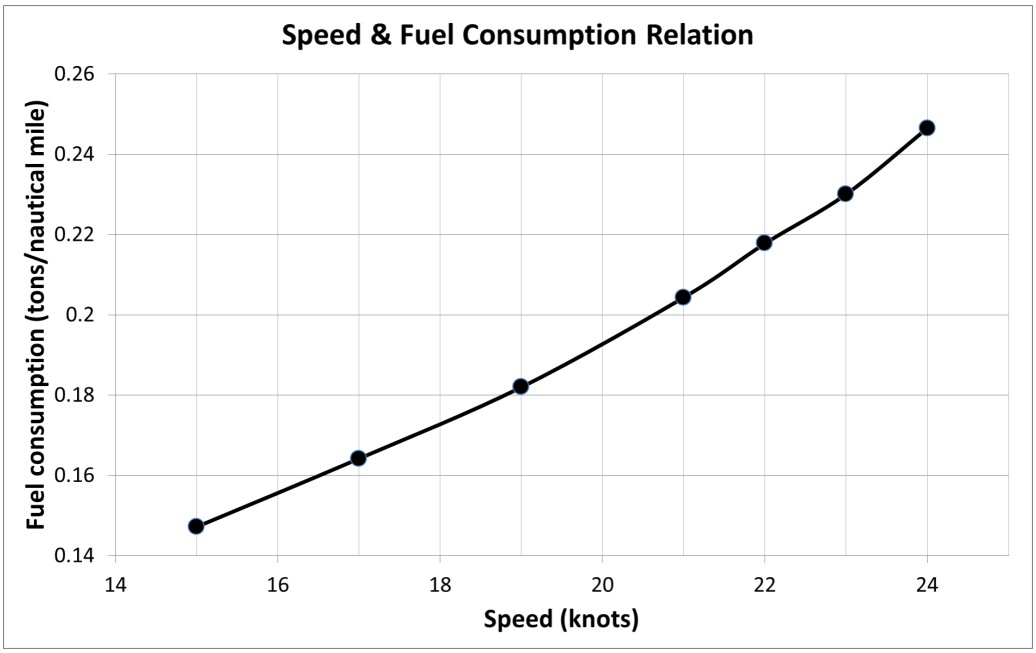

Figure 2.6: Speed and fuel consumption relation for the selected discrete speed points

them, and apply a version of the scenario-generating heuristic developed by Høyland et al. (2003) in order to generate scenarios for fuel prices. However, since fuel prices are significantly dependent over time, generating fuel prices using distributions derived from historical data directly can be problematic. For example, the generated fuel prices will not be representative if the historical data during the past booming period (e.g. 2008) is directly used in the process

of scenario generation, when the current market is actually in recession.

Therefore, we use a two-step approach to construct the scenarios for the spot-fuel prices for the next planning period. As a first step, we observe the latest fuel prices on the spot market and use them as base prices, which are also the *expected* spot prices during the planning period. Then, we generate *price increments* using the scenario generation heuristic, either positive or negative, and add them to the base prices. This approach corresponds to the special dynamic of the development of fuel price, which can be seen as a Lévy process with independent increments (Krichene, 2008; Gencer and Unal, 2012).

We use the historical data provided by Clarkson Research Services Limited (Clarkson, 2018a) to obtain an estimation of the distributions and correlation for the price increments. The data is collected from three major ports, Rotterdam, Houston and Singapore, and consists of monthly prices of the two fuels (HFO and MGO) at these ports from January 2000 to December 2015. According to the data, the price increments of HFO and MGO are positively correlated and the correlation coefficient is estimated at 0.75. Furthermore, we assume triangular distributions for the random increments. The lower limit, mode and upper limit that control the marginal distributions applied in the scenario-generating heuristic are set to (-40, 0, 40) and (-120, 0, 120) for HFO and MGO, respectively. The latest observations of the spot-fuel prices (used as base prices, or expected spot prices) are from December 2015, and the prices of HFO and MGO are 150 USD/tonne and 375 USD/tonne, respectively. Also note that in our model the forward prices are always set to be marginally higher than the corresponding expected spot prices to prevent speculation.

Finally, an in-sample stability test (Kaut and Wallace, 2007) is performed to check the reliability of the scenario generation process. By comparing the results with different scenario trees generated under the same conditions, this test checks whether the optimal objective function value has a significant dependence on the specific scenario tree used. In our case, 10 scenario trees, each with 100 scenarios, are generated. The difference among the objective values solved with all 10 scenario trees is smaller than 0.02%, which shows that the scenario generation process used in this paper is stable and reliable.

2.4 Computational study

In this section, we investigate how CO_2 emissions may be affected by a shipping company's risk attitude (Sect. 2.4.1), and its fuel hedging decisions (Sect. 2.4.2). The mathematical model in this paper is programmed in C++ with Microsoft Visual Studio. The commercial solver, CPLEX Optimization Studio V12.6.1, is called to solve the model in our tests. All computational tests are performed with an Intel Celeron 1.60 GHz CPU and 8 Gb RAM. The computational time does not exceed 1 minute for an individual test.

2.4.1 Impact of risk attitude on CO_2 emissions

In our model, the shipping company's risk attitude towards its total bunker costs, i.e. its risk aversion level, can be represented by a maximum tolerable CVaR value (A_γ) and a confidence level (γ, set to a fixed value of 95% in our study). The $A_{95\%}$ value determines an upper bound of the average total cost allowed in the worst (5%) cases. A larger $A_{95\%}$ then corresponds to a higher tolerance of extreme risk, and hence a lower risk aversion level. This allows us to use different $A_{95\%}$ values to represent the different levels of risk aversion, in order to study the impact of the company's risk attitude on its CO_2 emissions.

Effect of changing risk aversion levels

First, we assume a "standard" risk aversion level for our case study. The corresponding $A_{95\%}$ is set to 390,000 USD which is approximately 1%[1] higher than the optimal total bunker cost in a risk-neutral case, or the objective function value obtained when solving the problem without the CVaR constraints. The standard risk aversion level is then used as a benchmark for comparing the CO_2 emissions at different risk aversion levels.

We use in total 8 different $A_{95\%}$ values, ranging from 388,000 USD (extremely risk-averse) to 400,000 USD (least risk-averse). We also test the risk-neutral case which can be equivalently considered as having an enormously large $A_{95\%}$ value and the CVaR constraints are thus no longer binding. We then solve the problem with each of these $A_{95\%}$ values and observe, in each case, the optimal *fuel allocation* decisions, i.e. the forward-fuels (z_{js}^{MGO-F} and z_{js}^{HFO-F}) and spot-fuels (z_{js}^{MGO-S} and z_{js}^{HFO-S}) consumed for every scenario $s \in S$. The amount of CO_2 emitted (in tonnes) for every scenario s can then be calculated using the following formula:

$$CO_2 \ Emitted = \sum_{j \in J} \left[3.082(z_{js}^{MGO-S} + z_{js}^{MGO-F}) + 3.021(z_{js}^{HFO-S} + z_{js}^{HFO-F})\right] \tag{2.20}$$

Out of 100 scenarios, we can then find the five scenarios with the highest amounts of CO_2 emitted, and calculate their average as the worst-case CO_2 emission for each given $A_{95\%}$ value.

Table 2.3 displays the results comparing the worst-case CO_2 under different risk aversion levels ($A_{95\%}$ values). We may observe that the worst-case CO_2 emissions increase when the company lowers its risk aversion level (or accepts a higher $A_{95\%}$ value). We may also notice that the amount of CO_2 emitted stops increasing and remains at 6046 tonnes when $A_{95\%}$ is above 395,000 USD.

Table 2.3: Worst-case CO_2 emissions under different risk aversion levels

Value set for $A_{95\%}$ (maximum CVaR)									
[1000 USD]	388	389	**390***	391	392	393	395	400	Risk-neutral
%	-0.51	-0.26	**0.0**	+0.26	+0.51	+0.77	+1.28	+2.56	-
Worst-case CO_2 emitted (average of five worst scenarios out of 100)									
[tonnes]	5653	5695	**5785**	5787	5890	5930	6046	6046	6046
%	-2.28	-1.56	**0.0**	+0.03	+1.82	+2.51	+4.41	+4.41	+4.41

* Benchmark case with "standard" risk aversion.

Recall that the stochastics in our model come from the uncertain spot-fuel prices, creating risk on the total bunker costs. The introduction of CVaR constraints is therefore to contain such risk in the extreme cases. When the risk attitude is more relaxed in a shipping company's bunker risk management, i.e. with higher $A_{95\%}$, the company will have a higher willingness to take risks and rely more on the fuels from the spot market, rather than buying from the forward market. This actually allows the shipping company to operate the ship with higher flexibility in terms of more freedom to apply ECA-evasion and/or speed differentiation strategies, in order to avoid consuming the more expensive MGO. In contrast, for example, if a fair amount of MGO is already hedged, the shipping company's routing decisions may be restricted to the more traditional "shortest but more ECA involved" alternative, just to commit to the hedging contract and thus avoid paying too much penalty for unused MGO eventually. In Table 2.4, we

[1]It is feasible and reasonable to restrict the risk level to such extent in this test because the forward-fuel prices are set to be only marginally higher than the expected spot-fuel prices.

show the fuel consumption for a specific scenario (where the spot prices for MGO and HFO are 413 USD/tonne and 140 USD/tonne, respectively) under different risk aversion levels. We can see that the total fuel consumption (bottom row in Table 2.4) increases when setting a higher $A_{95\%}$, and hence the CO_2 emissions also increase (since the emission factors for MGO and HFO are practically the same). This is due to the fact that when relying more on spot fuels (at higher $A_{95\%}$) and in the light of the significant price difference between MGO and HFO, the ship is sailing more "aggressively": such as evading ECA at much as possible and sailing as slowly as possible inside ECA (see Appendix 2.1 for details). The aggressive sailing has brought down the consumption of MGO but increased HFO consumption even more, which is beneficial in terms of total bunker costs but leads to an increase in total fuel consumption and eventually more CO_2 emitted. Once the $A_{95\%}$ exceeds 395,000 USD, nevertheless, the pattern of fuel consumption for both fuels and thus the sailing behavior remain stable in the worst scenarios, since the sailing behavior in these scenarios has already been pushed to the most aggressive level. Therefore, the average CO_2 emissions in the worst scenarios remain unchanged after the $A_{95\%}$ surpasses 395,000 USD, as observed in Table 2.3.

Table 2.4: Example of fuel consumption for a particular scenario under different risk aversion levels

Value set for $A_{95\%}$ (1000 USD)	388	389	390	391	392	393	$\geq$ 395*
MGO consumption (tonnes)	482.2	473.1	455.4	454.4	435.5	426.5	404.8
HFO consumption (tonnes)	1379.4	1402.6	1449.8	1451.9	1504.5	1527.8	1588.5
Total consumption (tonnes)	1861.6	1875.7	1905.2	1906.3	1940.0	1954.2	1993.3

* Including the risk-neutral case.

It is important to notice that the above results are based on studying the *worst-case* CO_2 emissions under different risk aversion levels, which show a clear tendency that the imposition of financial risk control measures (CVaR constraints) is also, to a certain degree, able to contain the "environmental risk" (CO_2 emissions in the worst scenarios). On the other hand, the relationship between *average* CO_2 emissions and risk aversion level is more complicated, and is influenced by how much more expensive MGO is than HFO.

Influence of price gap between MGO and HFO

In our model, the base prices for MGO and HFO (see Sec. 2.3.2), 375 USD/tonne and 150 USD/tonne, respectively, refer to the spot prices observed in Dec 2015, and are used as expected spot prices for the planning period. This has lead to an Expected Spot Price Gap (ESPG in short) of 225 USD/tonne. In the following test, we aim to study how *average* CO_2 emissions change with different ESPG. This is done by altering the base price for MGO and hence the ESPG, solving the corresponding MFM problem, and observing the average amount of CO_2 emitted across all scenarios (instead of the 5-worst scenarios). We also test for two risk settings: standard risk-averse (see Sec. 2.4.1) and risk-neutral.

Table 2.5 displays the average amounts of CO_2 emitted, for both standard risk-averse and risk-neutral settings, at various ESPG ranging from 100 USD/tonne to 400 USD/tonne. The corresponding expected spot MGO ranges from 250 to 550 USD/tonne while the expected spot HFO is fixed at 150 USD/tonne. We can clearly see from Table 2.5 that for the risk-averse setting, the amount of CO_2 emitted becomes higher with increasing ESPG. It is also

Table 2.5: Average CO_2 emissions at different ESPG, for both standard risk-averse & risk-neutral settings.

ESPG (USD/tonne)	100	150	200	250	260	270	300	350	400
CO_2 (tonnes) Risk-averse	5586.7	5618.2	5655.6	5743.3	5852.3	5988.1	6023.1	6045.2	6046.4
CO_2 (tonnes) Risk-neutral	5561.0	5619.7	5670.7	5821.2	5869.0	5913.0	5999.2	6043.8	6046.4
Difference%*	0.46	+0.03	+0.27	+1.36	+0.29	-1.25	-0.40	-0.02	0.00

* Relative increase in CO_2 for the Risk-neutral case compared to the Risk-averse case.

the case for the risk-neutral setting. This is in fact consistent with the conclusion shown in Fagerholt et al. (2015), that is, in general, CO_2 emissions would also increase when the price gap between MGO and HFO increases, due to a higher tendency to implement ECA-evasion and speed differentiation strategies. However, when comparing the CO_2 emissions between risk-averse and risk-neutral settings, i.e. the **Difference%** row of Table 2.5, we cannot easily tell which risk attitude is more "environmentally friendly". We further illustrate in Fig. 2.7 the comparison of average CO_2 between risk-averse and risk-neutral settings.

In Fig. 2.7, the average CO_2 emitted at different ESPG under the standard risk-averse setting is represented by the solid line, and the risk-neutral setting by the dashed line. Unlike the results shown in Sec. 2.4.1, where stronger risk aversion leads to a lower worst-case CO_2 emissions (which is, in fact, a general trend regardless of ESPG according to our experiments), the effect of risk aversion on average CO_2 emissions is undetermined, and depends upon the specific ESPG that we face. For example, in Fig. 2.7, when the ESPG is around 250 USD/tonne, the risk-averse setting has lower average CO_2 emissions than the risk-neutral case; whereas at around 270 USD/tonne the opposite situation is observed.

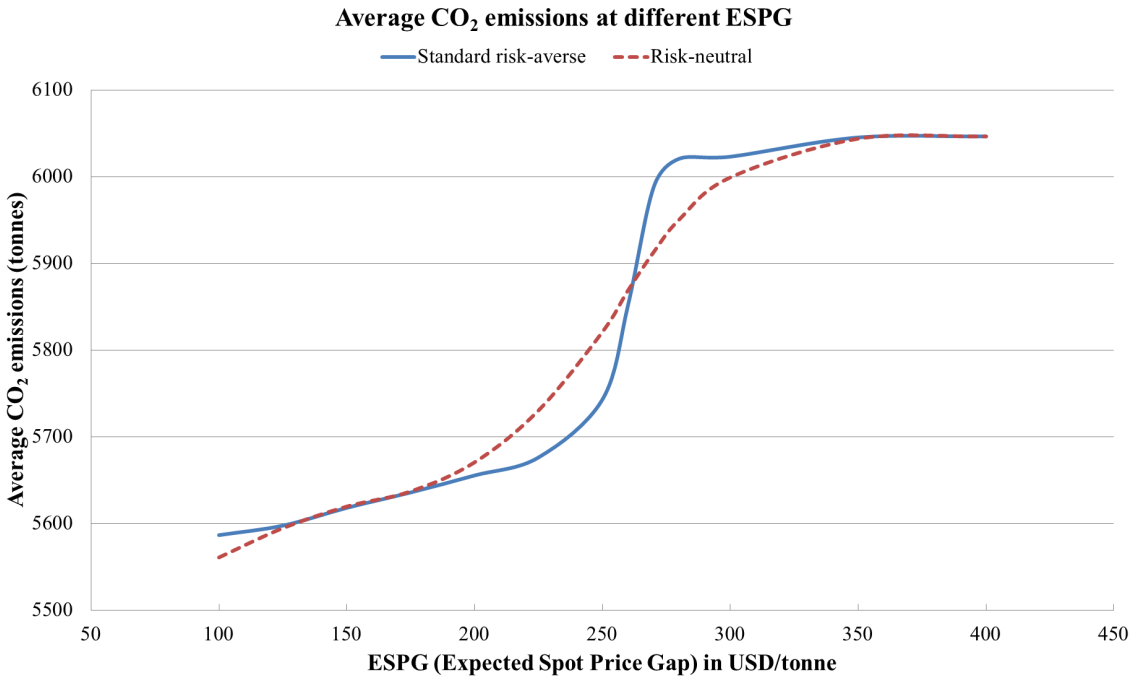

Figure 2.7: Difference of expected CO_2 emissions between risk-averse and risk-neutral cases under different levels of price gap

In order to explain this somewhat surprising result, we first need to explain what we call

a *jump* in sailing behavior. If there is no price gap between MGO and HFO, the shipping company has no incentive to change its sailing behavior, and thus sails the traditional leg option (shortest path) between two ports in the same ECA. When the price gap increases, a leg option change will not immediately occur. The vessel will stick to the shortest path until the price gap between MGO and HFO reaches a certain level, and then switch to another leg option, looking something like Leg Option 2 in Fig. 2.5; the sailing pattern makes a *jump*. Fig. 2.8 is used to illustrate the principle of a jump. The solid line represents the traditional leg option between two ports located inside the same ECA, the dash-dot line illustrates the leg option following a jump. For simplicity of the argument, let us simply assume that one universal speed is applied both in- and outside ECA. Hence, fuel consumption is proportional to distance. The fuel cost for the traditional leg is $P^{MGO} \times a$ while the total bunker cost for the "Jump-to" leg option is $P^{MGO} \times 2d + P^{HFO} \times (a - 2c)$. Hence, until the MGO price becomes $\frac{a-2c}{a-2d}$ times as high as the HFO price, it is cheaper to sail the shortest path and a jump will not be triggered. However, once the price gap exceeds that level, the optimal leg option switches to the "Jump-to" leg option and the jump occurs. Note that jumps are a natural part of the underlying problem and not caused by the fact that we have discretized sailing patterns into possible leg options. Furthermore, if time and speed considerations are involved, the "Jump-to" leg option will need a higher average speed, thus higher fuel consumption to maintain the schedule, which leads to a even higher price gap to trigger the jump.

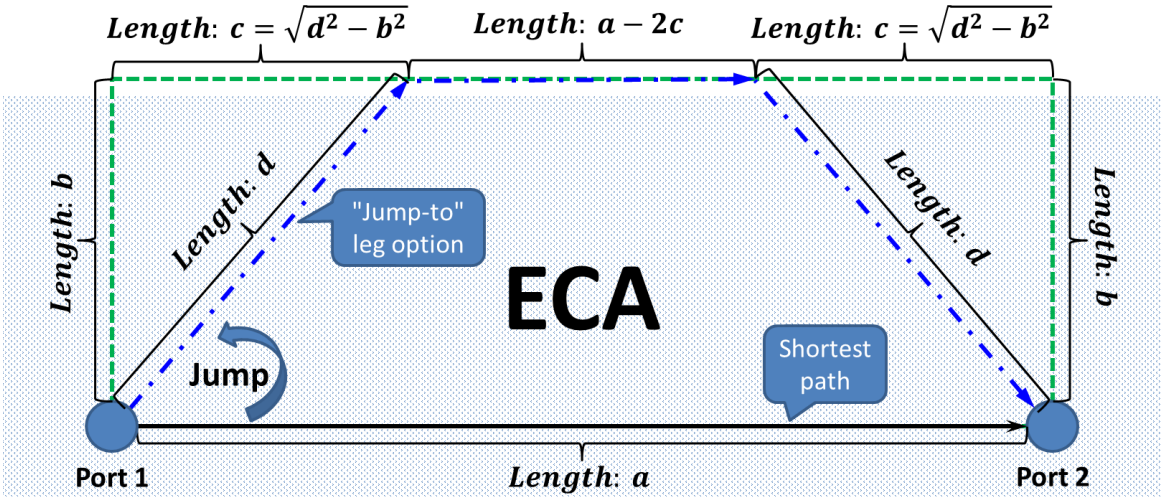

Figure 2.8: Simple example illustrating a jump in sailing behavior change

A risk-averse company relies mainly on the forward market while using small amounts of spot-fuels as supplements. Moreover, the forward price difference approximately equals the ESPG since the prices of the forward fuels are set to be just marginally higher than the expected spot fuel prices (basis prices). Therefore, the actual price gap which decides the sailing behavior in the risk-averse setting is significantly affected by the ESPG, and only slightly influenced by the Realized Spot Price Gap (RSPG in short) in each scenario. The RSPG in Scenario s can be expressed as:

$$RSPG_s = ESPG + (I_s^{MGO} - I_s^{HFO}) \tag{2.21}$$

where I_s^{MGO} and I_s^{HFO} represent the price increments of MGO and HFO, respectively, in Scenario s. The risk-neutral company, however, is more willing to take market risks and thus only buys from the spot market. Hence, in the risk neutral case, the sailing pattern in each specific scenario purely depends on the RSPG in that scenario. In sum, the price gaps in most scenarios

in the risk-averse setting are approximately the same as the ESPG while the price gaps in the risk-neutral setting (RSPG) differ substantially from scenario to scenario.

Since most scenarios in the risk-averse setting have similar price gaps, the jump happens almost simultaneously in these scenarios when the ESPG increases to the level that satisfies the requirement illustrated in Fig. 2.8. Such a clustered change in sailing behavior (thus CO_2 emissions) in most scenarios brings a sudden and major increase in average CO_2 emissions in the risk-averse setting, as observed in Fig. 2.7. From (2.21), we see that RSPG increases together with the ESPG, but such that the scenario with the largest price increment difference will also have the largest RSPG. Hence, when ESPG increases, these scenarios with large price increment differences will first trigger a jump. Then the scenarios with moderate price increment differences (thus moderate RSPGs) follow along with the increase of ESPG, and finally the jump occurs in the scenarios which have small price increment differences (thus small RSPGs). As we can see, contrary to the clustered jump in the risk-averse setting, the jump in the risk-neutral setting happens gradually from the scenarios with larger RSPGs to the ones with smaller RSPGs. The corresponding effect on average CO_2 emissions is much more widely distributed along the ESPG axis, which eventually leads to a smoother increasing curve for the risk-neutral setting, as witnessed in Fig. 2.7.

To summarize, in this section we show that the shipping company's risk attitude has impact on its CO_2 emissions in various ways. On one hand, the worst-case CO_2 emissions will be reduced by financial risk control measures, i.e. a stronger risk aversion will lead to less CO_2 emitted in the worst scenarios; on the other hand, the effect of risk aversion on average CO_2 emissions is undetermined, and is influenced by the expected price gap between MGO and HFO on the spot market.

2.4.2 Impact of hedging strategies on CO_2 emissions

We now study how different hedging strategies affect a shipping company's expected CO_2 emissions. For all experiments presented in this section, we assume the company's risk attitude is always standard risk-averse (see Sec. 2.4.1), and the expected CO_2 emissions refer to the average amount of CO_2 emitted across all scenarios.

Using the input data given in Sect. 2.3, we can first obtain the optimal hedging amounts of both MGO and HFO by solving the stochastic MFM problem to optimality. We then fix the hedging decision for one fuel, HFO for instance, and change the hedging amount of the other (MGO) to get different combinations of hedging decisions. For each such combination, we solve the problem after fixing the hedging decisions accordingly, and record the expected CO_2 emissions. The results are shown in Fig. 2.9a, where the hedged MGO varies from 70% to 120% of its optimal amount. We also show in Fig. 2.9b the opposite case in which we vary the hedging amount for HFO while fixing the hedged MGO at its optimal amount.

From the two charts in Fig. 2.9 we can see that the expected CO_2 emissions will (a) decrease when hedging more MGO, and (b) increase when hedging more HFO. These changes in CO_2 emissions may be explained by the changes in the company's willingness to apply ECA-evasion and speed differentiation strategies. As mentioned earlier, when more MGO is hedged, in order to commit to the forward contract and avoid paying too much penalty for unused forward MGO, the company may be restricted to the traditional "shorter but more ECA involved" routes. In this case, the *total* fuel consumption (MGO & HFO) is usually lower because of the shorter total distance sailed, hence the CO_2 emissions are also lower. On the other hand, when more HFO is hedged, the company may be more likely to sail "aggressively", e.g. with as little ECA involvement as possible, in order to consume more HFO. As a result, the total sailing distance is usually longer, which eventually leads to higher total fuel consumption and more CO_2 emitted.

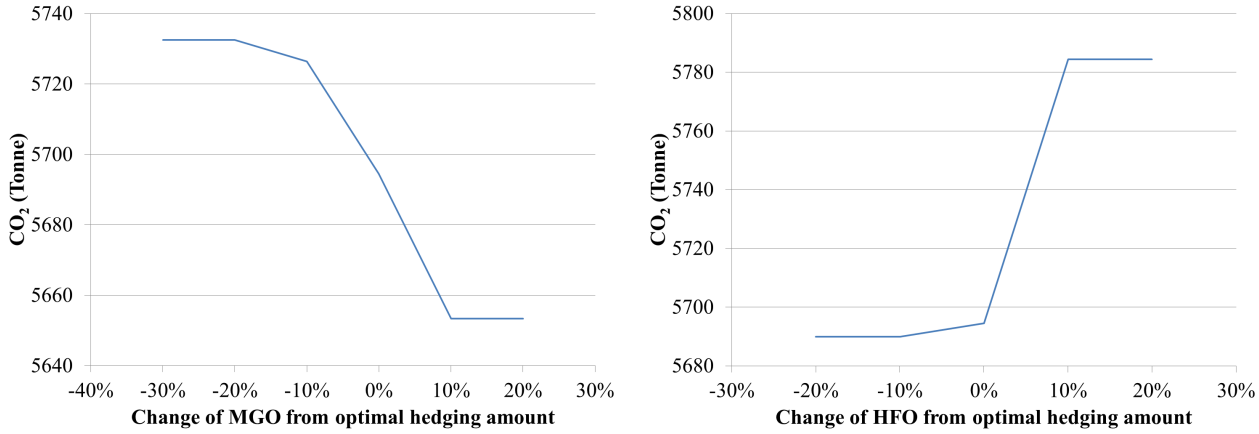

(a) CO_2 under different MGO hedging amount

(b) CO_2 under different HFO hedging amount

Figure 2.9: Expected CO_2 emissions under different fuel hedging strategies

Note that the above tests only show how expected CO_2 emissions change when altering the hedging amount of one type of fuel alone. In addition, apart from the environmental impact, different hedging decisions may also affect the total bunker costs, which is more of a concern for most shipping companies. Therefore in the following tests, we demonstrate the effects of simultaneously changing the hedging amounts of MGO and HFO, both environmentally (in terms of expected CO_2 emissions) and financially (in terms of expected total bunker costs and worst-case total bunker costs). We seek to provide an insight into the question: can we effectively reduce CO_2 emissions through different hedging strategies? And at what cost?

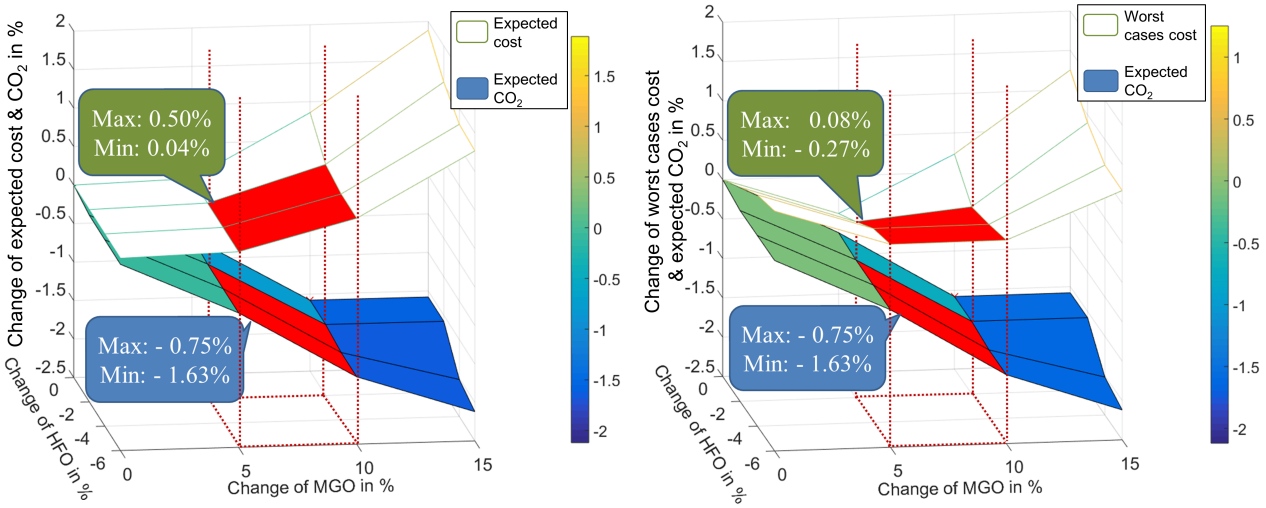

(a) Surfaces for Expected Total Bunker Costs & Expected CO_2 emissions

(b) Surfaces for Worst-case Total Bunker Costs & Expected CO_2 emissions

Figure 2.10: Illustration of the relation between CO_2 emissions and expected & worst-case total bunker costs under different hedging strategies.

Let us look at two 3-D charts in Fig. 2.10. In both charts, we use the changes (%) in the hedging amounts of MGO and HFO (relative to their respective optimal amounts) as x- and y- axes, respectively. For Fig. 2.10a, we show two plotted surfaces representing expected CO_2 emissions (bottom surface) and expected total bunker costs (top surface), both are changes (%) relative to their corresponding values obtained with the optimal hedging decisions. For Fig. 2.10b, the surface of expected CO_2 emissions remains the same, and we also show the surface for the worst-case total bunker costs, computed as the average of the five worst scenarios out of 100. Let us further focus on the red areas in the two charts, where the x- (change

in MGO) values and y- (change in HFO) values correspond to [+5%,+10%] and [-6%,-2%], respectively. Therefore, by hedging 5% to 10% more on MGO and 2% to 6% less on HFO, we are able to reduce expected CO_2 emissions by 0.75% to 1.63%. This is achieved at the expense of increasing the expected total bunker costs by 0.04% to 0.50%, which are not significant. Furthermore, we show in Fig. 2.10b that such reduction in CO_2 sometimes even coincides with an improved situation (decrease) in the worst-case bunker cost (ranging from -0.27% to 0.08%). These results are meant to provide an example that sometimes a shipping company can achieve noticeable reduction in CO_2 emissions with little sacrifice on its financial costs by changing the hedging strategies. For any single player in maritime transportation, such reduction may not be significant. But for the shipping industry on a global scale, this could become a sizeable contribution if more companies are coming to the realization of the potential environmental benefits of proper design of hedging and other bunker risk management measures.

2.5 Conclusion

Bunker risk management is widely practiced in the shipping industry to reduce financial risk and can be vital for a shipping company to remain competitive. Nevertheless, dramatic changes have taken place after the introduction of the ECA regulation. In this paper, we use a stochastic Maritime Bunker Management (MFM) model and a case study on a major liner shipping company to show that bunker risk management has impacts on the company's CO_2 emissions.

We first study the impact of the shipping company's risk attitude on its CO_2 emissions. The results show that stronger risk aversion can also lead to lower "environmental risk", i.e. less CO_2 emissions in the worst cases. Meanwhile, we also show that the effect of risk aversion on average CO_2 emissions is undetermined, and is influenced by the expected price gap between MGO and HFO on the spot market. We then study the impact of hedging strategies on CO_2 emissions. We show that a shipping company can sometimes achieve noticeable reduction in CO_2 emissions with little sacrifice on its financial costs by changing its hedging strategies.

Appendix 2.1

The detailed speed-routing decisions in scenario No. 26 under different maximum CVaR values are shown in the following table.

Table 2.6: Sailing behaviors in scenario No. 26 under different risk aversions

Max CVaR (1000 USD)		388	389	390	391	392	393	Neutral
Leg 1								
Leg Option		4	*5*	*5*	*5*	*5*	*5*	*5*
ECA/non-ECA (nautical mile)	distance	496/905	*408/1062*	*408/1062*	*408/1062*	*408/1062*	*408/1062*	*408/1062*
ECA/non-ECA (knot)	speed	15/15	15/15	15/15	15/15	15/15	15/15	15/15
Leg 2								
Leg Option		3	3	*5*	*5*	*5*	*5*	*5*
ECA/non-ECA (nautical mile)	distance	524/906	524/906	*397/1241*	*397/1241*	*397/1241*	*397/1241*	*397/1241*
ECA/non-ECA (knot)	speed	15/15	15/15	15/15	15/15	15/15	15/15	15/15
Leg 3								
Leg Option		1	1	1	1	*4*	*4*	*4*
ECA/non-ECA (nautical mile)	distance	632/0	632/0	632/0	632/0	*443/515*	*443/515*	*443/515*
ECA/non-ECA (knot)	speed	15/15	15/15	15/15	15/15	15/15	15/15	15/15
Leg 4								
Leg Option		4	4	4	4	4	4	*5*
ECA/non-ECA (nautical mile)	distance	889/2652	889/2652	889/2652	889/2652	889/2652	889/2652	*752/2903*
ECA/non-ECA (knot)	speed	15/20.6	15/20.6	*15/20.1*	*15/20.1*	*15/20.1*	*15/20.1*	*15/20.5*
Leg 5								
Leg Option		5	5	5	5	5	5	5
ECA/non-ECA (nautical mile)	distance	751/3428	751/3428	751/3428	751/3428	751/3428	751/3428	751/3428
ECA/non-ECA (knot)	speed	15/18.1	15/18.1	15/18.1	15/18.1	15/18.1	15/18.1	15/18.1

Chapter 3

Scrubber: a potentially overestimated compliance method for the Emission Control Areas - The importance of involving a ship's sailing pattern in the evaluation

Published at: Transportation Research Part D: Transport and Environment, Volume 55, 2017

Yewen Gu[1], Stein W. Wallace[1]

[1]Department of Business and Management Science, Norwegian School of Economics, Bergen, Norway

Abstract

Different methods for sulphur emission reductions, available to satisfy the latest Emission Control Areas (ECA) regulations, may lead to different sailing patterns (route and speed choices of a vessel) and thus have significant impact on a shipping company's operating costs. However, the current literature does not include sailing pattern optimization caused by ECA, and its corresponding cost effects, in the evaluation and selection process for sulphur abatement technology. This leads to an inaccurate estimation of the value of certain technologies and hence an incorrect investment decision. In this paper, we integrate the optimization of a ship's sailing pattern into the lifespan cost assessment of the emission control technology, so that such expensive and irreversible decisions can be made more accurately. The results shows that a considerable overestimation of the value of scrubbers, and thus a substantial loss, can occur if the sailing pattern of a ship is not considered in the decision-making process. Furthermore, we also illustrate that it is more important to involve a ship's sailing pattern when the port call density inside ECA is low.

Keywords: Scrubber, Fuel-switching, Emission Control Areas, Sailing pattern, Port call density, Lifespan cost evaluation

3.1 Introduction

Almost 90% of the world's trade is carried by sea. Therefore, the shipping industry plays a critical part in the global economy (ICS, 2017). However, since marine bunkers normally has a very high sulphur content, shipping activities actually emit more sulphur related exhausts per tonne-mile of cargo than other modes of transport (Wang and Corbett, 2007). Therefore, the International Maritime Organization (IMO) introduced the Emission Control Areas (ECA) regulation which is designated under MARPOL Annex VI on 19 May 2005 (IMO, 2016). The latest ECA regulation came into force in January 2015, see Figure 3.1. It requires that the vessels operating inside the regulated regions use fuel oil with a sulphur content of no more than 0.1%. In the meantime, the limit for sulphur content of fuel oil burnt outside ECA is 3.5%. However, this cap will decrease to 0.5% after 2020.

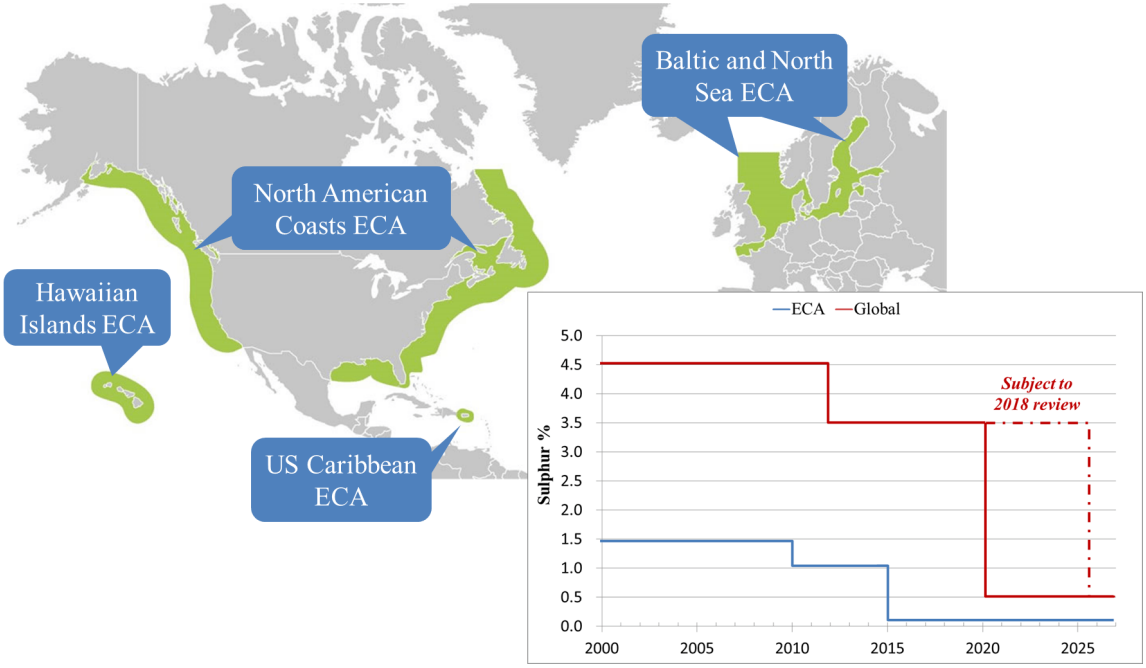

Figure 3.1: Map and requirements of the Emission Control Areas

Three alternatives that can be used to comply with the ECA regulation are currently available on the market. The first approach is fuel-switching, which allows a ship to change between heavy fuel oil (HFO) and marine gasoline oil (MGO). The HFO is the traditional fuel, with high sulphur content, and can only be used outside ECA. Note that after 2020 the HFO will be replaced by another ultra low sulphur fuel oil (ULSFO), which contains 0.5% sulphur, when the ship sails outside ECA. The MGO is the cleaner fuel, with less than 0.1% sulphur, and can be used inside ECA. The fuel-switching approach requires only slight modifications on the ship, and thus very limited initial investments. But the price of MGO is much higher than that of HFO, and its future replacement ULSFO, which means the operational costs of a vessel can increase dramatically if the fuel-switching approach is applied. On the other hand, the shipowner may also choose to install a scrubber system which absorbs the majority of the sulphur content in the exhaust, and therefore enables the ship to keep using cheap HFO in- and outside ECA. However, the capital costs of the scrubber installation is considerable. The last option is to use liquefied natural gas (LNG) as fuel for the ship's propulsion system. Similar to the scrubber approach, the LNG option can effectively avoid the consumption of expensive MGO in exchange for a substantial initial capital investment. Furthermore, the LNG approach also suffers from other problems, such as large space requirements and supply limitations at ports.

Since the three alternatives have different pros and cons, and the investments in certain technologies are irreversible, the choice of sulphur emission control method for a shipping company becomes critical and complex. The selection among the three abatement technologies mainly depends on the trade-off between their fix costs (e.g., capital costs and maintenance costs) and variable costs (fuel costs). The former is relatively clear, while the latter is uncertain. The fuel cost of a vessel is affected by its ***sailing pattern***, including route and speed decisions. Such patterns may change after choosing a certain emission control method. The major motivation for this paper is to study the impact of a ship's sailing pattern on the the selection of ECA compliance method as this is a costly, irreversible decision.

There is a solid body of literature on the selection of sulphur emission reduction technology. Ren and Lützen (2015) propose a multi-criteria approach to assist the decision-makers in a shipping company to choose the most sustainable emission reduction technology for all existing environmental regulations. Balland et al. (2013) develop a two-stage stochastic programming model to decide the selection of emission abatement technologies for a certain time period so that the vessel can comply with the air emission regulations in the most cost-efficient way. The model involves the consideration of the interaction between different abatement technologies and the pollution reduction uncertainties of different existing air emission controls. Patricksson et al. (2015) extend the maritime fleet renewal problem and include the ECA as a key factor in the decision-making process. A stochastic programming model is built to facilitate the selection between fuel-switching and scrubber system for the shipping company by minimizing the expected total costs including the initial capital cost and the expected operational cost in the future. Jiang et al. (2014) examine the costs and benefits of different sulphur reduction measures from a comprehensive viewpoint by integrating the private cost of the shipowners and the social benefits from emission reduction. Schinas and Stefanakos (2012) also use stochastic linear programming to minimize the total costs of a ship operator who has business in the ECA. The model determines the fleet-mix and the capacity under budgetary and fleet attribute constraints, while taking demand and growth patterns into account. The uncertainty in this research refers to the probability of the vessels sailing in ECA. Furthermore, Lindstad et al. (2015) evaluate costs as a function of emission abatement alternatives used in the ECA. Their study shows that there is no absolute answer to what is the best choice for emission reduction. The optimal option depends on several factors including engine size, annual fuel consumption in the ECA and future fuel prices. Lindstad and Eskeland (2016) claim that the scrubbing and tuning solution will become the dominant response after the global sulphur cap being implemented in 2020. However, such end-of-pipe solutions reduce energy efficiency and may deflect attention from developing cleaner fuels and improving energy efficiency. Hence, instead of extending to a global setting, the paper proposes to retain the current regulation. Öler and Ballini (2015) propose a comprehensive and holistic decision-making framework so as to overcome the barriers of cost-benefit analysis methodology by including all the decision-making parameters and their discrete values. Panasiuk and Turkina (2015) analyse the investment efficiency of a scrubber system installation to comply with the latest ECA regulation. The research calculates and evaluates the cash flow performance during the whole life cycle of the scrubber technology and compares it with the fuel-switching alternative. Other evaluation tools, such as the analytical hierarchy process (AHP) and the analytic network process (ANP), are also widely applied to support the decision-making of choosing technologies towards compliance with the ECA regulation (Schinas and Stefanakos, 2014; Yang et al., 2012).

During the assessment of the emission abatement methods in the papers mentioned above, all the authors have consciously or unconsciously made the assumption that the sailing pattern of a vessel will remain unchanged after a certain emission abatement technology is installed on board. This assumption is correct in the cases of the scrubber and LNG solutions, but not true in the fuel-switching approach. Doudnikoff and Lacoste (2014) and Fagerholt et al. (2015) have

pointed out two possible optimizations of ship's sailing pattern if the fuel-switching option is used to comply with the ECA regulation, see Fig. 3.2. The first type of optimization can be categorized as speed differentiation, which means that different speeds will be applied in- and outside ECA on the same voyage, see Fig. 3.2a. Normally, the ship will slow down inside ECA in order to reduce the consumption of the expensive MGO. Meanwhile, the speed outside ECA has to be increased so as to maintain the time schedule. The other type of optimization can be called as ECA-evasion. For example, if a vessel needs to carry out a trip from port-A to port-B that are both located inside the same ECA, it may choose to firstly quit the ECA zone after departing from port-A, then sail along the edge of the ECA and re-enter the control area when approaching port-B, rather than taking the shortest route between the two ports, see Fig. 3.2b. Such a strategy helps the shipping company avoid a substantial involvement of ECA sailings and hence reduces the consumption of MGO. However, it also leads to a longer total distance and a higher average speed to stay inside the schedule. Therefore, the consumption of HFO is increased. The spread between the prices of MGO and HFO decides the optimal combinations of these two strategies on a certain voyage. In general, comparing to navigating ships in the traditional way (shortest path and fixed speed), the shipping company can achieve a lower operating cost by smartly adopting these two strategies.

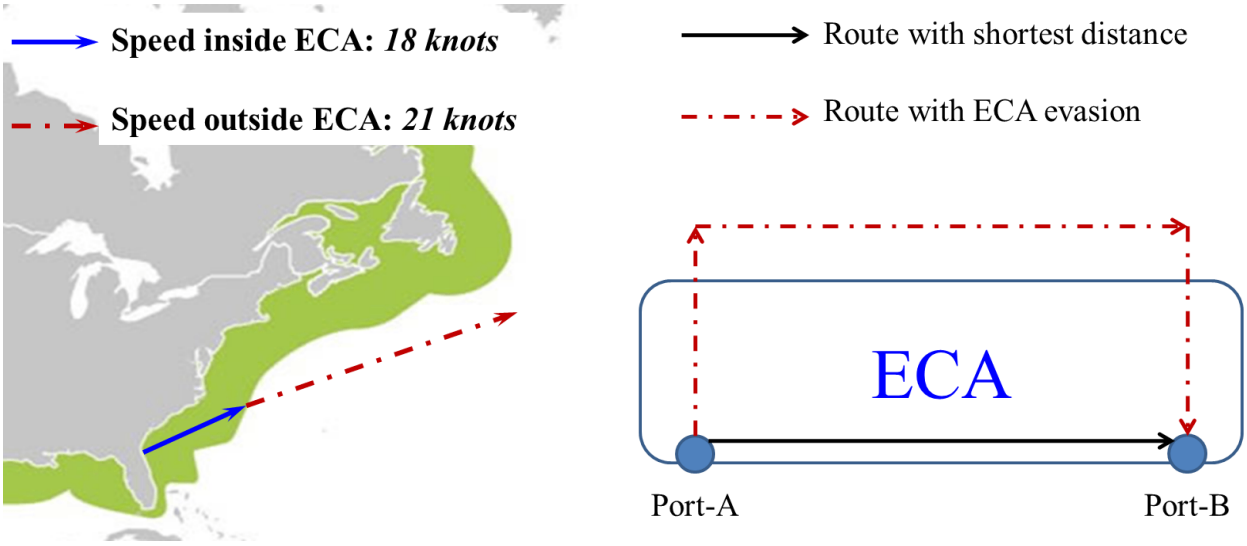

(a) Speed Differentiation **(b)** ECA-evasion

Figure 3.2: Two classifications of ship's sailing pattern optimization

The existing literature does not involve a ship's sailing pattern when evaluating sulphur emission abatement technologies for ECA. However, sailing pattern optimization in the fuel-switching case clearly affects a ship's fuel consumption and hence affects the variable costs of applying this technology. As mentioned in the previous paragraph, the choice of sulphur control method for a ship depends on both the fixed costs and the variable costs of adopting the technologies. Therefore, a ship's sailing pattern might have a significant impact on the selection. With such a knowledge gap in the literature, the value of certain sulphur emission control methods, such as scrubber and the LNG option, can be inaccurately estimated, which may lead to incorrect investment decisions and considerable financial losses. In this study we focus on fuel-switching and scrubber systems. Boscaratoa et al. (2015) point out that the scrubber system for maritime transportation is still not mature enough to perfectly work in an integrated system designed to handle all of the currently legislated emissions from marine engines. Meanwhile, Hilmola (2015) claims that the scrubber system is not widely applied today since the time span left before the regulation was implemented in 2015 was too short for the shipping companies to complete the research and adoption. These two papers express

some typical concerns about the application of scrubber systems in maritime transportation. In this study we use operational arguments to claim that the value of the scrubber option can be significantly overestimated if a ship's sailing pattern is not involved in the assessment. We integrate the optimization of the sailing pattern (e.g., speed and route choices) into the lifespan cost evaluation model for different sulphur emission reduction technologies. This closes the knowledge gap in the current literature and improves the accuracy in the decision-making process. Furthermore, this paper also tests how the density of port calls inside ECA on a voyage affects the size of such overestimation.

During the Marine Environment Protection Committee (MEPC) meeting in October 2016, IMO decided to introduce a global sulphur cap of 0.5% after 2020. The new regulation will certainly have impacts on the topic discussed in this paper. However, we argue that the phenomenon of optimizing a ship's sailing pattern in the fuel-switching case will continue to exist as long as there is a price difference between the MGO and the new fuel with 0.5% sulphur content used outside ECA. Therefore, the overestimation issue of scrubber will not simply disappear after 2020.

The rest of the paper is organized as follows. Section 3.2 gives a complete description of the problem and our mathematical model. In Section 3.3 we introduces the cases used for testing. Section 3.4 shows and analyses the results of the computational study. Last, conclusions of the study are given in Section 3.5.

3.2 Problem description and mathematical model

In this section, a formal description is offered. Section 3.2.1 describes the research problem and defines the terminology applied in this paper. Section 3.2.2 explains the structure of the model and gives the mathematical formulation.

3.2.1 Problem statment

The increased environmental requirements enforced by the latest ECA regulation and the even stricter global sulphur emission cap after 2020 bring great challenges to the shipping industry. It is vital for a shipping company to find the optimal compliance method, in our case between a scrubber system and a fuel-switching approach, so that the cost increase caused by the sulphur emission policy can be controlled. As mentioned in Section 3.1, the choice between scrubber and fuel-switching, from a cost perspective, is essentially a trade-off between capital investment in the beginning and operating costs in the future. Therefore, the problem faced by all shipping companies is to minimize its total lifespan costs including the fixed costs of installing a certain emission reduction technology and the variable costs of of operating the fleet with this technology on board during its life-time.

In this research we use mathematical programming models to calculate and compare the total lifespan costs of the two technologies; the scrubber system and the fuel-switching alternative. We can then compare the optimal emission control solutions in the cases that sailing pattern is ignored and considered. Therefore, we can see the difference between the two solutions and thus the impact of sailing pattern on the selection of emission abatement technology. The comparisons are also made under different scenarios of price gap between MGO and HFO and also with different settings of port call density inside ECA on the same trading line.

We also need to define the terminology applied in this research. The special terms used in this paper include *loop*, *leg*, *leg option* and *stretch*. A *loop* refers to a round trip consisting of several port calls in a predetermined order, while we define a *leg* as the voyage between two ports which are adjacent in the *loop* in terms of their calling sequences, see Fig. 3a. Figure 3b shows the concept of *leg option*. Different *leg options* represent different routing possibilities

that can be adopted to finish the trip on a certain *leg*. They normally differ not only in total travelling distance but also in ECA related miles.

One or more *stretches*, as shown in Fig. 3c, may be found on a *leg option*. The first *stretch* starts automatically when the ship leaves the origin port of the *leg* while the last *stretch* terminates after the vessel reaches the destination port. Furthermore, whenever the ship enters or exits the ECA zone, at which point the fuel used on board is switched, the previous *stretch* ends and simultaneously a new *stretch* begins. Certainly, if one *leg option* never crosses the border of ECA, there will be only one single *stretch* on that *leg option*. Although a certain *leg option* may have several *stretches*, same sailing speed is assumed to be applied on different *stretches* of the same kind, namely ECA and non-ECA *stretches*. Therefore, all the *stretches* under the same *leg option* will be consolidated into these two groups which characterises each *leg option* in the later modelling part.

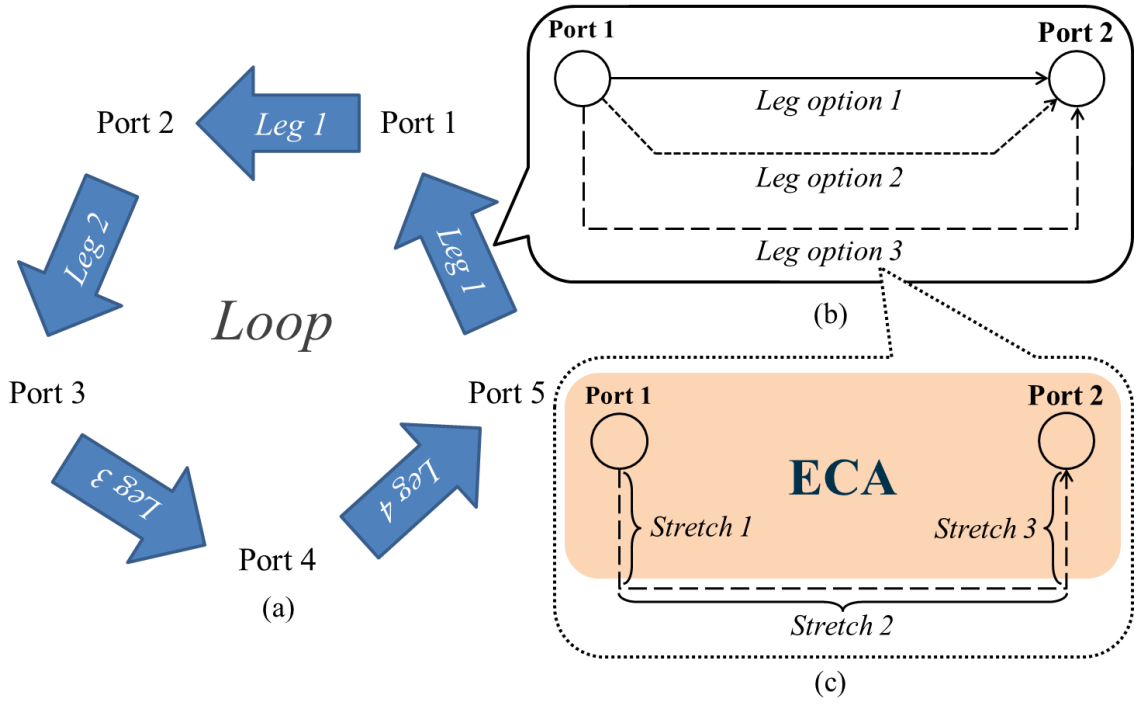

Figure 3.3: Illustration of loop, leg, leg option and stretch **cite the book paper**

3.2.2 Model formulation

The mathematical model applied in this paper compares the total lifespan costs of different compliance methods, and determines the optimal sulphur emission reduction technology for the vessel. The main observation of the model can be expressed as:

$$Cost^{life}_{difference} = Cost^{life}_{fuel\text{-}switching} - Cost^{life}_{scrubber} \tag{3.1}$$

where a negative cost difference means that the fuel-switching approach is optimal in terms of life cycle cost and a positive cost difference refers to the opposite.

Cost of scrubber system

The lifespan costs of applying the scrubber system on board can be roughly divided into two parts, the fixed costs and the operational costs (variable costs). Hence the total life cycle costs of the scrubber system can be calculated as:

$$Cost^{life}_{scrubber} = Cost^{fixed}_{scrubber} + Cost^{operation}_{scrubber} \tag{3.2}$$

The fixed costs of the scrubber system include initial capital investments, off-hire costs, cargo capacity losses and annual maintenance costs. When the shipping company decides to install a scrubber system on its vessel, a large initial cost must be paid for the system design, equipment procurement and installation. The old vessel automatically becomes unavailable on the chartering market during the retrofitting and installation of the scrubber system, which leads to a loss in revenue called off-hire cost. This cost does not apply in the newbuilding case. Moreover, since the installation of the scrubber system needs a considerably large space on the vessel, part of the room originally used for storing cargo now must be sacrificed. Therefore, the vessel's capability of generating revenue decreases due to such cargo capacity loss. Lastly, the additional cost caused by the daily maintenance of the equipment should also be considered in the calculation. The total fixed costs of the scrubber system can then be stated as:

$$Cost^{fixed}_{scrubber} = Cost^{capital}_{scrubber} + Cost^{off\text{-}hire}_{scrubber} + \sum_{t=0}^{T} \frac{Cost^{capacity}_{scrubber}}{(1+d)^t} + \sum_{t=0}^{T} \frac{Cost^{maintain}_{scrubber}}{(1+d)^t} \tag{3.3}$$

where $Cost^{capital}_{scrubber}$ refers to the initial capital investment cost, $Cost^{off\text{-}hire}_{scrubber}$ equals the revenue loss during the off-hire period due to the retrofitting of the scrubber, $Cost^{capacity}_{scrubber}$ and $Cost^{maintain}_{scrubber}$ represent the annual capacity loss and maintenance cost, T refers to the length of the scrubber system's lifespan, and d is the discount rate. Note that since the capacity losses and maintenance costs are yearly, they must be transformed into a net present value (NPV). Meanwhile, $Cost^{capital}_{scrubber}$ and $Cost^{off\text{-}hire}_{scrubber}$ occur immediately after the decision of installing scrubber system is made.

The operational costs here refer to the fuel costs generated during the ship operation with the prerequisite that the scrubber system is applied on board. The expression of the operation cost in the scrubber case can be formed as:

$$Cost^{operation}_{scrubber} = \sum_{t=0}^{T} \frac{n \times P^{HFO} \times F^{loop}_{traditional}}{(1+d)^t} \tag{3.4}$$

where n is the number of round trips that a vessel can perform on a loop in one year, P^{HFO} is the fuel price for HFO, and $F^{loop}_{traditional}$ refers to the amount of fuels needed for a round trip of a loop if the vessel operate in the traditional way. Recall that the vessel can still use the HFO as its bunker inside ECA as long as the scrubber system is on board. Hence, there is no incentive for the vessel to change its sailing pattern. Then the vessel will just continue to sail in the traditional way; the shortest path (no ECA-evasion) and the slowest possible speed (no speed differentiation) on each leg. The fuel consumption is therefore fixed as a constant. Furthermore, the cumulative operational costs during the entire lifespan of the scrubber also need to be calculated in the NPV form.

Cost of fuel-switching

Since the modification and additional maintenance needed for the vessel to run on MGO are insignificant, we assume that the fixed cost for the fuel-switching approach is neglectable. Therefore, the lifespan cost of using the fuel-switching approach comprises the operational costs only.

$$Cost^{life}_{fuel\text{-}switching} = Cost^{operation}_{fuel\text{-}switching} \tag{3.5}$$

However, the operation cost of the fuel-switching approach will be calculated in two different ways in this paper. Firstly, sailing pattern is not considered and the vessel follows its old-fashioned way of navigation. Secondly, the vessel is allowed to optimize its sailing pattern through the adoption of ECA-evasion and speed differentiation strategies.

- *When sailing pattern is ignored*

If the vessel sails in the traditional way, it will still choose to take the shortest path and the slowest possible speed on each voyage, like in the scrubber case. But the fuels used inside ECA is not HFO but MGO. Moreover, the fuels used outside ECA, before and after the global sulphur cap being introduced, are HFO and ULSFO respectively. The operation cost of the fuel-switching approach in the first situation then can be expressed as:

$$Cost^{operation}_{fuel\text{-}switching} = \sum_{t=0}^{T} \frac{n \times \left(P^N \times F^N_{traditional} + P^{ECA} \times F^{ECA}_{traditional}\right)}{(1+d)^t} \tag{3.6}$$

where P^N and P^{ECA} refers to the price of the fuels used outside and inside ECA, $F^N_{traditional}$ and $F^{ECA}_{traditional}$ are the corresponding fuel consumption of two types of fuel when the vessel is operated in the old-fashioned way. The sum of $F^N_{traditional}$ and $F^{ECA}_{traditional}$ equals $F^{loop}_{traditional}$ in Eq. 3.4. Since the fixed costs of the fuel-switching approach are set to zero 0 in the test, the lifespan of this technology no longer matters. In order to have a valid horizontal comparison in terms of cost between the fuel-switching approach and the scrubber system, however, we calculate the NPV of the accumulated total cost during the following T years (lifespan of the scrubber system).

- *When sailing pattern is considered*

If sailing pattern is considered in the calculation, the fuel consumptions of both fuels are no longer fixed. Due to the application of ECA-evasion and speed differentiation strategies, the amounts of MGO and HFO/ULSFO consumed will change according to the actual fuel price gap between the two fuels. Therefore, we adopt a deterministic optimization model from Fagerholt et al. (2015) to calculate the operational costs of the fuel-switching approach under the optimal sailing pattern. The model is formulated as follows:

Sets

J	Set of sailing legs along the loop
R_j	Set of leg options for Leg j
V	Set of feasible discrete speed points for the ship

Parameters

P^{ECA}	Price per ton of fuel used inside ECA
P^N	Price per ton of fuel used outside ECA
F^{ECA}_{jrv}	Fuel consumption on ECA stretches on Leg j under Leg Option r with Speed v
F^N_{jrv}	Fuel consumption on non-ECA stretches on Leg j under Leg Option r with Speed v
W^{ECA}_{jrv}	Sailing time on ECA stretches on Leg j under Leg Option r with Speed v
W^N_{jrv}	Sailing time on non-ECA stretches on Leg j under Leg Option r with Speed v
W_j	Scheduled starting time for Leg j
W^{Port}_j	Service time at port on Leg j

Decision variables

x_{jrv}^{ECA}	Weight of Speed v used on ECA stretches on Leg j with Leg option r
x_{jrv}^{N}	Weight of Speed v used on non-ECA stretches on Leg j with Leg option r
y_{jr}	Binary variables representing the decisions on route selection, equal to 1 if Leg Option r is adopted on Leg j, and 0 otherwise

The optimal operational costs of fuel-switching for a round trip of the loop when sailing pattern is involved can be calculated as:

$$Cost_{fuel\text{-}switching}^{loop} = \min \sum_{j\in J} \sum_{r\in R_j} \sum_{v\in V} \left(P^{ECA} F_{jrv}^{ECA} x_{jrv}^{ECA} + P^{N} F_{jrv}^{N} x_{jrv}^{N}\right) \tag{3.7}$$

Subject to

$$W_{j+1} \geq W_j + W_j^{Port} + \sum_{r\in R_j} \sum_{v\in V} \left(W_{jrv}^{ECA} x_{jrv}^{ECA} + W_{jrv}^{N} x_{jrv}^{N}\right) \qquad j \in J \tag{3.8}$$

$$\sum_{v\in V} x_{jrv}^{ECA} = y_{jr} \qquad j \in J, r \in R_j \tag{3.9}$$

$$\sum_{v\in V} x_{jrv}^{N} = y_{jr} \qquad j \in J, r \in R_j \tag{3.10}$$

$$\sum_{r\in R_j} y_{jr} = 1 \qquad j \in J \tag{3.11}$$

$$y_{jr} \in \{0,1\} \qquad j \in J, r \in R_j \tag{3.12}$$

$$x_{jrv}^{ECA},\ x_{jrv}^{N} \geq 0 \qquad j \in J, r \in R_j, v \in V \tag{3.13}$$

The objective function (3.7) minimizes the total fuel costs for a single loop. It consists of both MGO and HFO/ULSFO consumed on ECA and non-ECA stretches. Moreover, since the relationship between fuel consumption and speed is non-linear, we use a piecewise linearisation approach to handle the non-linearity in the computational study. The continuous sailing speed of a ship is then discretized into several speed points with known fuel consumption per unit distance. The speed related decision variables, x_{jrv}^{ECA} and x_{jrv}^{N}, represent the weights (summing to 1) of a certain speed point adopted in the solution. For example, if we know two speed points and their fuel consumption rates, Speed A (15 knots / 0.1 tons per nautical mile) and Speed B (25 knots / 0.3 tons per nautical mile), with a weight of 0.5 assigned to each speed, then the actual speed adopted in this example is $0.5*15+0.5*25 = 20$ knots while the corresponding fuel consumption at 20 knots is $0.5*0.1+0.5*0.3 = 0.2$ tons per nautical mile. A similar approach is also used to handle the estimation of travel time with discrete speed points. For more details about this piecewise linearisation technique, please see page 235 of Andersson et al. (2015). Constraints (3.8) guarantee that the starting time for a certain leg plus the service time at port and the corresponding travelling time needed on this leg will not exceed the scheduled starting time for next leg. Constraints (3.9) and (3.10) ensure that if a leg option is used ($y_{jr} = 1$), the sum of the speed weight variables on that leg option must equal 1 as well. Otherwise, the sum should be 0. This means a certain speed of the ship is used on a certain leg option if and only if that leg option itself is used. Constraints (3.11) state that one and only one leg option can be used on each leg. Otherwise, the speed is 0. Constraints (3.12) and (3.13) impose the binary and non-negativity requirements to the decision variables. In general, this model enables the

vessel to flexibly apply ECA-evasion and speed differentiation strategies and select the most suitable speed-routing choices based on the given fuel prices so that the operational costs of a round trip is minimized. For more details regarding the sailing pattern optimization, please see Fagerholt et al. (2015).

Finally, the NPV form of the total operational costs of the fuel-switching approach during the lifespan with the consideration of sailing pattern can be expressed as:

$$Cost^{operation}_{fuel\text{-}switching} = \sum_{t=0}^{T} \frac{n \times Cost^{loop}_{fuel\text{-}switching}}{(1+d)^t} \tag{3.14}$$

3.3 Test case

In this paper, we consider a shipping company assigning a new ship to a regular service on a specific loop with ECA involvement. The challenge faced by the shipping company is to decide which emission abatement technology they should invest in so as to comply with the ECA regulation and simultaneously minimize the total costs during the lifespan of that technology. Section 3.3.1 gives the general background settings of the test case while Section 3.3.2 introduces details regarding the different loops tested in this paper.

3.3.1 General information

Detailed information about the general settings in the test case is listed in Table 3.1. The vessel involved in the test is assumed to be a new container ship which started operating from 1st January 2015. The container ship has a capacity of 6000 TEU and its main engine power is 48000 kW. The minimum and maximum sailing speed of the ship is assumed to be 15 and 24 knots respectively. Within this speed range, we select seven speed points as input for the model. The fuel consumption per unit distance of these points are adopted from Notteboom and Cariou (2009) and is shown in Fig. 3.4.

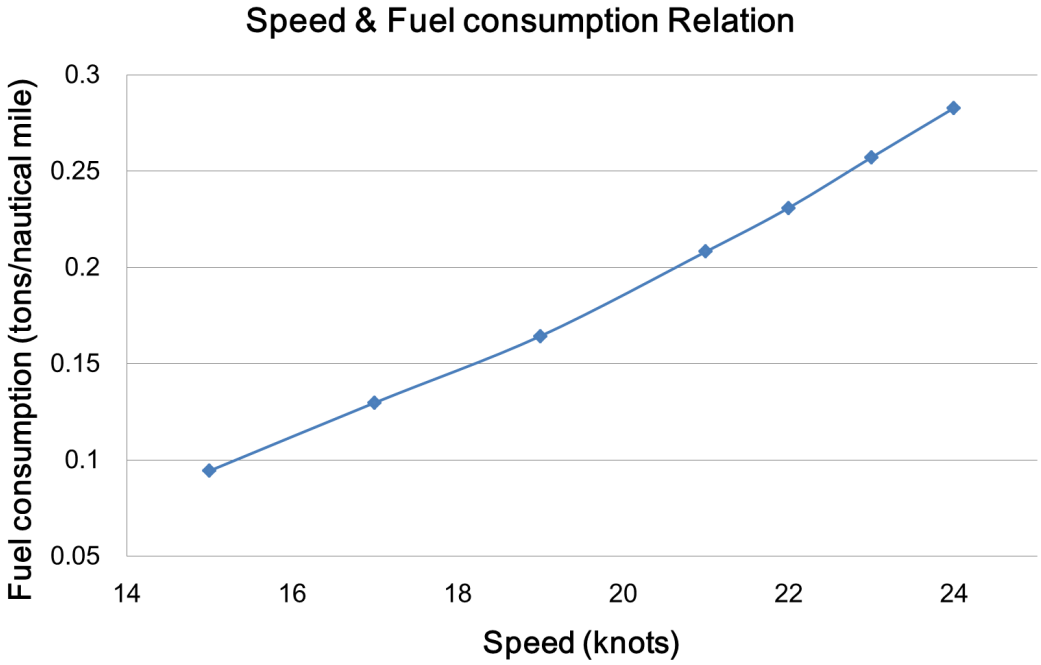

Figure 3.4: Fuel consumption rate for the selected speed points

Table 3.1: General settings in the test case

Ship assumptions	
Start service from	1st January 2015
Container capacity	6000 TEU
Main engine power	48000 kW
Speed range	15 – 24 knots
Assumptions for the scrubber system	
Lifespan	15 yeas
Initial capital cost	135 USD/kW
Annual maintenance cost	1% of the total capital cost
Off-hire cost	0 (newbuilding)
Cargo capacity loss	1%
Earnings	23000 USD/day
Days at sea	320 days/year
Annual cost of cargo capacity loss	$1\% \times 20000\ (USD/day) \times 320\ (days)$
Assumptions for fuel prices	
HFO	200 USD/ton
ULSFO	250 USD/ton
MGO	250 – 1000 USD/ton
Other assumptions	
Cost of capital	9%

The commonly used lifespan of the scrubber system in a newbuilding is 15 yeas which is also accepted in our tests. The capital costs for the scrubber system is assumed to be 135 USD/kW, while the annual maintenance cost for the system on a large vessel (main engine power $>$ 15000 kW) is considered to be 1% of the total capital costs (Entec, 2005). Since the scrubber system can be installed during the construction of the new ship, the off-hire cost is assumed to be 0. Moreover, the cargo capacity loss due to the installation of a scrubber system can be 2% in a retrofitting case (Brynolf et al., 2014). In the newbuilding case, however, the system can normally be better integrated in the ship design phase, which leads to a smaller space sacrifice and thus a lower cargo capacity loss. Therefore, we consider cargo capacity loss of 1% for the scrubber system on a newly built vessel in this paper. Meanwhile, the time-charter rate for a 6000 TEU container ship is assumed to be 23000 USD/day according to the historical data collected from June 2012 to November 2016 (Clarkson, 2018a), and the vessel is chartered out for 320 days a year. Then the annual cost caused by the cargo capacity loss equals 1% of the annual revenue of the vessel.

In the test, the prices of the fuels used outside the ECA are fixed while the the price of MGO varies. The fuels used outside ECA will be HFO (before 2020) and ULSFO (after 2020) if a fuel-switching approach is used. The price of the HFO is set to 200 USD/ton. The ULSFO is currently not available on the market and hence no price data for this fuel can be found. However, the price of ULSFO is estimated to be 20% higher than the LS 380 fuel (Notteboom et al., 2010) which, on average, is approximately 5% more expensive than the HFO according to the historical fuel price data collected for the port of Rotterdam from 2012 to 2014 (Clarkson, 2018a). Therefore, we assume the price of ULSFO to be 250 USD/ton. On the other hand, the price of MGO used inside ECA changes from 250 to 1000 USD/ton during the computational study. Finally, the cost of capital (discount rate) applied in this paper is set to be 9%.

3.3.2 Test loops

Three different loops between Europe and North America are are adopted in the test in this paper. Loop 1 contain three port calls while Loop 2 and 3 comprise four and seven port calls respectively. The details of the port calls and their corresponding sequence in the three loops can be found in Table 3.2. The cycle times for a round trip on the three loops are all assumed to be 40 days which includes 25 sailing days and 15 port days. Hence, a ship can finish $n = 8$ round trips per year. The sailing days are then assigned to each leg according to the shortest distance between two ports on that leg. Meanwhile, the port days are evenly distributed to all the port calls in each loop. Please note that the port time here is only for modelling purposes. It does not affect the speed and routing decisions in the optimization model and therefore has no impact on the final results.

Table 3.2: Details of port calls in the test loops

Loop 1 - Three Ports

Leg	*From*	*To*	*Shortest distance (nautical miles)*	*Sea days*	*Port days*
1	Gothenburg	Halifax	2860	6.95	5
2	Halifax	Houston	2323	5.65	5
3	Houston	Gothenburg	5105	12.40	5
				25	**15**

Loop 2 - Four Ports

Leg	*From*	*To*	*Shortest distance (nautical miles)*	*Sea days*	*Port days*
1	Gothenburg	Halifax	2860	6.87	3.75
2	Halifax	Norfolk	752	1.81	3.75
3	Norfolk	Houston	1683	4.05	3.75
4	Houston	Gothenburg	5105	12.27	3.75
				25	**15**

Loop 3 - Seven Ports

Leg	*From*	*To*	*Shortest distance (nautical miles)*	*Sea days*	*Port days*
1	Gothenburg	Halifax	2860	6.81	2.14
2	Halifax	New York	549	1.31	2.14
3	New York	Wilmington	485	1.16	2.14
4	Wilmington	Canaveral	361	0.86	2.14
5	Canaveral	Miami	491	1.17	2.14
6	Miami	Houston	641	1.53	2.14
7	Houston	Gothenburg	5105	12.16	2.14
				25	**15**

Furthermore, for each leg in a loop, we assign five leg options. Different leg options of a certain leg share origin and destination ports, but the sailing route and thus the ECA, non-ECA and total sailing distance of these leg options are different. For instance, Fig. 3.5 illustrates the five leg options of Leg 2 in Loop 2 (Halifax - Norfolk). Among all route alternatives, Leg Option 1 sails the shortest path between two ports, which is exactly the same as the traditional route used before ECA was introduced. However, Leg Option 5 takes the route with minimum ECA involvement although it leads to the longest total travelling distance. The other three leg options compromise differently between total sailing distance and ECA involvement. The detailed information regarding sailing distance on ECA/non-ECA stretches for all leg options in each loop can be found in Table 3.3.

3.4 Computational study

The influence of sailing pattern on the selection of sulphur emission abatement technology is firstly revealed in Section 3.4.1. Then in Section 3.4.2, we investigate how port call density inside ECA affects the emission reduction choice when sailing pattern is considered.

3.4.1 The impact of sailing pattern

We first calculate and compare the lifespan cost of the scrubber system and the fuel-switching approach on Loop 1 (3 ports). The lifespan cost difference ($Cost^{life}_{difference}$) between the two technologies under different MGO prices are shown in Fig. 3.6. Since the prices for the

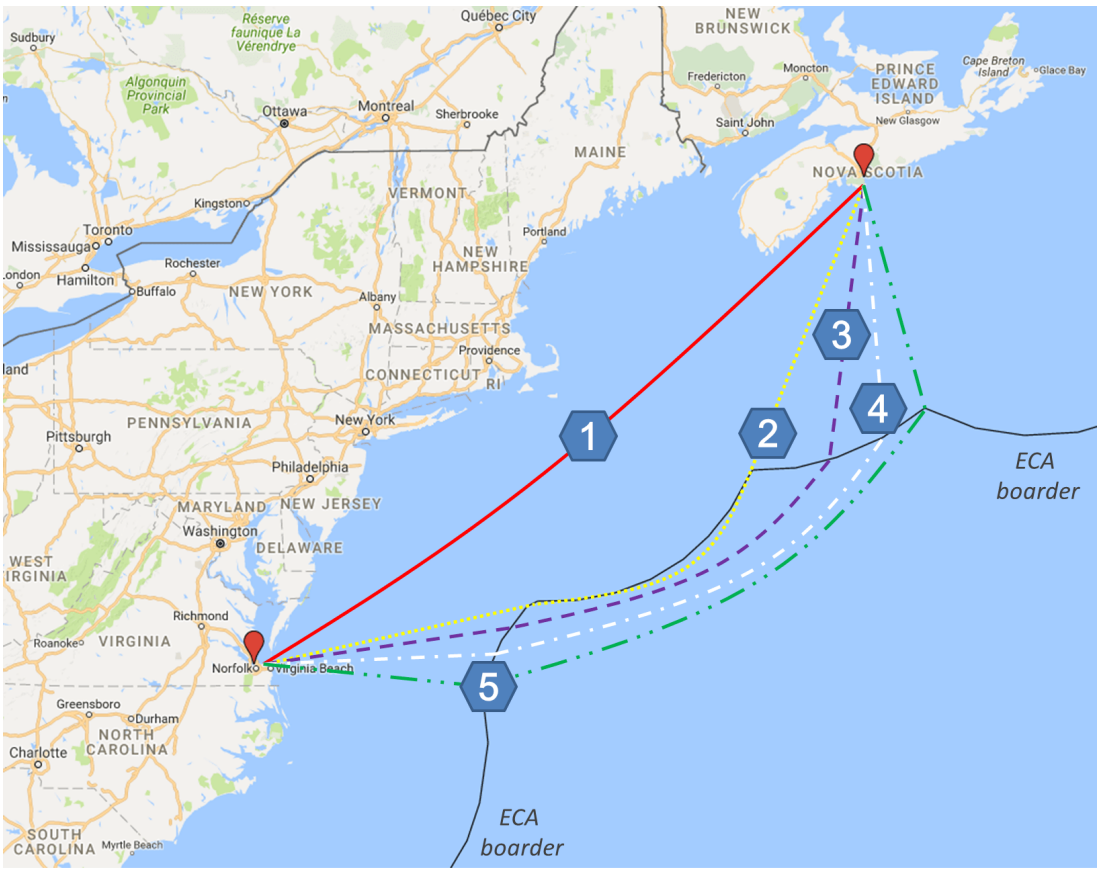

Figure 3.5: Five leg options for Leg 2 of Loop 2 (Halifax - Norfolk) (Google Maps, 2016)

Table 3.3: Detailed information for the leg options in each loop

Loop 1 (ECA/non ECA - nautical mile)

	Option 1	Option 2	Option 3	Option 4	Option 5
Leg 1	1225/1635	1133/1938	848/2302	788/2517	664/2760
Leg 2	2285/38	906/1477	624/1789	541/1925	442/2164
Leg 3	2422/2683	1586/3681	1257/4062	781/4610	661/4877

Loop 2 (ECA/non ECA - nautical mile)

	Option 1	Option 2	Option 3	Option 4	Option 5
Leg 1	1225/1635	1133/1938	848/2302	788/2517	664/2760
Leg 2	753/0	585/264	538/337	498/410	453/512
Leg 3	1652/31	1327/390	809/956	556/1432	455/1704
Leg 4	2422/2683	1586/3681	1257/4062	781/4610	661/4877

Loop 3 (ECA/non ECA - nautical mile)

	Option 1	Option 2	Option 3	Option 4	Option 5
Leg 1	1225/1635	1133/1938	848/2302	788/2517	664/2760
Leg 2	549/0	525/292	492/349	464/400	449/440
Leg 3	485/0	469/348	452/390	436/431	423/477
Leg 4	361/0	298/254	287/265	276/282	265/348
Leg 5	491/0	415/118	335/229	307/299	287/361
Leg 6	641/0	565/171	467/303	413/400	397/465
Leg 7	2422/2683	1586/3681	1257/4062	781/4610	661/4877

fuels outside ECA, HFO (before 2020) and ULSFO (after 2020), are fixed in the test, see Table 3.1, different MGO prices also represents different levels of price gap between fuels allowed in- and outside ECA. As mentioned in Section 3.2.2, a negative lifespan cost difference means that the fuel-switching approach has a lower total cost during the whole life cycle and thus is the optimal choice. A positive difference refers to the opposite. The solid line in Fig. 3.6a represents the lifespan cost difference under the assumption that sailing pattern is considered while the dashed line refers to the difference when sailing pattern is ignored.

Figure 3.6a shows that the break-even point for applying the scrubber system can be significantly different based on whether or not the sailing pattern is considered in the evaluation. In the former case a ship will switch to a scrubber system when the expected MGO price is higher than 540 USD/ton, while in the latter case the scrubber system will be used when the MGO

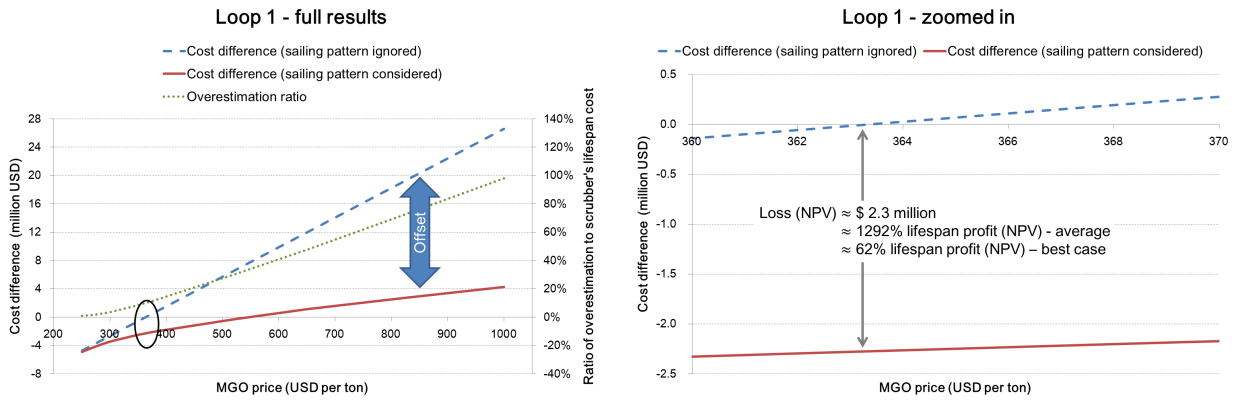

(a) Complete test result

(b) Potential loss

Figure 3.6: Cost difference between fuel-switching and scrubber system in Loop 1

price hits merely 363 USD/ton. In the case that a ship's sailing pattern is ignored, an incorrect investment decision will be made when the expected MGO price is still far from the real break-even point, which means the value of the scrubber system is significantly overestimated. In the worst case, such overestimation can reach 98% of the life cycle cost of the scrubber system when the expected MGO price is high.

The reason for such an overestimation can be explained as follows. In the case that a ship's sailing pattern is not considered, the vessel is assumed to be operated in the traditional way (the shortest path and fixed speed). Therefore, the fuel consumption in such a case is fixed no matter what emission reduction technology is installed, and the value of a scrubber increases linearly with the expected MGO price (dashed line). However, when a ship is allowed to optimize its navigation, a more aggressive sailing pattern will be adopted by a ship with fuel-switching on board in order to reduce the consumption of expensive MGO. A more aggressive sailing pattern refers to either a routing choice with lower ECA involvement but longer total travelling distance and higher average speed (e.g. Leg Option 5 in Fig. 3.5), or a greater speed differentiation on a certain leg option. Such routing and speed decisions normally lead to lower MGO but higher HFO/ULSFO consumption. The higher the MGO price is, the more aggressive the sailing pattern will be and thus the less MGO is consumed (see Table 3.4). The detailed routing and speed decisions for the table can be found in Appendix 1. In general, the total bunker costs for a ship with fuel-switching, using such an aggressive sailing pattern, becomes much lower than the fuel costs expected under the traditional navigation assumptions since the increasing fuel costs due to the high MGO price are substantially offset by adjusting the routing and speed choices and thus reducing the MGO consumption. Overlooking such offsetting through sailing pattern optimization in the fuel-switching case finally leads to the overestimation of the scrubber option as shown in Figure 3.6a.

Table 3.4: Fuel consumptions and cost offsetting for fuel-switching in Loop 1 under different MGO prices (sailing pattern considered)

MGO Price (USD/ton)	250	400	600	1000
Before 2020				
MGO consumption (ton/round trip)	458.6	251.8	216.6	203.6
HFO consumption (ton/round trip)	793.4	1101.5	1214.7	1257.3
Cost offsetting through sailing pattern optimization (1000 USD/round trip)	5.9	63.3	154.7	358.9
After 2020				
MGO consumption (ton/round trip)	698.8	251.8	251.8	203.6
ULSFO consumption (ton/round trip)	522.7	1101.5	1101.5	1257.3
Cost offsetting through sailing pattern optimization (1000 USD/round trip)	0	34.3	125.4	322.1

The actual consequences of such overestimation in the real world can be vital. Figure 3.6b shows a clearer picture of the circled area in Fig. 3.6a. The results show that if the shipping company ignores ship's sailing pattern and decides to install the scrubber system when the expected MGO price reaches 363 USD/ton, a substantial loss will occur. Instead of using the scrubber system, the shipping company can save 2.3 million USD (NPV) in total in the 15 years if they have selected fuel-switching approach and operated the vessel with proper sailing pattern. A recent survey by Alphaliner (2016) shows that the average margin rate of container shipping companies in 2015 was only slightly positive at 0.3%, while the best player on the market had a 6.3% margin rate. Therefore, for an average shipping company, the 2.3 million USD loss (NPV) is approximately 13 times as high as the NPV of the 15 years' total profit of a single container ship. Even for the best player, such a loss still equals to 62% of the NPV of the total margin.

A similar test is also carried out with the assumption that the vessel is purchased after the introduction of the global sulphur cap in 2020. The purpose of this test is to show the impact of the forthcoming regulation on the problem discussed in this paper. The results in Fig. 3.7a show that the overestimation of the scrubber system still exists if the sailing pattern is not considered. However, the size of the overestimation is smaller. The reason is that after 2020 a ship with fuel-switching has to purely rely on the new fuel (ULSFO) when sailing outside ECA, and ULSFO is more expensive than the current HFO. Therefore, the cost savings now brought by optimizing the sailing pattern through lower MGO but higher ULSFO consumption are smaller than before.

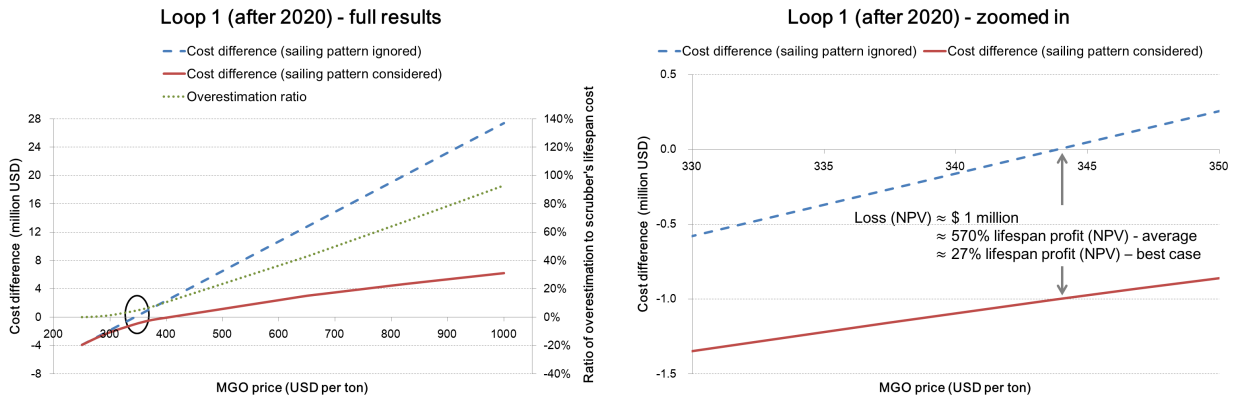

(a) Complete test result

(b) Potential loss

Figure 3.7: Cost difference between fuel-switching and scrubber system in Loop 1

However, the consequence of such a mistake can still be considerable after the global sulphur cap. Figure 3.7b shows that the shipping company can lose one million USD (NPV) due to the overestimation and incorrect investment decision in a scrubber. According to Alphaliner (2016), such a loss is about 6 times higher than the total profit of a single container ship for an average player during the life time of a scrubber, while it also equals 27% of the total margin for the best liner company. Therefore, it is safe to say that the new global sulphur policy does have an influence on the scrubber overestimation issue, but this problem will not automatically be fixed after 2020 and the importance of fixing this knowledge gap remains unchanged.

3.4.2 The impact of port call density in ECA

Besides Loop 1, we further test the effect of sailing pattern on the cost difference between the scrubber system and the fuel-switching approach on Loop 2 and 3. The results in Fig. 3.8

show that if sailing pattern is ignored in the evaluation, we will still be overly optimistic about the value of the scrubber system and experience a considerable loss.

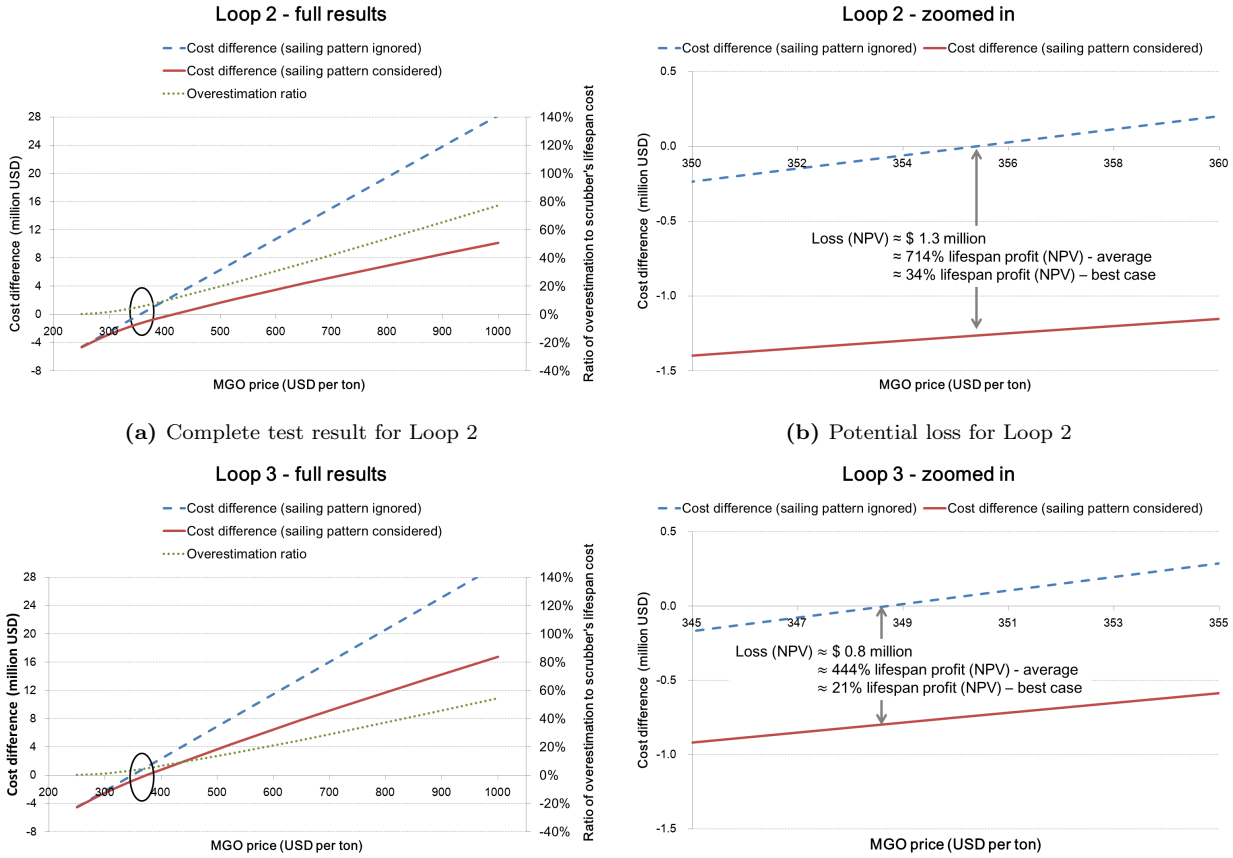

(a) Complete test result for Loop 2

(b) Potential loss for Loop 2

(c) Complete test result for Loop 3

(d) Potential loss for Loop 3

Figure 3.8: Cost difference between fuel-switching and scrubber system in Loop 2 & 3

In Fig. 3.9, the location of the ports in the different test loops are shown on the map. Meanwhile, the lines connecting these ports represents the traditional shortest sailing path. Clearly, the three loops involved in our test have different port call densities inside ECA, but approximately same ECA coverage and thus the same ECA sailing distances if the ships take the direct link between ports. Therefore, from a traditional point of view, it is reasonable to expect that identical optimal emission reduction solutions should be adopted on these loops. This is indeed true when sailing pattern is not considered, since the ships are then assumed to sail the shortest path with no ECA-evasion and speed differentiation. In that case, as shown in Fig. 3.10a, the break-even MGO prices for the scrubber system are nearly the same in the three tests. In the case that sailing pattern is involved in the consideration, however, the situation is totally different. The results in Fig. 3.10b indicate that the impact of sailing pattern on the cost difference between the two alternatives decreases when the port call density inside ECA increases. The overestimation of a scrubber system in Loop 3 is much smaller than those in the other two test. The break-even MGO price for the scrubber system in Loop 3 is also lower (about 370 USD/ton). Hence, even though from a traditional view point, the general ECA involvements in these three loops are similar, the optimal emission reduction choices for these loops are not identical when sailing pattern is considered. The scrubber system will be accepted as the favourite compliance method with a much lower MGO price in the loops with higher port call density inside ECA (e.g., Loop 3), while the vessels in the loops with less ECA port calls (e.g., Loop 1) will stick to the fuel-switching approach for rather high prices.

In order to explain the observed impact of port call density, we must first understand the

(a) Loop 1 - Three ports

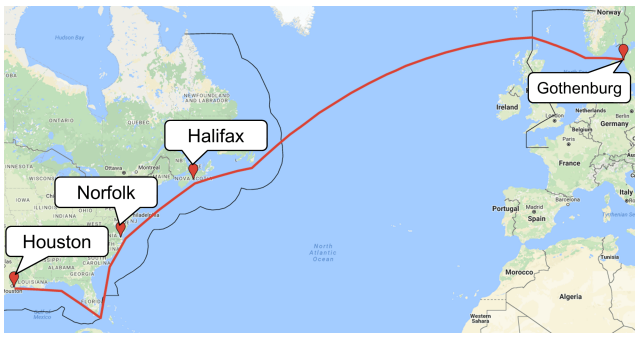

(b) Loop 2 - Four Ports

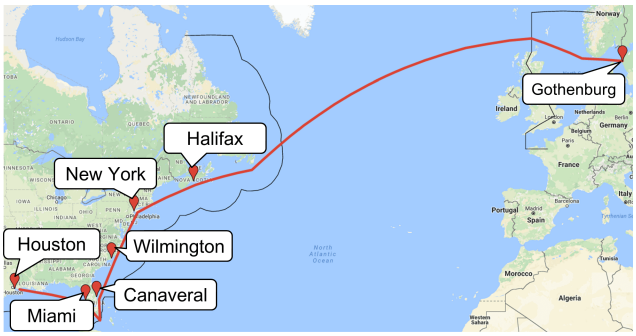

(c) Loop 3 - Seven Ports

Figure 3.9: Illustration of the test loops

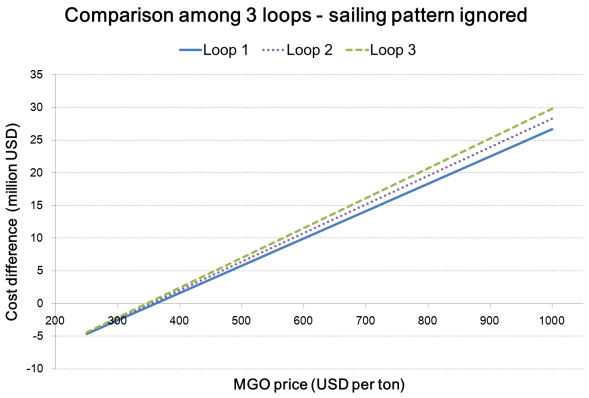

(a) Comparison when sailing pattern is ignored

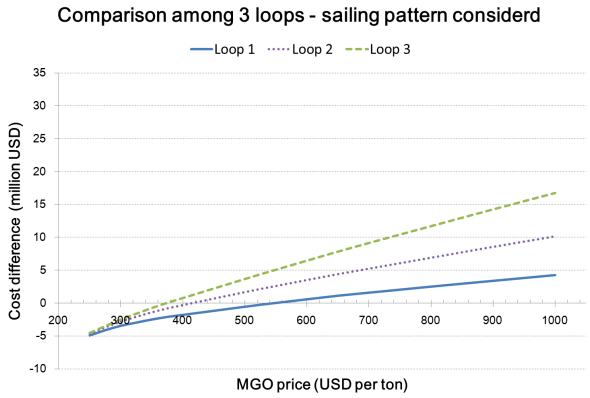

(b) Comparison when sailing pattern is considered

Figure 3.10: Cost difference between fuel-switching and scrubber system in all loops

basic principle of sailing pattern optimization. A simple example (Example 1), as shown in Fig. 3.11, is used for illustration. In Example 1, the vessel with fuel-switching technology on board needs to travel from Port 1 to Port 2. The two ports are located inside ECA and only two leg options are available. The solid line (Option 1) stands for the traditional shortest path while the dashed line (Option 2) represents the leg option with maximized ECA-evasion. The corresponding length of each stretch is given and we assume that $a > 2b$. To simplify, we further assume that the speed of the vessel is fixed at v during the whole voyage and no time constraints are applied. Therefore, the fuel cost of sailing on the two leg options can be

expressed as:

$$Cost^{Option\ 1} = P^{ECA} \times a \times f_v \tag{3.15}$$

$$Cost^{Option\ 2} = P^{ECA} \times 2b \times f_v + P^N \times a \times f_v \tag{3.16}$$

where P^{ECA} and P^N represent the price of fuels used in- and outside ECA, and f_v refers to the fuel consumption per unit distance under the fixed speed v. Therefore, it is easy to induce that the vessel will change its leg option from Option 1 to Option 2 when P^{ECA} becomes $\frac{a}{a-2b}$ times as high as P^N.

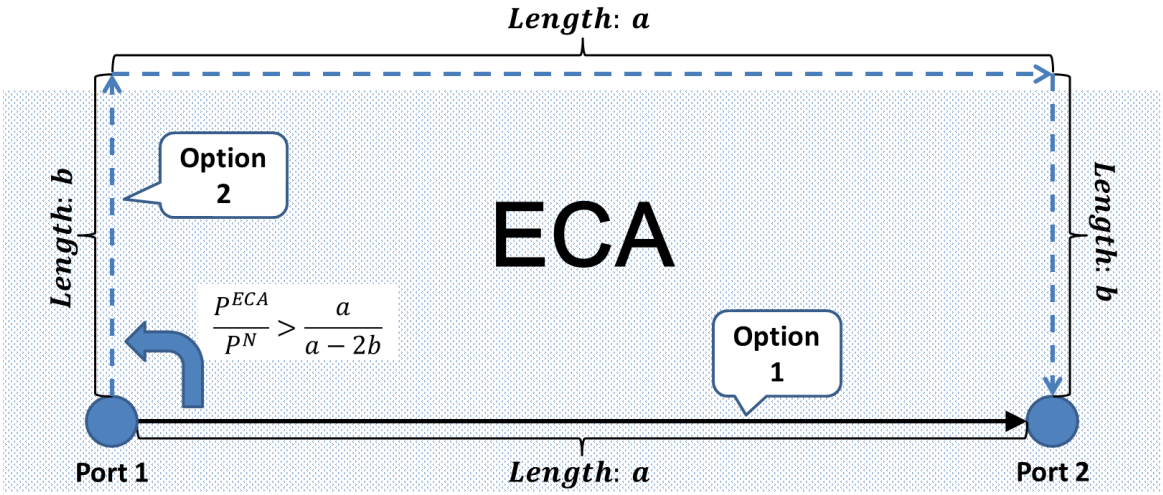

Figure 3.11: Example 1 to illustrate the principle of sailing pattern optimization

Now we increase the port call density in Example 2 by adding one more leg and port call in the previous example, but we keep the ECA coverage (total ECA sailing distance on the shortest path) unchanged, see Fig. 3.12. Again, the solid lines in Fig. 3.12 represent the leg options with shortest sailing distance on each leg, while the dashed lines refer to the leg options with maximized ECA-evasion. Moreover, we still assume that $c, d > 2b$ and the speed is fixed at v. Hence, when $\frac{P^{ECA}}{P^N} > \frac{c}{c-2b}$, the choice of optimal leg option changes from Option 11 to Option 12 on Leg 1. Regarding Leg 2, similarly, Option 22 becomes more cost efficient than Option 21 when P^{ECA} surpasses $\frac{d}{d-2b}$ times P^N. However, it is easy to prove that both $\frac{c}{c-2b}$ and $\frac{d}{d-2b}$ are larger than $\frac{a}{a-2b}$, which means a higher MGO price or a larger price gap between MGO and HFO/ULSFO is needed to trigger sailing pattern optimization when the port call density in ECA is higher (e.g. in Example 2).

Now we bring speed back into consideration and assume the total travelling time in both examples to be t. Hence the average speed needed to use Leg Option 2 in Example 1 is $v^* = \frac{a+2b}{t}$. In the meantime, the sailing times for Leg 1 and Leg 2 in Example 2 are $\frac{ct}{a}$ and $\frac{dt}{a}$ respectively (proportional to their distances on the traditional routes). Therefore, the vessel needs to adopt an average speed of $v_1^* = \frac{a+2ab/c}{t}$ for Option 12 and an average speed of $v_2^* = \frac{a+2ab/d}{t}$ for Option 22 if they are applied. It is easy to see that both v_1^* and v_2^* are bigger than v^*, which means a higher average speed (higher fuel consumption and fuel cost) is needed in Example 2 to apply the leg option with ECA-evasion. Therefore, when the speed

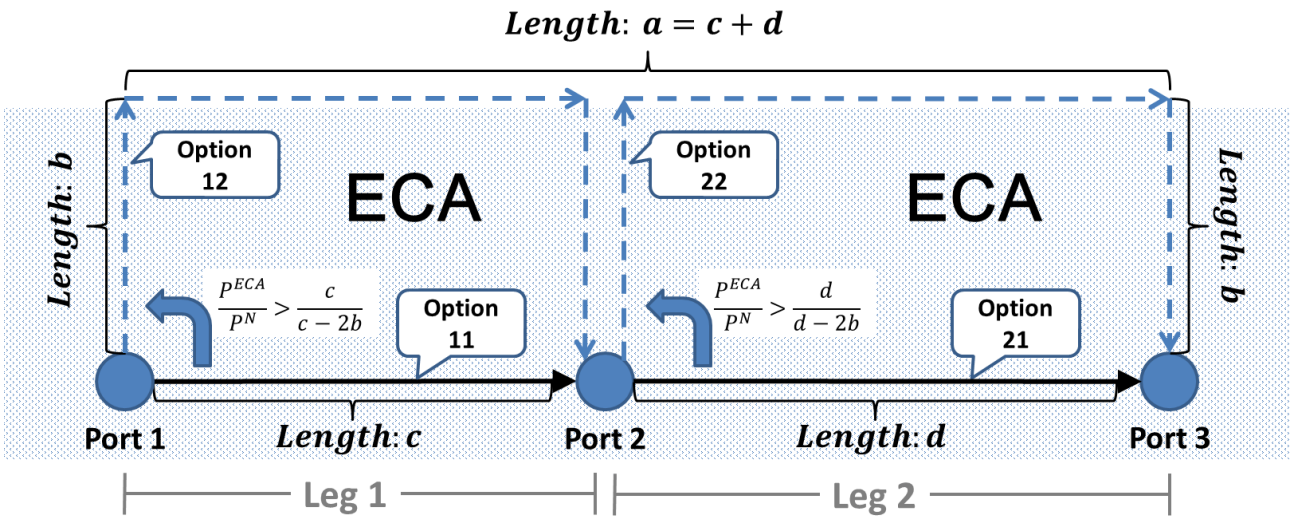

Figure 3.12: Example 2 to illustrate the principle of sailing pattern optimization

factor is considered, it becomes even more difficult to apply sailing pattern optimization in the case with higher ECA port call density.

The underlying reason for the results observed in Fig. 3.10b is well illustrated through the comparison between the two examples. Since it is harder to trigger sailing pattern changes in a loop with higher port call density inside ECA, the sailing pattern (leg option and speed choice) in Loop 3 are very close to the traditional way of navigation (shortest path and fixed speed), while a much more aggressive sailing pattern is adopted in Loop 1 under the same MGO price. Therefore, the savings caused by sailing pattern optimization for the vessels with fuel-switching in Loop 3 are more limited, which makes the overestimation on scrubber less significant. Comparing Fig. 3.10a and Fig. 3.10b, we can see that the break-even MGO prices for Loop 3 in both cases are very close (insignificant overestimation) while the beak-even MGO prices for Loop 1 in the two figures are very different (substantial overestimation). Hence, under certain circumstances, shipping companies that have fewer port calls inside ECA should be more worried about the scrubber problem discussed in this paper.

Normally, shipping companies and researchers only consider the travelling distance inside ECA when they evaluate a compliance method. However, the test results have clearly shown that the port call density inside ECA also affects a ship's sailing pattern and thus influences the operating costs. Therefore, it is important for us to include both considerations in the decision-making process. Fig. 3.10 shows that with similar ECA coverage, the scrubber system is more attractive for a vessel sailing in a loop with higher port call density in ECA, while the fuel-switching is more favourable in the opposite case.

3.5 Conclusion

After the ECA regulation was introduced, the selection of sulphur emission abatement technology becomes vital for shipping companies with business inside the regulated zones. The choice of sulphur emission control method used on board will not only affect the vessel's compliance with ECA regulation but also impact the financial costs of the shipping company substantially. Recent studies show that a vessel with fuel-switching technology has incentives to optimize its sailing pattern when sails inside ECA. However, none of the literature has integrated such sailing pattern optimization into the evaluation and selection of ECA compliance method.

In this paper we use a mathematical programming model to compare the lifespan cost of a scrubber system and a fuel-switching approach. Different from the classical cost assessment

model used in the current literature, the proposed model in this paper integrates the optimization of ship's sailing pattern into the evaluation. Compared to previous work, the results in this study show that the value of scrubber can be significantly overestimated and an incorrect emission reduction technology for ECA may be selected if a ship's sailing pattern is not considered in the decision-making process. Optimal decisions regarding ECA compliance can only be achieved by using an evaluation method which involves a ship's sailing pattern. Otherwise, a substantial loss may occur. Moreover, this study also points out that the port call density inside ECA will affect a ship's emission reduction choice, while previous works mainly focus on the sailing distance in ECA. The computational results show that the overestimation of scrubber becomes less severe when the port calls inside ECA on a voyage are denser. The scrubber system should be more attractive for shipping companies that have higher ECA port call density on their trade lines, while the fuel-switching approach is more suitable for vessels operating on loops with fewer port calls in ECA.

To summarize, this paper has two major contributions. First of all, it points to a knowledge gap in the literature, namely that a ship's sailing pattern must be included in the evaluation of sulphur emission control methods for ECA regulation. Potential severe financial consequences of this knowledge gap are revealed. Secondly, this paper integrates the optimization of a ship's sailing pattern into the lifespan cost assessment model for different compliance methods, thereby expanding earlier work.

Appendix 3.1

The detailed speed-routing decisions for the fuel-switching approach in Loop 1 under different MGO prices when sailing pattern optimization are considered are given in the following table.

Table 3.5: Speed-routing decisions for fuel-switching in Loop 1 under different MGO prices (sailing pattern optimization considered)

MGO Price (USD/ton)	250	400	600	1000
Leg 1				
Leg Option Before[After] 2020	1[1]	1[1]	3[1]	3[3]
ECA/non-ECA/Total distance (nautical mile) Before[After]	1225/1635/2860 [1225/1635/2860]	1225/1635/2860 [1225/1635/2860]	848/2302/3150 [1225/1635/2860]	848/2302/3150 [848/2302/3150]
ECA/non-ECA/Average speed (knot) Before[After] 2020	15.0/17.4/16.3 [16.3/16.3/16.3]	15.0/17.4/16.3 [15.0/17.4/16.3]	15.0/18.1/17.3 [15.0/17.4/16.3]	15.0/18.1/17.3 [15.0/18.1/17.3]
Leg 2				
Leg Option Before[After] 2020	2[1]	3[3]	3[3]	4[4]
ECA/non-ECA/Total distance (nautical mile) Before[After]	906/1477/2383 [2285/38/2323]	624/1789/2414 [624/1789/2414]	624/1789/2414 [624/1789/2414]	541/1925/2466 [541/1925/2466]
ECA/non-ECA/Average speed (knot) Before[After] 2020	16.6/17.0/16.8 [16.4/16.4/16.4]	15.0/17.9/17.0 [15.0/17.9/17.0]	15.0/17.9/17.0 [15.0/17.9/17.0]	15.0/18.3/17.4 [15.0/18.3/17.4]
Leg 3				
Leg Option Before[After] 2020	1[1]	4[4]	4[4]	4[4]
ECA/non-ECA/Total distance (nautical mile) Before[After]	2422/2683/5105 [2422/2683/5105]	781/4610/5391 [781/4610/5391]	781/4610/5391 [781/4610/5391]	781/4610/5391 [781/4610/5391]
ECA/non-ECA/Average speed (knot) Before[After] 2020	15.0/17.5/16.4 [16.4/16.4/16.4]	15.0/17.2/17.0 [15.0/17.2/17.0]	15.0/17.2/17.0 [15.0/17.2/17.0]	15.0/17.2/17.0 [15.0/17.2/17.0]

Chapter 4

Can the Maritime Emission Trading Scheme reduce CO_2 emissions in the short term? Evidence from a maritime fleet composition and deployment model

Yewen Gu[1], Stein W. Wallace[1], Xin Wang[2]

[1]Department of Business and Management Science, Norwegian School of Economics, Bergen, Norway
[2]Department of Industrial Economics and Technology Management, Norwegian University of Science and Technology, Trondheim, Norway

Abstract

Global warming is a major challenge for this planet, and its solution requires efforts from the whole mankind. Maritime transportation, which carries more than 90% of the global trade, plays a critical role in the contribution of greenhouse gas (GHG) emissions. However, the GHGs emitted by the global fleet still falls outside the emission reduction scheme established by the Kyoto Protocol. Alternative solutions are therefore sought. Several market-based measures are proposed and submitted to IMO for discussion and evaluation. In this paper, we focus on one of these measures, namely the Maritime Emissions Trading Scheme (METS). An optimization model integrating the classical fleet composition and deployment problem, but including of METS (global or regional) is proposed. This model is used as a tool to study the actual impact of METS on fleet operations and corresponding CO_2 emissions. The results of the computational study suggest that in the short term the implementation of METS may not guarantee further emission reductions in certain situations. However, in other scenarios with low bunker prices, high allowance costs or global METS coverage, a more significant CO_2 decrease in the short term can be expected.

Keywords: Maritime Emission Trading Scheme, market-based measure, fleet composition and deployment, CO_2 emissions

4.1 Introduction

Global warming has become a major issue in the past decades, particularly since it is a challenge needing global solutions. The emission of greenhouse gasses (GHGs) is the main reason for global warming, and one of the major sources of GHG emissions is transportation. Maritime transportation, which carries more than 90% of the global trade (ICS, 2017), plays a critical role. Although the CO_2 emission per tonne-km for shipping is only around 30% of that of road transport, maritime transport still accounts for 15% of the global transport CO_2 emissions (Goldsworthy, 2010) and 2.6% the global anthropogenic CO_2 emission (IMO, 2014). Furthermore, according to Buhaug (2009), the GHG emissions from ships are expected to increase by 150 - 250% in the next few decades if the world trade continuously increases without a proper measure for mitigation.

Recently, the support for implementing a market-based measure (MBM) in the shipping sector has become strong. An MBM addresses the negative externalities of a market, such as pollution, through market mechanisms. Different from command-and-control measures (e.g., legislations), an MBM offers economic incentives rather than fixed rules to achieve a more cost-effective and sustainable pollution control (Miola et al., 2011). In terms of shipping, an MBM can help to internalise the external costs of the fleet emission by making the ship owner or operator pay for the CO_2 emitted from their ships, which finally creates an incentive for them to cut the emissions (Psaraftis, 2012).

Although seven MBM proposals have been submitted to the IMO for discussion and evaluation, it seems that only two of them, namely the Emissions Trading Scheme (ETS) and the GHG Fund, are favoured and widely studied in the literature (Shi, 2016). The ETS is a type of cap-and-trade system. In such a system, first a legally binding limit on total emissions (cap) during a certain period is set by the authority. Then the equivalent amount of emission allowances are issued by the administration and assigned to or purchased by different concerned parties. In the system, participants can choose to submit the allowance for their own emissions or trade with other players for cash based on the market price of the allowance. However, if all the issued allowances are consumed, no more emissions will be allowed due to the legal limit. Such a market-based cap-and-trade system will help achieve the emission reduction target with certainty as well as minimal costs. However, the uncertainty of the allowance price may cause problems, for example cost volatility and investment risks for the participants. The application of an ETS can be either global or regional. On the other hand, the GHG Fund proposal can be considered as a bunker levy scheme. In such a scheme, a fixed levy will be collected by the authority from the ship owners or operators based on their fuel consumption and the money raised will eventually enter the GHG Fund and finance future CO_2 emission reduction projects. Compared to the ETS approach, the bunker levy scheme guarantees the CO_2 price and therefore brings less volatility and risk to the shipping industry. However, the reduction of CO_2 emissions remains uncertain under such a scheme. In this paper, we choose to focus on the Maritime Emission Trading Scheme (METS) option (Kågeson, 2008) as the potential MBM for emission reduction in maritime transportation.

In general, the expected emission reduction brought by the MBM (METS in this paper) can be divided into long-term and short-term effects. In the long term, the market-based scheme offers strong incentives for the shipping companies to invest more in technological change and innovation, which can help them significantly reduce their vessel's CO_2 emissions and save money (IMO, 2011). Normally, such emission reduction will not occur immediately due to the difficulties of technological breakthroughs. Hence, such reduction effects are expected in the long term. On the other hand, the amount of CO_2 emitted from a ship is proportional to its fuel consumption which is positively correlated to the ship's sailing speed. In the short term, therefore, the shipping companies may also slow down their ships in order to reduce the fuel

consumption, and thus reduce the emissions and the corresponding METS allowance costs.

However, the fuel consumption and corresponding CO_2 emissions of a ship depend not only on its sailing speed but also on its sailing route. Moreover, the price of CO_2 allowance is just one of many factors that will affect a ship's sailing speed and route. Other factors, such as fuel price and charter rate, can impact these operational decisions as well. Therefore, whether or to what extent an METS can cut the CO_2 emissions of a ship, based on its daily operations in the short term, remains unclear and should be examined. Therefore, in this paper we propose an optimization model integrating the fleet composition and deployment problem with the application of METS (global or regional). Note that the main purpose of this study is not to develop a practical model for direct application. In the computational study, however, we use this model as a tool to test and observe the actual impacts of METS on short-term emission reduction in different scenarios. Other variables, including fuel price and charter rate, are also investigated. We believe that through this study, a better understanding of METS (especially its ability to decrease CO_2 emissions in the short term) can be reached, which may help policy makers to make a more informed decisions in the future.

The rest of the paper is organized as follows. A comprehensive literature review is made in Section 4.2. The description of the problem and research assumptions are given in Section 4.3, while in Section 4.4, the mathematical formulation of the optimization model is presented. Section 4.5 introduces the test case and the relevant settings. In Section 4.6, the results of the computational study and the corresponding insights are shown and explained. Finally, we conclude this paper in Section 4.7.

4.2 Literature review

The maritime fleet composition and deployment are two classical problems which have been intensively studied in the literature of operations research in maritime transportation. The maritime fleet composition decisions affects the size and mix of the fleet in a shipping company, while the fleet deployment aims to find the optimal match between available transport capacity and freight demand. The readers can find more comprehensive information about these two types of problem in the surveys conducted by Wang and Meng (2017) and Pantuso et al. (2014). Wang et al. (2017) develop a stochastic programming model that integrates the fleet composition and deployment problem. In this paper, we further extend the model by taking the environmental policies into consideration.

The shipping industry falls outside the scheme of GHG emissions reduction established by the Kyoto Protocol. Alternative solutions are therefore necessary. The Marine Environment Protection Committee (MEPC) of the International Maritime Organization (IMO) has made its efforts. Two new measures, namely Energy Efficiency Design Index (EEDI) and Ship Energy Efficiency Management Plan (SEEMP), were adopted in the MARPOL Annex VI and came in to force in 2013 (IMO, 2013). The former (EEDI) is a non-prescriptive but performance-based mechanism which puts mandatory technical requirement on the ship design so that the required energy efficiency level can be attained. Meanwhile, the latter (SEEMP) builds a scheme to improve the energy efficiency of shipping from an operational perspective. Nevertheless, Shi (2016) argues that the technical approach may not achieve breakthroughs in the short run, while the operational measure can bring negative impacts (e.g., longer supply chain lead times) on international seaborne trade. Hence, using EEDI and SEEMP alone may not achieve absolute emission reductions from shipping and market-based measures (MBMs) should be adopted to complete the whole mechanism.

Studies dealing with METS are limited in the literature. Psaraftis (2012) and Psaraftis (2016) comprehensively review all the potential MBMs (including the METS) proposed to the IMO and analyse their pros and cons. Meanwhile, Kågeson (2007) and Kågeson (2008)

discuss the most basic details of the METS proposal, such as cap setting, allowance allocation and use of revenues. Luo (2013) evaluates the impact of adopting an open METS on various perspectives, for instance world trade pattern, net exporting countries and market concentration in the shipping industry. Miola et al. (2011) discuss the possibility of including the shipping sector in the existing EU ETS and compare this proposal with other alternatives, such as a bunker levy scheme and Maritime Sector Crediting Mechanism (MSCM). Shi (2016) examines whether now is the right timing to adopt ETS in shipping, and suggests his own revised MBM based on existing solutions. Koesler et al. (2015) conduct a case study involving ship operators to assess the organizational and operational implications of the METS on shipping companies. The results of this study show that shipping companies are optimistic about the potential performance of METS. Franc and Sutto (2014) explore the impacts of a cap-and-trade system on liner companies and European ports. Substantial and differentiated effects in different scenarios are found in this study. Wang et al. (2015) compare the applications of METS in an open and in a maritime only environment. The paper shows that the sailing speed of vessels will decrease in both cases, while challenges for specific shipping sectors vary from scenario to scenario. Gritsenko (2017) carries out a qualitative research discussing the suitable geographical scope of METS. Hermeling et al. (2015) conduct an analysis of including shipping in the current EU ETS from both economic and legal considerations. They argue that such an attempt may run into a dilemma where it is difficult to achieve a cost efficient emission reduction and comply with the existing international law simultaneously.

Obviously, the advantages and disadvantages of applying METS are properly discussed according to the literature review. To the best of our knowledge, however, no previous paper has quantitatively examined the short-term emission reduction performance of a global or regional METS together with the consideration of other determining factors, for instance fuel price and charter rate. As mentioned in the previous section, these factors also affect a fleet's operation and hence its CO_2 emission in the short term. Any analysis without seeing the whole picture and ignoring these determining factors can lead to an incorrect estimation of METS on its capability of emission reduction in the short term.

4.3 Problem description and assumptions

In the traditional maritime fleet composition and deployment problem, a shipping company needs to make a plan so that its fleet is optimally utilized to fulfil the shippers' demands in the next planning period. The demands from the customers normally consist of two parts, the fixed contracts which are mandatory and the spot cargoes which are optional. In order to meet the specific volume and frequency requirements of these demands, the shipping company has to first ensure enough ships and cargo capacity available. Hence they need to decide the number and type of ships to time-charter in from the spot market. In the mean time, the company also has to think about how to deploy and operate these ships, so that the demands of the consignors are fulfilled in a timely and cost efficient manner.

In this paper, the concept of *trade lanes* between geographical areas is introduced. The trade lanes are considered as the carrier of a highly abstracted demand of freight transportation. Such high level abstraction can also be found in the literature, e.g., Pantuso et al. (2016) and Wang et al. (2017). In a trade lane, ships pick up different cargoes from a number of adjacent loading ports located in the same geographical area, then transport these cargoes to another geographical area and finally unload the cargoes at the corresponding destination ports. An example trade lane from Western Europe to the East Coast of the US can be found in Figure 4.1. In this example, cargoes from three loading ports in Western Europe are collected first, then transported cross the Atlantic Ocean and finally delivered at the unloading points in the US. If the demands served by the trade lane are contractual, specific frequency requirement (e.g.,

once every month) may need to be fulfilled. Furthermore, the type of ship that can serve the trade lane may also be restricted if there is a cargo compatibility issue, typically in the bulk or tanker sectors.

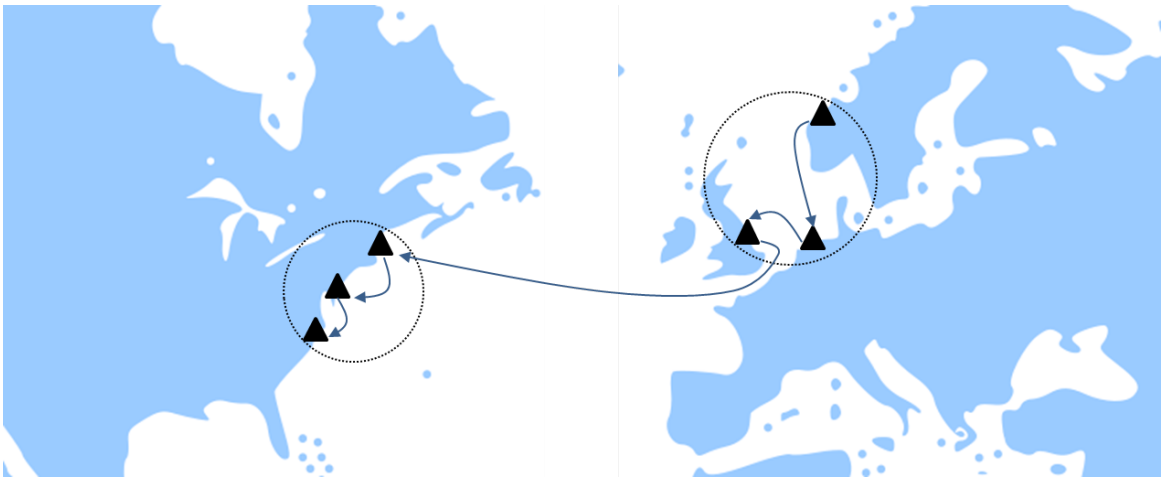

Figure 4.1: An example of trade lane from Western Europe to the East Coast of the US

Besides these classical settings in the maritime fleet composition and deployment problem, some additional new decisions need to be made by the shipping company due to the implementation of METS. First, the company has to decide the amount of emission allowance they want to buy so that the CO_2 emission of its fleet can be covered. Moreover, if the METS is regional, the operation cost inside the regulated areas will be higher than the cost outside due to the extra allowance cost for the METS regions. Such cost difference offers the shipping company an incentive to differentiate its vessel's speed in- and outside the METS regions. For instance, in Figure 4.2, the ship can choose to slow down inside METS areas so as to emit less CO_2 and consume less allowances, which helps to save money. However, the sailing speed outside METS areas may increase so that the total travelling time or transport capacity can still be guaranteed. In general, the total cost can be minimized through such a speed differentiation strategy. Hence, rather than one universal speed, the shipping company now needs to make two separate speed decisions for a single voyage which crosses the border of the METS areas. Similar applications of speed differentiation can also be found in the cases of the Emission Control Area in e.g., Fagerholt et al. (2015), Gu and Wallace (2017) and Gu et al. (2018b).

The shipping company's aim is to minimize its total cost from both tactical and operational levels. On the tactical level, caused by the METS, the fixed cost in this new fleet composition and deployment problem consists of the chartering expenses and the allowance procurement fees. The chartering strategy offers an adequate number of ships and cargo capacity, while the purchasing of allowance, on the other hand, ensures the emission of the fleet during operation complies with the regulation of METS. However, if there is an excess transport capacity in the existing fleet of the shipping company or a surplus of unused allowance, the company can charter out the redundant vessel and sell the unneeded allowance on the spot market for profit. On the operational level, the variable cost (mainly fuel consumption) is affected by the decisions of routing, ship deployment and sailing speed. These decisions make sure that the fleet and its corresponding transport capacity are fully utilized to fulfil the frequency and volume requirement of the demand with CO_2 emission less than the amount of allowance bought. Different from the traditional fleet composition and deployment problem, this extended version of the problem captures the three dimensional trade-off among chartering cost, bunker cost and allowance cost.

Due to the consideration of METS in this study, the following assumptions about the details of this scheme need to be made first.

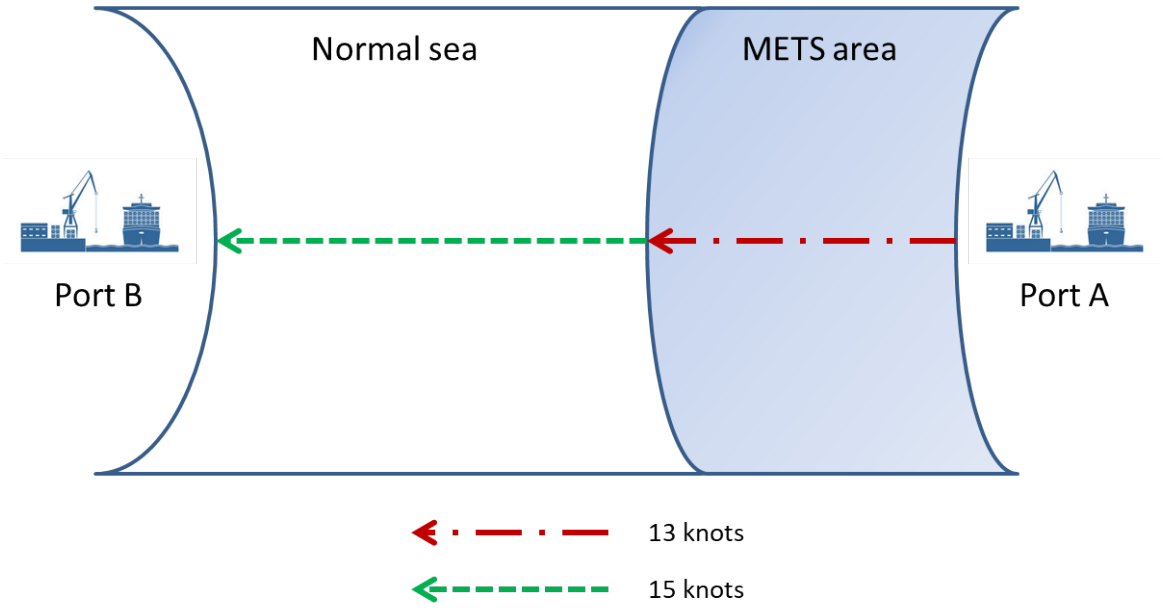

Figure 4.2: An example of speed differentiation

- We assume that the allowance for CO_2 emission needs to be bought through auctioning in the scheme. Other options, such as *grandfathering* based on historic data or *grandfathering* based on benchmark, are found impractical for the shipping industry due to its volatility and complexity (Kågeson, 2007, 2008; Miola et al., 2011). The market situation in the shipping industry is very volatile. Hence the historical data of fuel consumption or emission in a recession period is not reliable as the basis for the cap setting in the booming years. On the other hand, the enormous number of ship types and sizes also bring significant challenges in the design of a fair benchmark.

- According to the literature, a cap-and-trade scheme can be either an open or a closed system (Kågeson, 2007, 2008; Koesler et al., 2015; Wang et al., 2015). The former allows the companies in the system to trade with other sectors, while the latter requires the trade of allowance to be restricted inside this cap-and-trade scheme. The disadvantage of a close system is that the cap of CO_2 emissions for the whole sector needs to be set cautiously or even generously (Kågeson, 2008). According to Kågeson (2007), the shipping sector is expected to become a net-buyer of allowances due to the relatively high abatement cost in this industry. Hence, without an emergency exit available in the system, a too tight cap may lead to a skyrocketing allowance price when the availability of allowance is low on the market (Psaraftis, 2012). However, too much "mercy" in the cap setting process may also bring negative effects to the original intention, emission reduction, of the cap-and-trade scheme. Therefore, we assume the METS in this paper to be an open system in which the shipping companies can trade with other sectors, e.g., electricity generation, that have a lower marginal CO_2 abatement cost (Wang et al., 2015; Koesler et al., 2015). Furthermore, an open system with a larger volume of allowance in the pool can lead to a more transparent and stable system (Kågeson, 2008).

- In a global setting of METS, it is easy to understand that all emissions of a vessel need to be covered by the equivalent amount of allowances. In a regional METS, however, the scope of a vessel's emission liability is controversial. Some studies suggest that the ship is responsible for the entire emission during the whole voyage between two ports as long as one of them is located inside the METS areas (Franc and Sutto, 2014; Kågeson, 2008). Such a route-based approach used to be adopted by the aviation sector in the early

stage when it was included in the EU ETS. However, this approach failed due to massive complaints and boycotts from the non-EU countries because these countries questioned the legitimacy of EU to charge the emissions outside its territorial airspace (Meleo et al., 2016; Li et al., 2016; Scheelhaase et al., 2018). Moreover, the route-based approach may be easily evaded in the shipping sector as long as a transshipment is arranged at a hub outside but near the METS area (Kågeson, 2007; Franc and Sutto, 2014). Therefore, we assume a geographical area-based approach proposed in Hermeling et al. (2015) and Miola et al. (2011) to calculate the liability of a ship's emission for the regional METS in this study. In this approach, the shipping company only needs to submit the allowances for the CO_2 of its fleet emitted inside the territorial waters and the exclusive economic zone (EEZ) of the regulating authorities. Such approach seems to be more reasonable and feasible for a regional METS.

4.4 Mathematical model

In this section, we present the mathematical model for the fleet composition and deployment problem with METS. Section 4.4.1 introduces the modelling approaches and relevant assumptions. The mathematical formulation of the model is presented in Section 4.4.2

4.4.1 Model development

The optimization model proposed in this paper is deterministic. Therefore, the tactical decisions including chartering strategy and allowance procurement plan are made immediately in the beginning of the planning horizon. Simultaneously, the corresponding operational decisions during the planning horizon, such as route choice, vessel allocation and sailing speed, are also determined to support the tactical decision-making. In Section 4.3, we mentioned that a highly abstract demand based on trade lanes is used. Every freight contract is associated with one corresponding trade lane that covers the loading and unloading areas in this contract. One trade lane may have several associated freight contracts and each of these contracts represents the aggregated demand compatible with the same type of ship from the same origin area to the same destination area.

In order to serve all the demands, the shipping company needs to make the routing and fleet deployment decisions based on their own ships and the chartering plan. Due to the abstraction of the demand, the routing and fleet deployment decisions are also kept at an aggregated level. For the routing decisions, we use the concept of *loop* defined in Pantuso et al. (2016) and Wang et al. (2017). According to the definition, a loop means a round trip involving one or several trade lanes which begin and finish in the same geographical area. In the case of multiple trade lanes, ballast sailing may be performed so as to connect two consecutive trade lanes, if the destination port of one trade lane is different from the loading port of the subsequent trade lane. In Figure 4.3, a simple example of several trade lanes and the potential loops derived from these trade lanes are illustrated. The solid arrows in Figure 4.3a shows the trade lanes, TL 1, TL 2 and TL 3, while the dotted arrows represent examples of ballast sailings that connect two consecutive trade lanes. TL 1, TL 2 and the ballast voyages together constitute the example loop in Figure 4.3a. Hence, if a ship is assigned to this example loop, it first sails TL 1 from Northern Europe to the East Coast of the US. Then the ship takes the ballast voyage to the North Coast of South America and then performs TL 2 which ends in Southern Europe. Finally, the ship returns the origin of TL 1 and finishes the loop. Figure 4.3b further illustrates this example loop with bold arrows as well as all other potential loops that can be generated in the three trade lanes case. Note that a loop which consists of a single trade lane needs to have a ballast sailing back to the origin area of this trade lane after unloading at the destination.

This is represented by the dotted loop out of a node in Figure 4.3b. With all potential loops constructed based on the trade lanes, the fleet will then be deployed. The available vessels and their corresponding transport capacity will be assigned to different loops so that the demand of all trade lanes can be met.

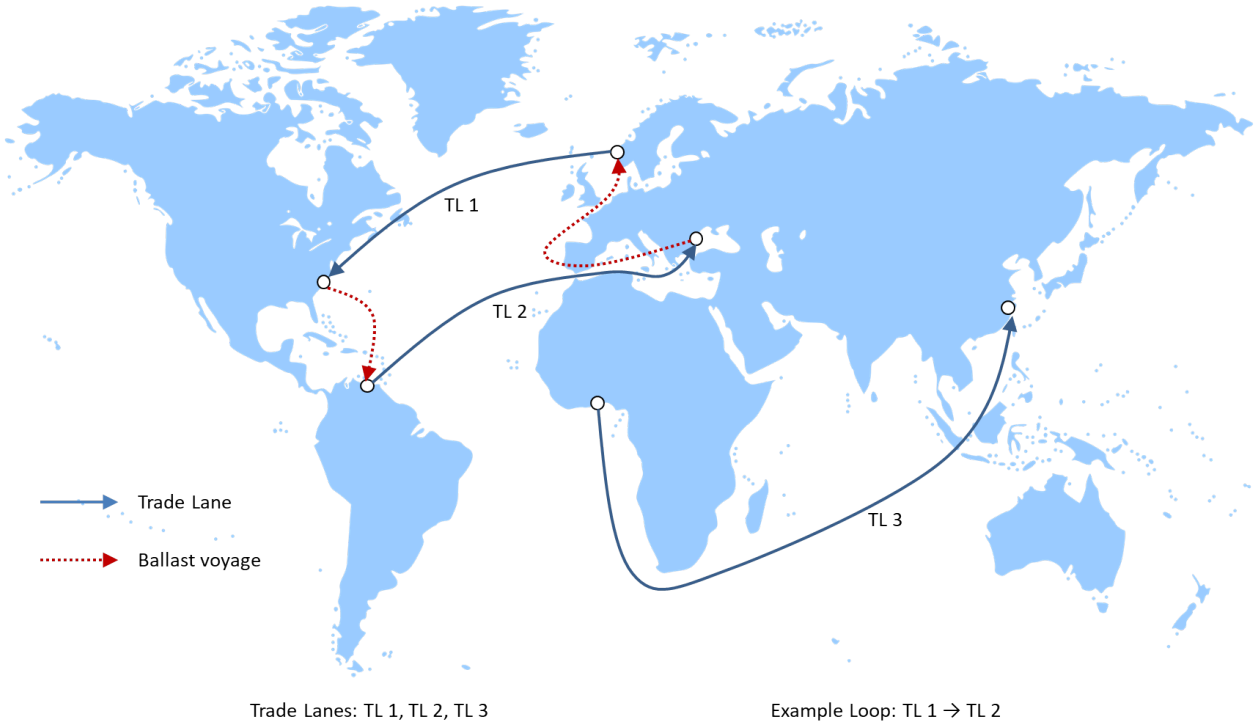

(a) Example loop

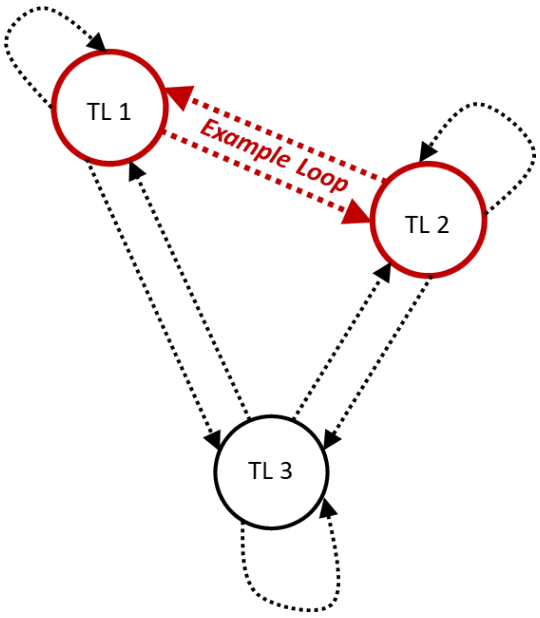

(b) Potential loops for three trade lanes

Figure 4.3: Example of three trade lanes and possible loops

Another important factor considered in the fleet deployment decisions is the sailing speed of the ships. Speed optimization is critical for the problem since it affects the travelling time and fuel consumption. The former impacts the number of ships needed to meet the demand and hence the chartering cost, while the latter decides the fuel costs. Moreover, another important outcome depending on sailing speed is the CO_2 emission of the ship which influences the

allowance cost due to the existence of METS in this paper. It is widely recognized that the fuel consumption per time unit of a ship is approximately proportional to the third power of its sailing speed (Ronen, 1982; Psaraftis and Kontovas, 2013). Nevertheless, shipping companies usually only have fuel consumption data for their ships for a few discrete speed points, which also applies for the case in this paper. Hence, a piecewise linearisation, adopted from Andersson et al. (2015) is used here to handle the non-linearity of the function of speed and fuel consumption. For example, if we want to estimate the fuel consumption rate of a particular speed v^* which can be represented by a linear combination of speed v_1 and v_2 (see Figure 4.4), then the same linear combination can also be used in the estimation of the corresponding fuel consumption rate F^*_{est}. Note that such an approximation normally leads to an overestimation, but the gap is normally negligible as long as enough discrete speed points are adopted (see Andersson et al. (2015) for detailed explanations).

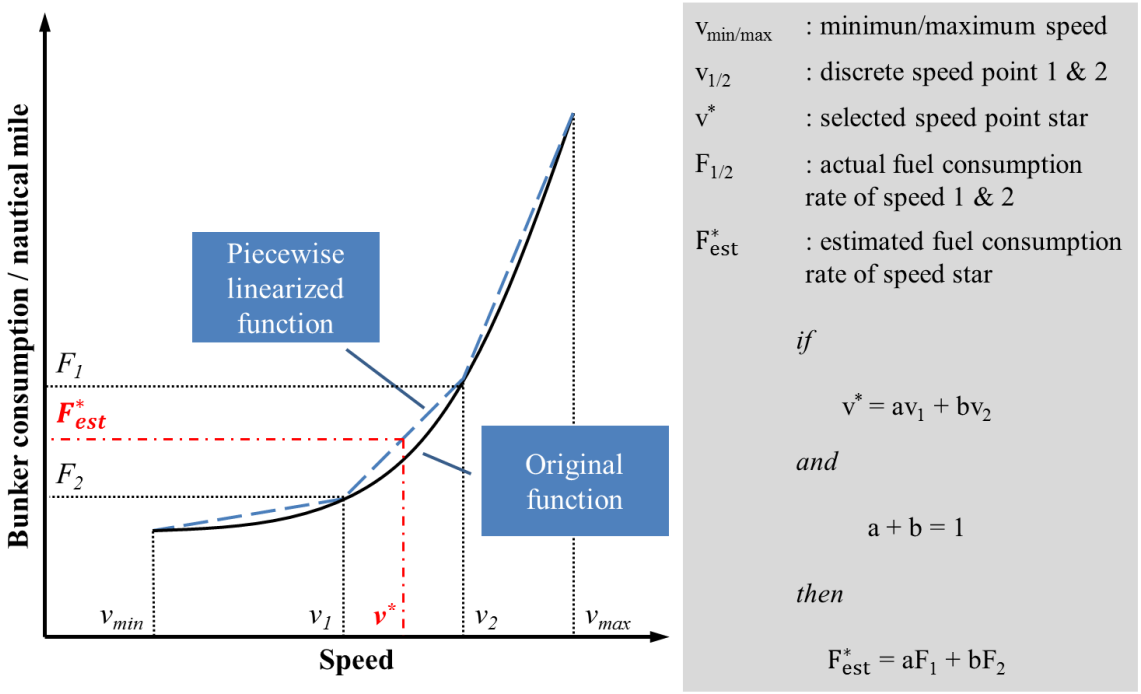

Figure 4.4: Piecewise linearisation of fuel consumption (Gu et al., 2018a)

Lastly, in the case of a regional METS, the sailing speed inside the METS area can be different from the speed outside. In order to achieve such speed differentiation in the decision-making process, we consider a loop crossing the regulated region as two separated stretches in the model, see Figure 4.5. Two groups of speed related decision variables are assigned to each stretch of the loop and different speeds may be applied on different stretches. However, the interdependency between these two groups of variables, such as the consistency in the total number of round trips sailed on both stretches with different speeds, need to be guaranteed with specific constraints which is further explained in the next section. In general, the model balances among the travelling time (chartering cost), fuel consumption (bunker cost) and emission (allowance cost) to decide the most economic speed on each stretch. Please note that in the case of a loop involving only an METS area or normal sea, i.e., a global METS or a business as usual (no METS) scenario, only one stretch will be observed.

4.4.2 Mathematical formulation

The mathematical formulation of the fleet composition and deployment problem with METS and its notation are shown as follows.

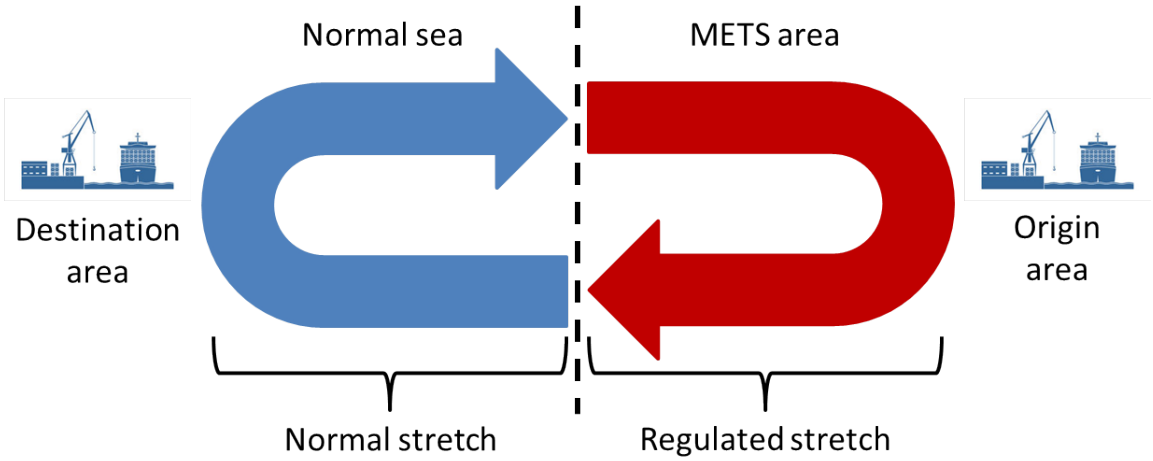

Figure 4.5: Two stretches of a loop in the regional METS scenario

Sets

$\mathcal{V}$, $\mathcal{C}$	Set of ship types and contracts
$\mathcal{N}$, $\mathcal{R}$	Set of of trade lanes and loops
$\mathcal{E}_v$	Set of speed alternatives for ship type v
$\mathcal{R}_v \subseteq \mathcal{R}$	Set of loops that can be sailed by ship type v
$\mathcal{R}_{iv} \subseteq \mathcal{R}$	Set of loops serving Trade Lane i and compatible with ship type v
$\mathcal{C}_i^{\mathcal{TR}} \subseteq \mathcal{C}$	set of contracts serviced by Trade Lane i
$\mathcal{V}_i \subseteq \mathcal{V}$	Set of ship types that can sail Trade Lane i

Parameters

N_v	No. of ships of type v owned by the shipping company
M_v	No. of available service days for a ship of type v owned by the shipping company
Q_v	Volume of ship type v
T_{vre}^{ETS}	Time for ship type v to complete the METS stretch of a round trip on Loop r with speed e
T_{vre}^{N}	Time for ship type v to complete the normal stretch of a round trip on Loop r with speed e
F_c	Frequency requirement of contract c
D_c	Demand of contract c

C_{vre}^{ETS}	Cost for ship type v to complete the METS stretch of a round trip on Loop r with speed e
C_{vre}^{N}	Cost for ship type v to complete the normal stretch of a round trip on Loop r with speed e
C_{v}^{In}	Daily charter-in rate for a ship of type v
R_{v}^{Out}	Daily charter-out revenue for a ship of type v (lower than C_{v}^{In})
R_{i}^{SP}	Freight rate for a unit of spot cargo on Trade Lane i
D_{i}^{SP}	Demand of spot cargo on Trade Lane i
E_{vre}^{ETS}	CO_2 emitted from ship type v to complete the METS stretch of a round trip on Loop r with speed e
C^{A}	Cost of the METS allowance for a ton of CO_2

Decision variables

w_v	No. of days that ship of type v is chartered in
z_v	No. of days that ship of type v is chartered out
x_{vre}^{ETS}	No. of times sailed by a ship of type v on the METS stretch of Loop r with speed alternative e
x_{vre}^{N}	No. of times sailed by a ship of type v on the normal stretch of Loop r with speed alternative e
q_{ivc}	Volume carried by ship type v for contract c on Trade Lane i
q_{iv}^{SP}	Volume of spot cargo carried by ship type v on Trade Lane i
y^{ETS}	Amount of METS allowance bought in

Objective function

$$\begin{aligned} \min \quad & \sum_{v\in\mathcal{V}} C_{v}^{In} w_v - \sum_{v\in\mathcal{V}} R_{v}^{Out} z_v - \sum_{i\in\mathcal{N}}\sum_{v\in\mathcal{V}} R_{i}^{SP} q_{iv}^{SP} \\ & + \sum_{v\in\mathcal{V}}\sum_{r\in\mathcal{R}_v}\sum_{e\in\mathcal{E}_v} (C_{vre}^{ETS} x_{vre}^{ETS} + C_{vre}^{N} x_{vre}^{N}) + C^{A} y^{ETS} \end{aligned} \tag{4.1}$$

Subject to

$$\sum_{r\in\mathcal{R}_v}\sum_{e\in\mathcal{E}_v}(T^{ETS}_{vre}x^{ETS}_{vre}+T^{N}_{vre}x^{N}_{vre})+z_v=M_vN_v+w_v \qquad v\in\mathcal{V} \tag{4.2}$$

$$\sum_{e\in\mathcal{E}_v}x^{ETS}_{vre}=\sum_{e\in\mathcal{E}_v}x^{N}_{vre} \qquad v\in\mathcal{V}, r\in\mathcal{R}_v \tag{4.3}$$

$$\sum_{v\in\mathcal{V}_i}\sum_{r\in\mathcal{R}_{iv}}\sum_{e\in\mathcal{E}_v}x^{ETS}_{vre}\geq F_c \qquad i\in\mathcal{N}, c\in\mathcal{C}^{\mathcal{TR}}_i \tag{4.4}$$

$$\sum_{v\in\mathcal{V}_i}q_{ivc}=D_c \qquad i\in\mathcal{N}, c\in\mathcal{C}^{\mathcal{TR}}_i \tag{4.5}$$

$$\sum_{r\in\mathcal{R}_{iv}}\sum_{e\in\mathcal{E}_v}Q_vx^{ETS}_{vre}\geq\sum_{c\in\mathcal{C}^{\mathcal{TR}}_i}q_{ivc}+q^{SP}_{iv} \qquad i\in\mathcal{N}, v\in\mathcal{V}_i \tag{4.6}$$

$$\sum_{v\in\mathcal{V}_i}q^{SP}_{iv}\leq D^{SP}_i \qquad i\in\mathcal{N} \tag{4.7}$$

$$\sum_{v\in\mathcal{V}}\sum_{r\in\mathcal{R}_v}\sum_{e\in\mathcal{E}_v}E^{ETS}_{vre}x^{ETS}_{vre}=y^{ETS} \tag{4.8}$$

$$w_v, z_v\geq 0 \qquad v\in\mathcal{V} \tag{4.9}$$

$$x^{ETS}_{vre}, x^{N}_{vre}\geq 0 \qquad v\in\mathcal{V}, r\in\mathcal{R}_v, e\in\mathcal{E}_v \tag{4.10}$$

$$q_{ivc}\geq 0 \qquad i\in\mathcal{N}, v\in\mathcal{V}_i, c\in\mathcal{C}^{\mathcal{TR}}_i \tag{4.11}$$

$$q^{SP}_{iv}\geq 0 \qquad i\in\mathcal{N}, v\in\mathcal{V}_i \tag{4.12}$$

$$y^{ETS}\geq 0 \tag{4.13}$$

The objective function (4.1) minimizes the total cost including the ship chartering cost, fleet operation cost and the emission allowance cost. Furthermore, the revenue of chartering out surplus ships and carrying spot cargo are also considered as negative costs in the objective function. Constraints (4.2) keep the balance between the transport capacity available and the capacity needed for each type of vessel. The available capacity consists of the self-owned fleet and the ships chartered in, while the needed capacity covers the demand for freight transport and the possible chartering out. Constraints (4.3) make sure that for each ship type v and Loop r, the corresponding number of times sailed on the METS stretch and the normal stretch must be the same. Constraints (4.4) - (4.5) guarantee that the contractual demands, including both frequency and volume requirements, are fulfilled with enough transport capacity. Constraints (4.6) state that the total cargo volume offered by ship type v on Trade Lane i should be sufficiently large to carry the contractual and spot demands on Trade Lane i assigned to ship type v. Constraints (4.7) restrict the total amount of spot cargo can be picked up. Constraint (4.8) enforces METS requirement that the emission generated during the fleet operation in side METS areas must be covered by the allowance bought. Constraints (4.9) - (4.13) define the domains of the decision variables. Please note that the fleet deployment variables (x^{ETS}_{vre} and x^{N}_{vre}) are allowed to be continuous in this paper. The fractional part of the solution means a round trip to be finished in the future planning period.

4.5 Test case

In this study we consider a shipping company which offers transportation services of chemical liquid bulk among different geographical areas. We assume that there are two types of chemical tankers owned by this shipping company while these two types of ship are also available on the spot market for chartering. The basic information about these two types of tankers is collected through the statistics of a peer group analysis made by Clarkson (2018b). The detailed data are listed in Table 4.1. Moreover, we assume that the shipping company in the case owns four type 1 tankers and one type 2 tanker. All owned vessels in the fleet have 250 days available per year for freight transportation.

Table 4.1: Basic information of two types of chemical tanker

	Type 1	Type 2
Deadweight tonnage	49503	10239
Cargo Capacity (cu.m.)	45127	10921
Draft	12.96	8.05
Speed - Low/Medium/High ***(Knots)***	12.5/14.4/15.5	12.5/14.4/15.5
Fuel Consumption - Low/Medium/High ***(Tonne/Nautical mile)***	0.084/0.091/0.101	0.042/0.054/0.058
No. of vessel owned	4	1

For demand, we assume that the shipping company needs to serve three trade lanes with corresponding long-term contracts, see Figure 4.6. In Trade Lane 1, the vessel travels from Northern Europe to the East Coast of North America. The contract served by Trade Lane 2 requires the cargo to be picked up at the South-east Coast of the US and delivered at the West Coast of Africa. The last trade lane in the case starts in the Persian Gulf and finishes in Southern Europe. Other detailed contractual terms for each trade lane, such as frequency and freight volume, can be found in Table 4.2. In a real world case, there might be several loading or unloading ports in a specific trade lane. However, we use one origin and destination port representing all demands and deliveries in the same geographical area for simplicity. Moreover, we exclude the consideration of spot cargo in this test case because the spot freight market in the chemical shipping industry is quite limited due to restrictions from both the demand and supply sides. Different from other shipping sectors, the specialized tankers compatible for the cargo on the spot market are not always available on short notice. More importantly, the main goal of this study is to examine the impact of METS on fleet's CO_2 emission during operation rather than a direct application. Therefore, we believe such simplification will not affect the original purpose of the test.

Table 4.2: Trade Lanes and Contracts

	Trade Lane 1	*Trade Lane 2*	*Trade Lane 3*
Origin port	Mongstad	Houston	Ras Tanura
Destination port	Saint John	Luanda	Rijeka
Frequency	12 visits per year	12 visits per year	10 visits per year
Total freight demand ***(1000 cu.m.)***	490	450	95

Different loop options are then formed as input for the computational study. As mentioned in Section 4.4.1, each potential loop covers one or several trade lanes. Figure 4.7 shows an

Figure 4.6: Three trade lanes in the case

example of the loop serving both Trade Lane 2 and Trade Lane 3. The ballast sailing connecting these two trade lanes are marked as dotted arrows in the figure. The detailed data of travelling distance for each loop is measured through Google Map. The amount of CO_2 emitted from the ship on a loop with certain speed equals the product of sailing distance (nautical mile), fuel consumption rate (tonne/nautical mile) and CO_2 emission factor (tonne/tonne fuel). The emission factor applied in this case is *3.021* (Psaraftis and Kontovas, 2009).

4.6 Computational Study

In this section, different settings of the tests and the corresponding results of the computational study are given. Section 4.6.1 introduces different scenarios applied in the tests. Then the observations from the tests and the insights gained are presented in Section 4.6.2.

4.6.1 Tested Scenarios

As mentioned in Section 4.1, the main purpose of this study is to examine the actual impact of METS on short-term emission reduction when other relevant factors, such as charter rate, are also considered. Therefore, different scenarios for these determinants are assumed in the computational study and the corresponding results of these tests are compared to identify the real impact of different determinants on CO_2 emissions. The considered determinants include the charter rate of the vessels, the price of emission allowance, bunker price and the geographical scope of METS.

First, for charter rate, we introduce three scenarios. When the freight market is booming, the charter rate is usually high due to the high demand for transportation. But when the economy is in recession, the total supply of ships may exceed the demand on the market. Therefore, if the shipping company has surplus capacity, it normally has to (a) accept the minimum charter rate which equals the mandatory cost for running the ship, (b) lay up the

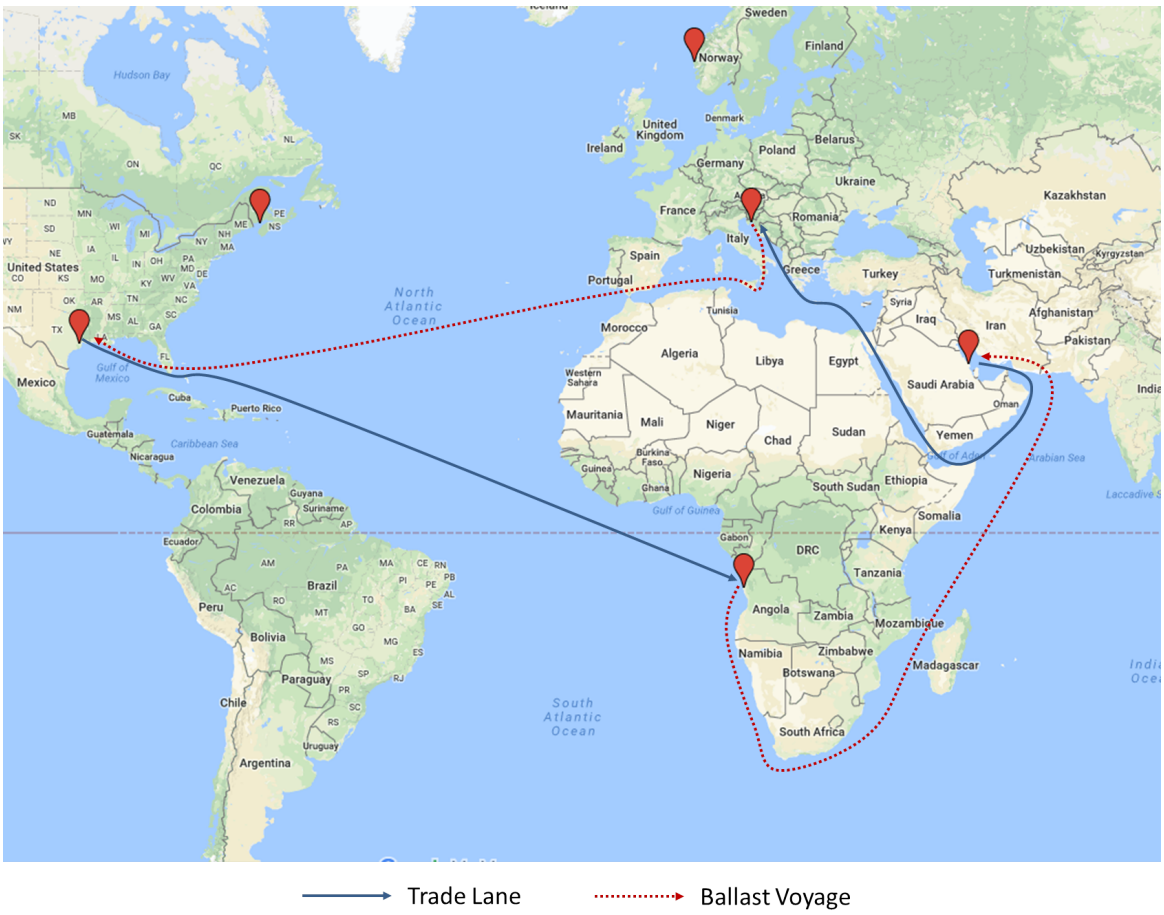

Figure 4.7: Loop for Trade Lane 2 & 3

vessel or (c) send the vessel for demolition. In the latter two cases, the value of a surplus vessel is almost zero. Therefore, the expected earnings for charter-out in the bad market can be very low. The charter rates are otherwise based on historical data observed in Clarkson (2018a). Note that the actual value of a surplus vessel during a recession should be much lower than the recorded charter rates in the historical data due to the unrecorded lay-ups or demolition cases. With that in mind, we further adjusted the average charter-out rate in the low scenario, which should better represent the situation in the real world.

Second, we also assume two different situations, namely high and low, for the price of emission allowance issued by the METS. Since there is no real world data for the allowance price of METS, we have to make reasonable assumptions based on the price of allowance traded in EU ETS. Similarly, high and low bunker prices are also adopted in the tests. Since we have assumed an open system for the METS in Section 4.3, we consider no correlations between the allowance price and the other two factors. Furthermore, the type of chartering applied in this paper is time charter. Hence, the charter rate is also independent of the bunker price. Detailed information about charter rates, allowance prices and fuel prices are listed in Table 4.3.

Table 4.3: Scenarios for charter rate, allowance price and bunker price (USD)

Scenario	*High*	*Normal*	*Low*
Charter-in rate per day (type 1/2)	22000/15000	11000/8000	5000/4000
Charter-out rate per day (type 1/2)	22000/15000	11000/8000	2000/1500
Allowance price per tonne CO_2	65	*n/a*	10
Bunker price per tonne	600	*n/a*	200

Last, for the geographical scope of METS, three possible scenarios are assumed, namely global METS, regional METS and business-as-usual. In a global METS, the entire voyage of a vessel is regulated and an emission allowance needs to be submitted for the total CO_2 emission. For the regional METS in this study, we assume the regulation is only implemented in EU and U.S. As already assumed in Section 4.3, the EEZ of the regulating country or authority is accepted as the territory of the regional METS, see Figure 4.8. Hence, the shipping company is only liable for the emissions of its fleet inside the regulated areas in the regional METS scenario. In the business-as-usual scenario, no METS is introduced and therefore no allowance is required for any emissions.

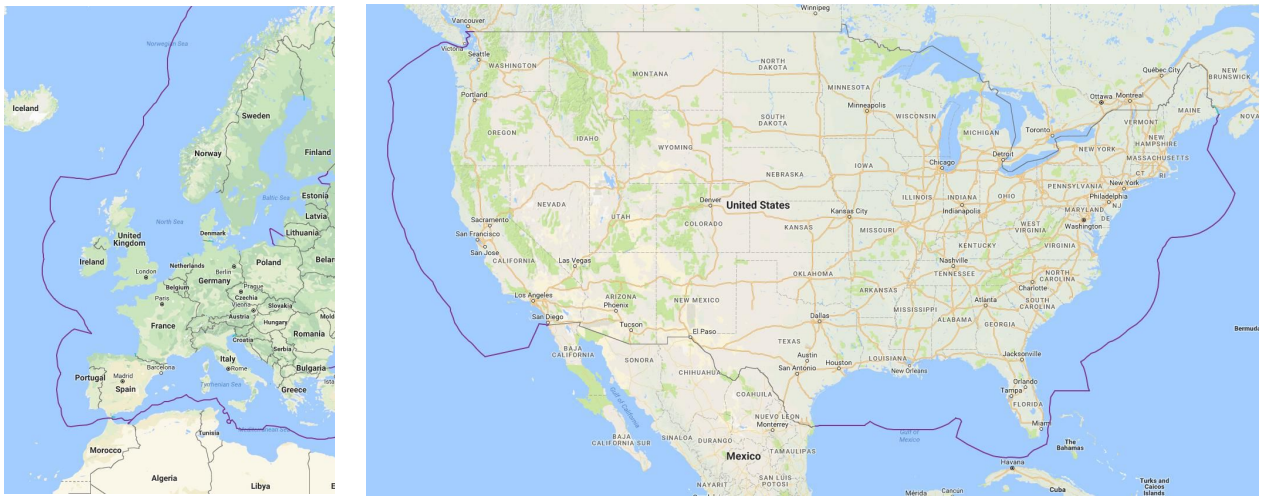

(a) EU METS **(b)** U.S. METS

Figure 4.8: The geographical scope of the regional METS

4.6.2 Main Results

In this section, we present the main results of the computational study. In the following analysis, we compare the results obtained under different METS settings (e.g., geographical scope and allowance cost) with the benchmark case (business-as-usual), while other two factors, namely bunker price and charter rate, remain fixed during the comparison. The purpose of such tests is to clearly observe the real emission reduction impact of METS under the optimal plan for fleet composition and deployment when other determinants are also considered. We also compare the results with the same METS settings but different bunker price or charter rate, so as to find out how these two factors influence the CO_2 reduction performance of METS. A brief summary of the findings will be offered at the end of this section.

We first consider a low bunker price scenario, and run the model with different combinations of all other parameters. The results are shown in Table 4.4. The numbers in the table represents the total amount of CO_2 emitted by the ships in the optimal fleet composition and deployment solution. Meanwhile, the percentages listed in the parentheses show the volume change of emission comparing to the benchmark scenario. A negative percentage refers to a emission reduction, while a positive ratio means an increase.

Scenario: low bunker price, normal charter rate

In this subsection, a low bunker price and normal charter rate is assumed. Based on the results in Table 4.4, we see that when the freight market is in a normal situation, the application of METS will lead to a decrease of CO_2 emissions. Moreover, the reduction in the global METS

Table 4.4: Result summary in the low bunker price scenario

CO_2 Tonne (% of change)	**Business-as-usual (Benchmark)**	**Regional METS**		**Global METS**	
		Low allowance cost	*High allowance cost*	*Low allowance cost*	*High allowance cost*
Low charter rate	66288.2 (n/a)	66291.5 (0.0%)	73195.4 (10.4%)	66288.2 (0.0%)	66288.2 (0.0%)
Normal charter rate	79043.6 (n/a)	77076.8 (−2.5%)	77076.8 (−2.5%)	72693 (−8.0%)	72693 (−8.0%)
High charter rate	79043.6 (n/a)	79040.1 (0.0%)	79040.1 (0.0%)	79043.6 (0.0%)	79043.6 (0.0%)

case is much stronger than in the regional setting. The underlying reasons for these observations can be found in the following paragraphs.

In the business-as-usual case, Loop 1, 2, 3 and 6 are adopted in the solutions. The former three loops cover Trade Lane 1, 2 and 3 correspondingly while the latter serves both Trade Lane 1 and 2. According to the optimal solutions listed in Table 4.5, ships of type 1 sail Loop 1 and Loop 6 for 0.31 and 11.69 times respectively, while ships of type 2 complete 0.31 and 10 round trips on Loop 2 and Loop 3. A high speed is adopted during the voyages on all loops and the surplus capacity (447 days) are chartered out for profit.

Table 4.5: Solutions summary in the business-as-usual case with normal charter rate and low bunker price

	No. of round trips Vessel Type 1	Speed - knots Vessel Type 1	No. of round trips Vessel Type 2	Speed - knots Vessel Type 2
Loop 1 (TL1)	0.31	15.5	0	0
Loop 2 (TL2)	0	0	0.31	15.5
Loop 3 (TL3)	0	0	10	15.5
Loop 6 (TL1 & TL2)	11.69	15.5	0	0
	Vessel Type 1		Vessel Type 2	
Chartered days in/out (+/−)	−447		0	

But if a regional METS is included in the consideration, the emission from the fleet start to decrease. In the solution summary of this scenario offered in Table 4.6, we see that the loop decisions are almost the same comparing to the decisions in the business-as-usual case. But a lower speed is adopted on the METS stretches of Loop 1 and 6 by the ships of type 1. Such operational change is triggered by the additional allowance cost due to the implementation of the regional METS. In order to adapt to the new regulation and simultaneously minimize the total cost, the ship choose to decrease its sailing speed inside the METS areas so that less emission is generated and thus less allowances need to be purchased. In return, nevertheless, more transport capacity is occupied since the total sailing time to finish the same loop becomes longer. Therefore, the chartered out days of the surplus ships decline.

In the case of a global METS, the emission of CO_2 is further reduced. The shipping company decides to utilize more of its surplus transport capacity, rather than charter them out for profit, and slow down its operation on Loops 1 and 6 during the entire voyage, so as to minimize its consumption of emission allowances, see Table 4.7. Note that the composition and deployment decisions are indifferent in the scenarios with the same METS scope but different allowance cost. The reason is that the difference between a high and low allowance cost here is not large enough to motivate the vessel to deviate from its current loop choices or further slow down its navigation for allowance saving purpose which needs more transport capacity and leads to a

Table 4.6: Solutions summary in the regional METS case with normal charter rate and low bunker price

	No. of round trips Vessel Type 1	Speed (normal stretch) - knots Vessel Type 1	Speed (METS stretch) - knots Vessel Type 1	No. of round trips Vessel Type 2	Speed (normal stretch) - knots Vessel Type 2	Speed (METS stretch) - knots Vessel Type 2
Loop 1 (TL1)	0.32	15.5	14.4	0	0	0
Loop 2 (TL2)	0	0	0	0.32	15.5	15.5
Loop 3 (TL3)	0	0	0	10	15.5	15.5
Loop 6 (TL1 & TL2)	11.68	15.5	14.4	0	0	0
	Vessel Type 1			Vessel Type 2		
Chartered days in/out (+/-)	−434			0		

higher charter-in cost or lower charter-out revenue.

Table 4.7: Solutions summary in the global METS case with normal charter rate and low bunker price

	No. of round trips Vessel Type 1	Speed - knots Vessel Type 1	No. of round trips Vessel Type 2	Speed - knots Vessel Type 2
Loop 1 (TL1)	0.31	14.4	0	0
Loop 2 (TL2)	0	0	0.31	15.5
Loop 3 (TL3)	0	0	10	15.5
Loop 6 (TL1 & TL2)	11.69	14.4	0	0
	Vessel Type 1		Vessel Type 2	
Chartered days in/out (+/−)	−405		0	

Scenario: low bunker price, high charter rate

However, if we assume a booming freight market (high charter rate) with still a low bunker price, the effect of METS on emission reduction witnessed in the previous tests disappears, see Table 4.4. The high charter rate offers significant incentives for the fleet to speed up so that it can use as little transport capacity as possible to finish the job, which minimizes its demand for costly chartering in or maximizes its possibility of profitable chartering out. Therefore, in spite of the extra allowance cost, the introduction of the METS, both regional and global, is not sufficient to make the fleet composition and deployment decisions more environmental friendly. The optimal solutions show that a high speed is adopted in all scenarios in the high charter rate case. The composition and deployment decisions in the high charter rate scenarios are identical with the solutions listed in Table 4.5.

Scenario: low bunker price, low charter rate

Similar results are also observed when the market is in a recession (low charter rate). The enforcement of the METS does not lead to any further emission reduction in this case. But comparing to the cause just discussed in the high charter rate scenario, the reason for the observation here is actually the opposite. In the business-as-usual case with market recession, the optimal solutions choose to fulfil all contractual demands with Loop 3 and 6 only and slow down its operation considerably while more transport capacity is involved, see Table 4.8.

When the charter rate is low, the value of the surplus vessels or the cost of supplementing the insufficiency of transport capacity become low as well. This means it is more cost efficient for the shipping company to fully utilize its own idle ships or take advantage of the cheap resources on the chartering market so as to reduce the sailing speed during the operation for bunker saving purpose, although such slow steaming strategy requires more vessels which leads to a decrease/increase in the profit/cost of chartering out/in. Since a minimum speed has already been applied in the business-as-usual scenario, the additional cost of METS allowance can not push the speed to an even lower level, which therefore stops further emission reduction in other METS scenarios.

Table 4.8: Solutions summary in the business-as-usual case with low charter rate and bunker price

	No. of round trips Vessel Type 1	Speed - knots Vessel Type 1	No. of round trips Vessel Type 2	Speed - knots Vessel Type 2
Loop 3 (TL3)	1.55	12.5	8.45	12.5
Loop 6 (TL1 & TL2)	12	12.5	0	0
	Vessel Type 1		Vessel Type 2	
Chartered days in/out (+/−)	−256		0	

Surprisingly, in the scenario with high allowance cost and regional METS, an increase of CO_2 emission is observed. The optimal solution in Table 4.9 suggests the shipping company to use the loop options with minimum sailings in the METS areas so that the effect of high allowance cost can be minimized. Hence comparing to the solutions in the business-as-usual case in Table 4.8, the new plan here abandons Loop 6 (more METS involvement) while uses Loop 1 and Loop 2 (less METS involvement) to serve Trade Lane 1 and Trade Lane 2 separately, see Figure 4.9. Unfortunately, the total travelling distance of Loop 1 and Loop 2 is longer than that of Loop 6, which leads to the total emission increase (although decrease inside METS areas) observed in Table 4.4. The longer voyage also causes an increased fuel consumption (higher bunker cost) and vessel demand (higher chartering cost). Nevertheless, the saving on the allowance side still exceeds these cost increases since the bunker price and charter rate are both low in this scenario. With such a new fleet composition and deployment plan, the O_2 emission inside the METS regions does decrease, while the emission outside increased significantly, which brings us a typical example of *carbon leakage*.

Table 4.9: Solutions summary in the regional METS case with low allowance cost, charter rate and bunker price

	No. of round trips Vessel Type 1	Speed (normal stretch) - knots Vessel Type 1	Speed (METS stretch) - knots Vessel Type 1	No. of round trips Vessel Type 2	Speed (normal stretch) - knots Vessel Type 2	Speed (METS stretch) - knots Vessel Type 2
Loop 1 (TL1)	12	12.5	12.5	0	0	0
Loop 2 (TL2)	12	12.5	12.5	0	0	0
Loop 3 (TL3)	0.06	12.5	12.5	9.94	15.5	12.5
	Vessel Type 1			Vessel Type 2		
Chartered days in/out (+/-)	−231			0		

Now we change the setting of bunker price from low to high and repeat the tests again with all other assumptions. The results under different scenarios in the high bunker price cases are summarized in Table 4.10. We observe a similar pattern which is also witnessed in the low

(a) Routes of Loop 1 & 2

(b) Route of Loop 6

Figure 4.9: Different METS coverage of Loop 1, 2 & 6

bunker price case in Table 4.4. The emission reduction caused by the implementation of METS is only experienced in the scenarios with a normal charter rate. Moreover, a higher allowance cost facilitates more emission reduction, while a global geographical scope of the regulation also encourage the ships to emit less. However, comparing to the benchmark, no further emission reduction is observed in the high and low charter rate scenarios after introducing either regional or global METS.

Table 4.10: Result summary in the high bunker price scenario

CO_2 Tonne (% of change)	**Business-as-usual (Benchmark)**	**Regional METS**		**Global METS**	
		Low allowance cost	*High allowance cost*	*Low allowance cost*	*High allowance cost*
Low charter rate	66288.2 (n/a)	66291.5 (0.0%)	66291.5 (0.0%)	66288.2 (0.0%)	66288.2 (0.0%)
Normal charter rate	72693 (n/a)	72108.4 (−0.8%)	70772.6 (−2.6%)	72109.8 (−0.8%)	67983.9 (−6.5%)
High charter rate	72693 (n/a)	72690.6 (0.0%)	72690.6 (0.0%)	72693 (0.0%)	72693 (0.0%)

Scenario: high bunker price, normal charter rate

Firstly, a high bunker price and a normal charter rate are assumed in this subsection. Table 4.11 shows the detailed optimal composition and deployment decisions in the business-as-usual case with high bunker price and normal freight market. Compared to the results in Table 4.5 (low bunker price, normal charter rate), we find that the ships on loops 1 and 6 start slow steaming due to the higher bunker price. Certainly, more transport capacity is used as well, which leads to less chartering out.

If a regional METS with low allowance cost is implemented, the optimal solutions propose a simpler deployment plan and further speed reduction on the METS stretch of Loop 3, see Table 4.12. However, the speeds on Loop 6 and normal stretch of the Loop 3 remain unchanged. Furthermore, the sailing on the METS stretch of Loop 3 (see Figure 4.10) is just a small part of the entire voyage including all other used loops (approximately 5% based on travelling distance). Hence, the further speed reduction on the METS stretch of Loop 3 here has very limited impact on the total emission. Therefore, a merely 0.8% reduction of CO_2 is observed in Table 4.10. A similar situation also happens in the scenario with a global METS and low allowance cost. Although the global coverage of METS forces the ships to slow down on the entire voyage on Loop 3, the low allowance cost can only lead to a relatively slight speed reduction, see Table 4.13, which again has minor impact on the total emission.

Table 4.11: Solutions summary in the business-as-usual case with normal charter rate and high bunker price

	No. of round trips Vessel Type 1	Speed - knots Vessel Type 1	No. of round trips Vessel Type 2	Speed - knots Vessel Type 2
Loop 1 (TL1)	0.31	14.4	0	0
Loop 2 (TL2)	0	0	0.31	15.5
Loop 3 (TL3)	0	0	10	15.5
Loop 6 (TL1 & TL2)	11.69	14.4	0	0

	Vessel Type 1	Vessel Type 2
Chartered days in/out (+/−)	−405	0

Table 4.12: Solutions summary in the regional METS case with low allowance cost, normal charter rate and high bunker price

	No. of round trips Vessel Type 1	Speed (normal stretch) - knots Vessel Type 1	Speed (METS stretch) - knots Vessel Type 1	No. of round trips Vessel Type 2	Speed (normal stretch) - knots Vessel Type 2	Speed (METS stretch) - knots Vessel Type 2
Loop 3 (TL3)	0	0	0	10	15.5	12.8
Loop 6 (TL1 & TL2)	12	14.4	14.4	0	0	0

	Vessel Type 1	Vessel Type 2
Chartered days in/out (+/-)	−394	0

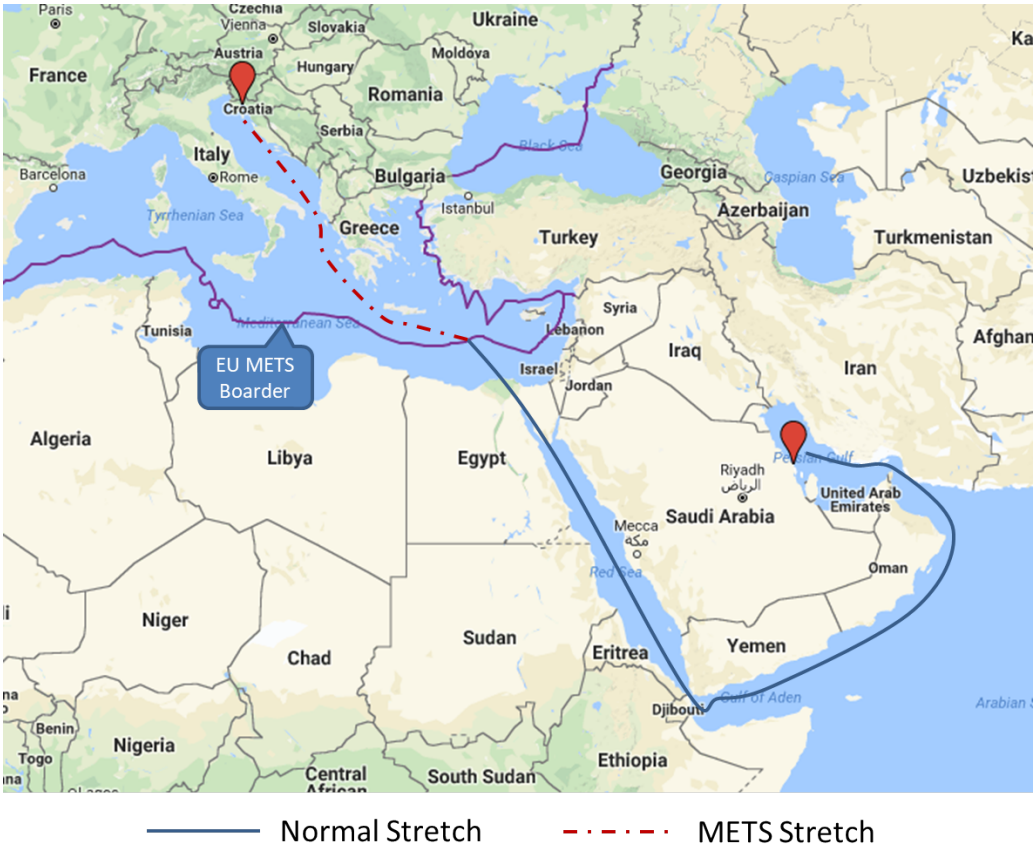

Figure 4.10: The normal and METS stretches on Loop 3

Table 4.13: Solutions summary in the global METS case with low allowance cost, normal charter rate and high bunker price

	No. of round trips Vessel Type 1	Speed - knots Vessel Type 1	No. of round trips Vessel Type 2	Speed - knots Vessel Type 2
Loop 3 (TL3)	0	0	10	14.8
Loop 6 (TL1 & TL2)	12	14.4	0	0
	Vessel Type 1		Vessel Type 2	
Chartered days in/out (+/−)	−394		0	

Compared to the results observed in the previous paragraph with low allowance costs, the emission decreases significantly in the scenarios with higher allowance cost, see Table 4.10. The reason for the lower emission is that the sailing speed of the vessel further declined due to the higher cost of the CO_2 allowance. In the setting of a regional METS, the vessels start slow steaming not only on the METS stretch of Loop 3, as already mentioned in Table 4.12, but also on the METS part of Loop 6, see Table 4.14. The regulated part of Loop 6 accounts for a much larger percentage of the total travelling distance than it does in Loop 3, see Figure 4.9b. Therefore, the speed reduction on the METS stretch of Loop 6 brings a substantial impact on the total emission. Similar observation of such upgraded slow steaming is also found in the global METS case, see Table 4.15. A minimum speed is adopted during the entire trip on Loop 6, which leads to a most dramatic CO_2 reduction in the tests in this study.

Table 4.14: Solutions summary in the regional METS case with high allowance cost, normal charter rate and high bunker price

	No. of round trips Vessel Type 1	Speed (normal stretch) - knots Vessel Type 1	Speed (METS stretch) - knots Vessel Type 1	No. of round trips Vessel Type 2	Speed (normal stretch) - knots Vessel Type 2	Speed (METS stretch) - knots Vessel Type 2
Loop 3 (TL3)	0.1	14.4	12.5	9.9	15.5	12.5
Loop 6 (TL1 & TL2)	12	14.4	12.5	0	0	0
	Vessel Type 1			Vessel Type 2		
Chartered days in/out (+/-)	−364			0		

Table 4.15: Solutions summary in the global METS case with high allowance cost, normal charter rate and high bunker price

	No. of round trips Vessel Type 1	Speed - knots Vessel Type 1	No. of round trips Vessel Type 2	Speed - knots Vessel Type 2
Loop 3 (TL3)	0	0	10	14.8
Loop 6 (TL1 & TL2)	12	12.5	0	0
	Vessel Type 1		Vessel Type 2	
Chartered days in/out (+/−)	−302		0	

Scenario: high bunker price, high/low charter rate

However, for the scenarios with high bunker price but low or high charter rate, the implementation of the METS, whether regional or global, leads to no further emission reduction compared to the situation in the business-as-usual case, see Table 4.10. The reason is the same as the one explained in the previous paragraphs for the scenarios with low bunker price and low or high charter rate. In a booming freight market or a recession, the high or low charter rate plays the dominant role which influences the fleet's composition and deployment decisions.

In the business-as-usual case with high charter rate, the model suggests the same optimal solution (with limited slow steaming) as the one obtained in the benchmark case with normal charter rate, see Table 4.11. With METS, a further slow steaming can help to save more allowance and fuel costs, but the total travelling time becomes longer, which leads to an increased need for transport capacity. When the charter rate is high, the additional savings brought by the further speed reduction can not compensate the increased charter-in cost (or decreased charter-out revenue) for more vessels. Hence, no further slow steaming is triggered and the introduction of the METS in the booming freight market scenario does not contribute additional emission reduction compared to the benchmark.

In a market recession, the low charter rate has already motivated the fleet to slow down to its minimum speed in the business-as-usual case in order to fully utilize the cheap vessel resources on the spot market or the idle capacity in its own fleet which is not very profitable for chartering out at that time. Therefore, a high or low extra allowance cost can not bring any more reduction on this minimum speed (same as the solutions in Table 4.8), which leaves an unaffected CO_2 emission even though the METS is implemented.

Low bunker price v.s. high bunker price

The last insight of the computational study can be obtained from the comparison between the results with low bunker price (Table 4.4) and the results with high fuel cost (Table 4.10). Based on the comparison we find that a high bunker price can substantially undermine the capability of METS on short-term emission reduction through the fleet's operation. The reason for this observation is that a high fuel cost has already initiated slow steaming of the ships, which leaves limited room for the METS to trigger further speed reduction. Therefore, the emission reduction in the high bunker price scenarios brought by the METS also becomes limited.

To briefly summarize, the findings obtained from this computational study include the following points. First, the introduction of METS may not lead to further short-term emission reduction in certain situations. Second, a larger geographical scope and higher allowance cost bring positive impact on the emission reduction performance of METS. Last, high bunker price significantly undermines the capability of METS on short-term emission reduction.

4.7 Conclusion

The Maritime Emission Trading Scheme is one of the most popular market-based measures that might be implemented in the shipping industry for CO_2 emission control purposes. The advantages and disadvantages of METS are widely discussed by researchers in the literature. The impact of the METS on emission reduction is normally divided into two categories. First, it is commonly agreed that the adoption of an MBM, such as METS, can bring strong incentives for the industry to invest in new technology which can lead to long-term emission reduction. Moreover, it is also believed that due to the extra allowance cost, the application of METS can also force the shipping company to adjust its fleet's operation, for example slow steaming,

and hence achieve emission reduction in the short-term as well. However, besides the allowance cost, other factors including bunker price and charter rate will also affect the operational behaviour of the vessels. Hence, whether the enforcement of the METS can still lead to emission reduction should remain in doubt when other mentioned variables are simultaneously considered. Nevertheless, previous studies in the literature seem to ignore this question and take the emission reduction effect of METS in the short term for granted. Therefore, the authors of this study try to fill this gap in the literature and examine the actual capability of METS in the short-term emission reduction with a more comprehensive setting.

We have proposed an optimization model integrating the fleet composition and deployment problem with the METS, which may be implemented in the future. A computational study is performed with a case of chemical tanker company. Different scenarios, covering all factors affecting the fleet's CO_2 emission are tested in the study and the corresponding emission level in the optimal solution of each scenario is observed and compared. The results show three main insights which are believed to be valuable reference for policy makers in the future. First, the implementation of METS will not guarantee a short-term emission reduction. Other factors, for example the charter rate, may be more important for the fleet's operational decisions in certain situations, while the impact of the METS becomes minor. In certain special case, such as the scenario with low bunker price, low charter rate, regional METS and high allowance cost, the application of METS can even increase the fleet's CO_2 emissions. Second, if the scenario allows the METS to have substantial effect on the fleet's operation, for example with a normal freight market, then a high allowance cost or a global coverage of the scheme may have the best performance in emission reduction. Last, a stronger impact of the MEST on CO_2 emission is expected in a low bunker price scenario.

Bibliography

Alizadeh, A. H., Kavussanos, M. G., and Menachof, D. A. (2004). Hedging against bunker price fluctuations using petroleum futures contracts: constant versus time-varying hedge ratios. *Applied Economics*, 36(12):1337–1353.

Alphaliner (2016). Alphaliner Newsletter No. 14 - 2016. http://www.alphaliner.com/get_public_newsletter.php?file=2016/no14/Alphaliner%20Newsletter%20no%2014%20-%202016.pdf. (accessed 05.12.2016).

Andersson, H., Fagerholt, K., and Hobbesland, K. (2015). Integrated maritime fleet deployment and speed optimization: case study from roro shipping. *Computers & Operations Research*, 55:233–240.

Balland, O., Erikstad, S. O., Fagerholt, K., and Wallace, S. W. (2013). Planning vessel air emission regulations compliance under uncertainty. *Journal of Marine Science and Technology*, 18(3):349–357.

Boscaratoa, I., Hickeya, N., Kašpara, J., Pratib, M. V., and Mariani, A. (2015). Green shipping: Marine engine pollution abatement using a combined catalyst/seawater scrubber system. 1. Effect of catalyst. *Journal of Catalysis*, 328:248–257.

Brynolf, S., Magnusson, M., Fridell, E., and Andersson, K. (2014). Compliance possibilities for the future ECA regulations through the use of abatement technologies or change of fuels. *Transportation Research Part D*, 28:6–18.

Buhaug, Ø. (2009). *Second IMO GHG Study 2009*. International Maritime Organization, London, UK.

Cames, M., Graichen, J., Siemons, A., and Cook, V. (2015). Emission reduction targets for international aviation and shipping. http://www.europarl.europa.eu/thinktank/en/document.html?reference=IPOL_STU(2015)569964. (accessed 25.06.2016).

Cariou, P. (2011). Is slow steaming a sustainable means of reducing co_2 emissions from container shipping? *Transportation Research Part D*, 16(3):260–264.

Christiansen, M., Fagerholt, K., and RonenShip, D. (2004). Routing and scheduling: Status and perspectives. *Transportation Science*, 38(1):1–18.

Clarkson (2018a). Clarkson Research Services website. https://sin.clarksons.net/. (accessed 11.01.2018).

Clarkson (2018b). Clarkson World Fleet Register. https://www.clarksons.net/wfr2/. (accessed 11.02.2018).

Corbett, J. J., Wang, H., and Winebrake, J. J. (2009). The effectiveness and costs of speed reductions on emissions from international shipping. *Transportation Research Part D*, 14(8):593–598.

Dan-Bunkering (2016). Dan-bunkering website. http://dan-bunkering.com/Pages/Solutions/Risk-management/Fixed-Price-Agreement.aspx. (accessed 12.08.2016).

De, A., Mamanduru, V. K. R., Gunasekaran, A., Subramanian, N., and Tiwari, M. K. (2016). Composite particle algorithm for sustainable integrated dynamic ship routing and scheduling optimization. *Computers & Industrial Engineering*, 96:201–215.

Doudnikoff, M. and Lacoste, R. (2014). Effect of a speed reduction of containerships in response to higher energy costs in sulphur emission control areas. *Transportation Research Part D*, 28:51–61.

Entec (2005). Service contract on ship emissions: Assignment, abatement and market-based instruments, task 2c SO_2 abatement. Final report, Entec UK Limited.

Fagerholt, K., Gausel, N. T., Rakke, J. G., and Psaraftis, H. N. (2015). Maritime routing and speed optimization with emission control areas. *Transportation Research Part C*, 52:57–73.

Fagerholt, K., Laporte, G., and Norstad, I. (2010). Reducing fuel emissions by optimizing speed on shipping routes. *Journal of the Operational Research Society*, 61(3):523–529.

Franc, P. and Sutto, L. (2014). Impact analysis on shipping lines and european ports of a cap-and-trade system on co2 emissions in maritime transport. *Maritime Policy & Management*, 41(1):61–78.

Gencer, M. and Unal, G. (2012). Crude oil price modelling with Lévy process. *International Journal of Economics and Finance Studies*, 4(2):139–148.

Ghosh, S., Lee, L. H., and Ng, S. H. (2015). Bunkering decisions for a shipping liner in an uncertain environment with service contract. *European Journal of Operational Research*, 244:792–802.

Goldsworthy, L. (2010). Exhaust emissions from ship engines-significance, regulations, control technologies. *The Australian and New Zealand Maritime Law Journal*, 24:21–30.

Gritsenko, D. (2017). Regulating GHG Emissions from shipping: Local, global, or polycentric approach? *Marine Policy*, 84:130–133.

Gu, Y. and Wallace, S. W. (2017). Scrubber: A potentially overestimated compliance method for the emission control areas: The importance of involving a ships sailing pattern in the evaluation. *Transportation Research Part D*, 55:51–66.

Gu, Y., Wallace, S. W., and Wang, X. (2018a). The impact of bunker risk management on co2 emissions in maritime transportation under ECA regulation. In Cinar, D., Gakis, K., and Pardalos, P. M., editors, *Sustainable Logistics and Transportation*, pages 199–224. Springer International Publishing, Switzerland.

Gu, Y., Wallace, S. W., and Wang, X. (2018b). Integrated maritime fuel management with stochastic fuel prices and new emission regulations. *Journal of the Operational Research Society*. https://www.tandfonline.com/doi/full/10.1080/01605682.2017.1415649.

Hermeling, C., Klement, J. H., Koesler, S., Köhler, J., and Klement, D. (2015). Sailing into a dilemma: An economic and legal analysis of an EU trading scheme for maritime emissions. *Transportation Research Part A*, 78:34–53.

Hilmola, O.-P. (2015). Shipping sulphur regulation, freight transportation prices and diesel markets in the Baltic Sea region. *International Journal of Energy Sector Management*, 9(1):120–132.

Hoff, A., Andersson, H., Christiansen, M., Hasle, G., and Løkketangen, A. (2010). Industrial aspects and literature survey: Fleet composition and routing. *Computers & Operations Research*, 37(12):2041–2061.

Høyland, K., Kaut, M., and Wallace, S. W. (2003). A heuristic for moment-matching scenario generation. *Computational optimization and applications*, 24(2):169–185.

ICS (2017). International Chamber of Shipping website. http://www.ics-shipping.org/shipping-facts/shipping-and-world-trade. (accessed 17.02.2018).

IMO (2011). Feasibility Study and Impact Assessment. http://www.imo.org/en/OurWork/Environment/PollutionPrevention/AirPollution/Pages/Feasibility-Study-and-Impact-Assessment.aspx. (accessed 01.05.2018).

IMO (2013). A new chapter for MARPOL Annex VI requirements for technical and operational measures to improve the energy efficiency of international shipping. http://www.imo.org/en/KnowledgeCentre/PapersAndArticlesByIMOStaff/Documents/A%20new%20chapter%20for%20MARPOL%20Annex%20VI%20-%20E%20Hughes.pdf. (accessed 19.02.2018).

IMO (2014). Third IMO GHG Study 2014. http://www.imo.org/en/OurWork/Environment/PollutionPrevention/AirPollution/Pages/Greenhouse-Gas-Studies-2014.aspx. (accessed 15.02.2018).

IMO (2016). International Maritime Organization website. http://www.imo.org/en/OurWork/Environment/PollutionPrevention/AirPollution/Pages/Emission-Control-Areas-(ECAs)-designated-under-regulation-13-of-MARPOL-Annex-VI-(NOx-.aspx. (accessed 05.02.2016).

Jiang, L., Kronbak, J., and Christensen, L. P. (2014). The costs and benefits of sulphur reduction measures: Sulphur scrubbers versus marine gas oil. *Transportation Research Part D*, 28:19–27.

Kågeson, P. (2007). Linking CO2 emissions from international shipping to the EU ETS. http://www.natureassociates.se/wp-content/uploads/2011/03/Linking-CO2-Emissions-from-International-Shipping-to-the-EU-ETS.pdf. (accessed 15.02.2018).

Kågeson, P. (2008). The Maritime Emissions Trading Scheme. http://www.natureassociates.se/pdf/METS%20final.pdf. (accessed 15.02.2018).

Kaut, M. and Wallace, S. W. (2007). Evaluation of scenario-generation methods for stochastic programming. *Pacific Journal of Optimization*, 3(2):257–271.

Koesler, S., Achtnicht, M., and Köhler, J. (2015). Course set for a cap? A case study among ship operators on a maritime ETS. *Transport Policy*, 37:20–30.

Kontovas, C. A. (2014). The green ship routing and scheduling problem (gsrsp): A conceptual approach. *Transportation Research Part D*, 31:61–69.

Krichene, N. (2008). Crude oil prices: Trends and forecast. Working Paper WP/08/133, International Monetary Fund.

Li, Y., zhang Wang, Y., and Cui, Q. (2016). Has airline efficiency affected by the inclusion of aviation into European Union Emission Trading Scheme? Evidences from 22 airlines during 2008 - 2012. *Energy*, 96:8–22.

Lindstad, H., Asbjørnslett, B. E., and Strømman, A. H. (2011). Reductions in greenhouse gas emissions and cost by shipping at lower speeds. *Energy Policy*, 39(6):3456–3464.

Lindstad, H. and Eskeland, G. S. (2016). Environmental regulations in shipping: Policies leaning towards globalization of scrubbers deserve scrutiny. *Transportation Research Part D*, 47:67–76.

Lindstad, H., Sandaas, I., and Strømman, A. H. (2015). Assessment of cost as a function of abatement options in maritime Emission Control Areas. *Transportation Research Part D*, 38:41–48.

Luo, M. (2013). Emission reduction in international shipping the hidden side effects. *Maritime Policy & Management*, 40(7):694–708.

Maloni, M., Paul, J. A., and Gligor, D. M. (2013). Slow steaming impacts on ocean carriers and shippers. *Maritime Economics & Logistics*, 15(2):157–171.

Meleo, L., Nava, C. R., and Pozzi, C. (2016). Aviation and the costs of the European Emission Trading Scheme: The case of Italy. *Energy Policy*, 88:138–147.

Menachof, D. A. and Dicer, G. N. (2001). Risk management methods for the liner shipping industry: the case of the bunker adjustment factor. *Maritime Policy & Management*, 28(2):141–155.

Meng, Q., Wang, S., Andersson, H., and Thun, K. (2013). Containership routing and scheduling in liner shipping: Overview and future research directions. *Transportation Science*, 48(2):265–280.

Miola, A., Marra, M., and Ciuffo, B. (2011). Designing a climate change policy for the international maritime transport sector: Market-based measures and technological options for global and regional policy actions. *Energy Policy*, 39:5490–5498.

Norstad, I., Fagerholt, K., and Laporte, G. (2011). Tramp ship routing and scheduling with speed optimization. *Transportation Research Part C*, 19(5):853–865.

Notteboom, T. and Cariou, P. (2009). Fuel surcharge practices of container shipping lines: Is it about cost recovery or revenue-making. In *Proceedings of the 2009 International Association of Maritime Economists (IAME) Conference*, Copenhagen, Denmark.

Notteboom, T., Delhaye, E., and Vanherle, K. (2010). Analysis of the consequences of low sulphur fuel requirements. Final report, European Community Shipowners Associations (ECSA).

Öler, A. and Ballini, F. (2015). The development of a decision making framework for evaluating the trade-off solutions of cleaner seaborne transportation. *Transportation Research Part D*, 37:150–170.

Panasiuk, I. and Turkina, L. (2015). The evaluation of investments efficiency of SO_x scrubber installation. *Transportation Research Part D*, 40:87–96.

Pantuso, G., Fagerholt, K., and Hvattum, L. M. (2014). A survey on maritime fleet size and mix problems. *European Journal of Operational Research*, 235(2):341–349.

Pantuso, G., Fagerholt, K., and Wallace, S. W. (2016). Uncertainty in fleet renewal: A case from maritime transportation. *Transportation Science*, 50(2):390–407.

Patricksson, Ø. S., Fagerholt, K., and Rakke, J. G. (2015). The fleet renewal problem with regional emission limitations: Case study from roll-on/roll-off shipping. *Transportation Research Part C*, 56:346–358.

Pedrielli, G., Lee, L. H., and Ng, S. H. (2015). Optimal bunkering contract in a buyerseller supply chain under price and consumption uncertainty. *Transportation Research Part E*, 77:77–94.

Plum, C. E. M., Jensen, P. N., and Pisinger, D. (2014). Bunker purchasing with contracts. *Maritime Economics & Logistics*, 16:418–435.

Prodhon, C. and Prins, C. (2014). A survey of recent research on location-routing problems. *European Journal of Operational Research*, 238:1–17.

Psaraftis, H. N. (2012). Market-based measures for greenhouse gas emissions from ships: a review. *WMU Journal of Maritime Affairs*, 11(2):211–232.

Psaraftis, H. N. (2016). Green maritime transportation: Market based measures. In Psaraftis, H. N., editor, *Green Transportation Logistics*, pages 267–297. Springer International Publishing, Switzerland.

Psaraftis, H. N. and Kontovas, C. A. (2009). CO_2 emission statistics for the world commercial fleet. *WMU Journal of Maritime Affairs*, 8(1):1–25.

Psaraftis, H. N. and Kontovas, C. A. (2010). Balancing the economic and environmental performance of maritime transportation. *Transportation Research Part D*, 15(8):458–462.

Psaraftis, H. N. and Kontovas, C. A. (2013). Speed models for energy-efficient maritime transportation: A taxonomy and survey. *Transportation Research Part C*, 26:331–351.

Qi, X. and Song, D.-P. (2012). Minimizing fuel emissions by optimizing vessel schedules in liner shipping with uncertain port times. *Transportation Research Part E*, 18(4):26–31.

Ren, J. and Lützen, M. (2015). Fuzzy multi-criteria decision-making method for technology selection for emissions reduction from shipping under uncertainties. *Transportation Research Part D*, 40:43–60.

Rockafellar, R. T. and Uryasev, S. (2002). Conditional value-at-risk for general loss distributions. *Journal of Banking & Finance*, 26(7):1443–1471.

Ronen, D. (1982). The effect of oil price on the optimal speed of ships. *Journal of the Operational Research Society*, 33(11):1035–1040.

Ronen, D. (2011). The effect of oil price on containership speed and fleet size. *Journal of the Operational Research Society*, 62(1):211–216.

Scheelhaase, J., Maertens, S., Grimme, W., and Jung, M. (2018). EU ETS versus CORSIA - A critical assessment of two approaches to limit air transport's CO2 emissions by market-based measures. *Journal of Air Transport Management*, 67:55–62.

Schinas, O. and Stefanakos, C. (2012). Cost assessment of environmental regulation and options for marine operators. *Transportation Research Part C*, 25:81–99.

Schinas, O. and Stefanakos, C. (2014). Selecting technologies towards compliance with MARPOL Annex VI: The perspective of operators. *Transportation Research Part D*, 28:28–40.

Shi, Y. (2016). Reducing greenhouse gas emissions from international shipping: Is it time to consider market-based measures? *Marine Policy*, 64:123–134.

Stopford, M. (2009). *Maritime Economics*, page 225. London: Routledge, 3rd edition.

Tai, H.-H. and Lin, D.-Y. (2013). Comparing the unit emissions of daily frequency and slow steaming strategies on trunk route deployment in international container shipping. *Transportation Research Part D*, 21:26–31.

Wang, C. and Corbett, J. J. (2007). The costs and benefits of reducing SO_2 emissions from ships in the US west coastal waters. *Transportation Research Part D*, 12(8):577–588.

Wang, K., Fu, X., and Luo, M. (2015). Modeling the impacts of alternative emission trading schemes on international shipping. *Transportation Research Part A*, 77:35–49.

Wang, S. and Meng, Q. (2012). Sailing speed optimization for container ships in a liner shipping network. *Transportation Research Part E*, 48(3):701–714.

Wang, S. and Meng, Q. (2015). Robust bunker management for liner shipping networks. *European Journal of Operational Research*, 243(3):789–797.

Wang, S. and Meng, Q. (2017). Container liner fleet deployment: A systematic overview. *Transportation Research Part C*, 77:389–404.

Wang, S., Meng, Q., and Liu, Z. (2013). Bunker consumption optimization methods in shipping: A critical review and extensions. *Transportation Research Part E*, 53:49–62.

Wang, X., Fagerholt, K., and Wallace, S. W. (2017). Planning for charters: A stochastic maritime fleet composition and deployment problem. *Omega*. https://doi.org/10.1016/j.omega.2017.07.007.

Wang, X. and Teo, C. C. (2013). Integrated hedging and network planning for container shipping's bunker fuel management. *Maritime Economics & Logistics*, 15(2):172–196.

Wong, E. Y., Tai, A. H., Lau, H. Y., and Raman, M. (2015). An utility-based decision support sustainability model in slow steaming maritime operations. *Transportation Research Part E*, 78:57–69.

WWL (2016). Wallenius Wilhelmsen Logistics website. http://www.2wglobal.com/global-network/. (accessed 19.02.2016).

Xia, J., Li, K. X., Ma, H., and Xu, Z. (2015). Joint planning of fleet deployment, speed optimization, and cargo allocation for liner shipping. *Transportation Science*, 49(4):922–938.

Yang, Z., Zhang, D., Caglayan, O., Jenkinson, I., S. Bonsall, J. W., Huang, M., and Yan, X. (2012). Selection of techniques for reducing shipping NO_x and SO_x emissions. *Transportation Research Part D*, 17(6):478–486.

Yao, Z., Ng, S. H., and Lee, L. H. (2012). A study on bunker fuel management for the shipping liner services. *Computers & Operations Research*, 39(5):1160–1172.